A Fuzzy Logic Based Microgrid Energy Management System
(Case Study Oda Bultum University)

Birhanu Feye Tola

A Thesis Submitted to the Department of Electrical Power and Control Engineering
School of Electrical Engineering and Computing

Presented in Partial Fulfillment of the Requirement for the Degree of Master's in Electrical Power and Control Engineering
(Control Engineering)

Office of Graduate Studies
Adama Science and Technology University

June, 2024

Adama, Ethiopia

A Fuzzy Logic Based Microgrid Energy Management System (Case Study Oda Bultum University)

Birhanu Feye Tola

Advisor:- Dr. Tafesse Asrat

A Thesis Submitted to the Department of Electrical Power and Control Engineering

School of Electrical Engineering and Computing

Presented in Partial Fulfillment of the Requirement for the Degree of Master's in Electrical Power and Control Engineering (Control Engineering)

Office of Graduate Studies

Adama Science and Technology University

June, 2024

Adama, Ethiopia

DECLARATION

I, hereby declare that this Master Thesis entitled **"A Fuzzy Logic Based Microgrid Energy Management System (Case Study Oda Bultum University)"** is my work. That is, it has not been submitted for the award of any academic degree, diploma, or certificate in any other university. All resources of materials that are used for this thesis have been duly acknowledged through citation.

Birhanu Feye Tola	_________________________	________________
Name of student	Signature	Date

RECOMMENDATION

I, the advisor of this thesis, hereby certify that I have read the revised version of the thesis entitled **"A Fuzzy Logic Based Microgrid Energy Management System (Case Study Oda Bultum University)"** prepared under my guidance by Birhanu Feye Tola submitted in partial fulfillment of the requirements for the degree of Masters of Science in Electrical Power and Control Engineering (Control Engineering). Therefore, I recommend the submission of a revised version of the thesis to the department following the applicable procedures.

Dr. Tafesse Asrat	______________________	______________
Advisor	Signature	Date

APPROVAL PAGE

I, the advisor of the thesis entitled **"A Fuzzy Logic Based Microgrid Energy Management System (Case Study Oda Bultum University)"** and developed by Birhanu Feye Tola, hereby certify that the recommendation and suggestions made by the board of examiners are appropriately incorporated into the final version of thesis.

Dr.Tafesse Asrat	____________________	______________
Advisor	Signature	Date

We, the undersigned, members of the board examiners of the thesis by Birhanu Feye Tola have read and evaluated the thesis entitled **"A Fuzzy Logic Based Microgrid Energy Management System (Case Study Oda Bultum University)"** and examined the candidate during open defense. This is, therefore, to certify that the thesis is accepted for partial fulfillment of the requirement of the degree of Master of Science in Electrical Power and Control Engineering (Control Engineering).

________________	____________________	______________
Chairperson	Signature	Date
________________	____________________	______________
Internal Examiner	Signature	Date
Dr Beteley Teka	____________________	June 21, 2024
External Examiner	Signature	Date

Final approval and acceptance of the thesis are contingent upon the submission of its final copy to the Office of Postgraduate (OPGS) through the Department Graduate Council (DGC) and School Graduate Committee (SGC).

____________________	____________________	______________
Department Head	Signature	Date
____________________	____________________	______________
School Dean	Signature	Date
____________________	____________________	______________
Office of Postgraduate Studies, Dean	Signature	Date

ACKNOWLEDGEMENT

First and foremost, I wish to express my heartfelt gratitude to Almighty God, the creator of all life and the wellspring of all knowledge. I am deeply thankful that He has granted me the wisdom and perseverance needed to complete this research paper.

I am truly grateful for the precious gift of life that the Almighty has bestowed upon me, as well as the strength. I would like to sincerely acknowledge and convey my heartfelt gratitude to my advisor, **Dr. Tafesse Asrat,** for his steadfast guidance, encouragement, and unrelenting support encompassing both the technical and personal dimensions of my research work. I am profoundly moved by his unwavering patience, his steadfast motivation, and his unwavering dedication in supporting me throughout this process. I am profoundly thankful to **Dr. Endalew Ayenew** for his excellent assistance and guidance. His continual encouragement, insightful input, and rigorous supervision have all helped shape and elevate our study undertaking. I appreciate his patience and willingness to willingly share his vast expertise, which has significantly improved the quality of my research paper.

I am deeply appreciative of the staff members at the National Meteorology Service Agency's Adama branch, for their essential support in supplying me with vital data collected at the Chiro station. Lastly, I would like to convey my most heartfelt gratitude to my cherished mother and father, as well as to my treasured sister and brother, whose steadfast love and sacrifices have been the very foundation of my success. I am also profoundly thankful to my dear friends, whose companionship and support have imbued this journey with profound meaning and significance.

TABLE OF CONTENTS

LIST OF FIGURES

LIST OF TABLES

LIST OF ABBREVIATIONS AND ACRONYMS

AC	Alternative Current
Bpb	Battery parallel
Bsb	Battery series
Bt	Battery total
CB	Capacity Battery
DC	Direct Current
DER	Distributed energy resources
DFIGs	Double-fed induction generators
DOD	Depth of discharge
DP	Change power
DV	Change voltage
EEA	Ethiopia Electric Authority
EEP	Ethiopian Electric Power Corporation
EMS	Energy management system
FIS	Fuzzy inference system
FLC	Fuzzy logic control
HAWT	Horizontal axis wind turbine
IC	Incremental conductance
IGs	Induction Generators
MPP	Maximum power Point
MPPT	Maximum power point track
MUP	Main utility power
MW	Megawatt
OBU	Oda Bultum University
PB	Power battery
PD	Power demand
PMSGs	Permanent magnet generators
P&O	Pertub and Observation
PS	Power solar
PV	Photovoltaic

PW	Power wind
PWM	Pulse width Modulation
RPM	Revolution per minute
VAWT	Vertical axis wind turbine

ABSTRACT

In response to the increased demand for electricity and the need for reliable power sources, microgrid systems have gained importance. However, power systems have become more complex and vulnerable, resulting in unstable power supply, and limited access, particularly at Oda Bultum University. The university heavily relies on diesel generators and the national grid, which are expensive and unreliable. As a result, fuzzy logic-based microgrid energy management system has become necessary. The load demand, solar and wind weather conditions were collected from a select site. This thesis uses Matlab/Simulink to develop a hybrid solar/wind microgrid system with battery backup. The system served as a small-scale alternative power source for three power-sensitive areas at Oda Bultum University (library, registrar's office, and data center). The total load demand energy consumption is approximately 367kWh. Load demand energy consumption covered by solar panels is 76% of the total load demand energy consumption which was 278.92kWh with wind turbines contributing around 24% of total load demand energy consumption which was 88.1kWh. Battery used as a backup for high-priority loads during solar and wind power outages, as well as when main utility power is unavailable. The available resources were intelligently managed using fuzzy logic, and it examined the type and quantity of resources before making an informed selection on the power demand. The fuzzy rule editor was used to create fuzzy rules, and Matlab/Simulink was used to simulate the components of the hybrid system. Based on the selected appropriate components to meet the site's energy demand. Specifically, SPR-305E-WHT-D photovoltaic panels, wind turbines, maximum power points, bidirectional DC-to-DC converters, inverters, and 12V, 200Ah deep cycle batteries were chosen. Simulation results show the system maintains a stable 400V DC bus with 212A DC current from renewable sources. An inverter then converts this 400V DC to 400V AC, providing with 125A AC current. The inverter-based design helps manage fluctuations in renewable power generation, balancing supply and demand. Overall, the integrated system was designed to be efficient, reliable, and able to properly meet the site's electrical load requirements.

Keywords*:- Solar Photovoltaic, Batteries, Wind turbine, Matlab/Simulink, Microgrid, and Fuzzy logic*

CHAPTER ONE

1. INTRODUCTION

1.1 Background of Study

Energy is crucial to modern civilization since it ensures a high standard of existence and supports all other aspects of the economy. Cost increases and environmental concerns about traditional electrical energy. Alternative forms of energy have received significant attention. Numerous civilizations throughout the world now have a strong desire for electrical energy. This demand has been fueled by the simplicity with which energy can be created delivered, and used, as well as the wide range of uses. It is debatable whether electricity consumption should be allowed to be unfettered, yet the truth remains that there is an ever-increasing need for this energy source. It is obvious that to fulfill this requirement, the world’s electrical power generation capacity must continue to rise. Almost all energy is produced nowadays in central power plants, which employ fissile nuclear material, oil, coal, water, and gas as their principal fuel sources. The further development of systems based on any of these common fuels presents obstacles. However, generation is limited to physically appropriate places, and coal deposits, while substantial, are not renewable.

Renewable energy management involves using renewable energy sources to meet an organization's energy needs. This can include generating renewable energy on-site, purchasing renewable energy from the grid, or using a combination of both. Sustainable energy management goes beyond renewable energy to include other practices that reduce energy consumption and environmental impact. This can include energy efficiency measures such as improving insulation and upgrading to energy-efficient appliances and equipment. Wind power, geothermal energy, and solar energy all are examples of sustainable energy sources that may be used to minimize dependency on petroleum and coal. Environmentally conscious energy management is critical for a variety of reasons. It may help companies save money on their energy costs, minimize emissions of greenhouse gases, and enhance their overall sustainability performance. Unfortunately, many organizations do not consider the sustainable aspects of energy management until after they have already shifted to renewable energy sources.

This can result in missed opportunities to save money and lessen environmental impacts (Muayad Younus & Najeeb Zaidan, 2022).

Ethiopia is no exception to the rising demand for electricity worldwide. The reason for this is rapid population growth and industrial development. Ethiopia and other countries employ sustainable energy sources such as wind, solar, biomass, and biogas to satisfy their energy demands. Renewable energy sources are pollution-free and can be produced more economically than traditional energy sources, such as coal and oil. This is important because many countries are facing energy-related problems, such as pollution and limited energy resources (Shallo et al., 2020). Ethiopia is changing its power sector to make electricity more accessible, attract foreign investment, and use more renewable energy. The government wants to increase and diversify its energy-generating capacity to 25,000 MW by 2030, including 6,000 MW from the Grand Ethiopian Renaissance Dam. The EEA's main goals are to make the energy sector more competitive, ensure that electricity is supplied efficiently and reliably, and promote energy efficiency and conservation. The Ethiopian Electric Power Corporation (EEP) is the main company that generates electricity in Ethiopia. Approximately 98% of the installed capacity of the nation is produced by hydroelectric dams. Some private companies are building projects to generate electricity from geothermal, wind, and solar sources, but these projects are not yet finished because there is no more attention to renewable energy sources (Ayele & Shen, 2022).

Solar power is regarded as one of Ethiopia's most potent and viable, environmentally friendly power sources. In Ethiopia, the average monthly sun radiation throughout a day on a flat surface ranges from 3.45 kWh/m2/day to 7.47 kWh/m2/day, with a mean of year 5.83 kWh/m2/day. This suggests that Ethiopia can generate a substantial quantity of electricity from solar energy. This might help minimize the nation's dependency on fossil fuels while also increasing access to power for all. The solar radiation potential in Ethiopia varies by region, with the highest levels of solar radiation found in Afar, Somalia, and Oromia. In contrast, the Amhara and Tigray regions have a low level of solar radiation (Benti et al., 2022). Wind energy is a kind of power generated by the inconsistent heating of the land and ocean surfaces of the Earth. Because of the inconsistent heating, the atmosphere experiences pressure changes, which push air from areas of high pressure to areas of low pressure. Wind energy is converted into a more usable form, such as electricity, by wind power. Wind turbines use kinetic energy from the wind to generate electricity. Ethiopia has considerable wind energy potential, estimated at 10,000 MW of useable wind power, which is concentrated in two significant wind zones separated by the Rift Valley. The first wind energy zone, which covers the highland plateaus, has two separate peak wind speed periods, one from March to May and the other from September to November. The second wind energy zone, which includes the Ogaden and eastern lowland regions, has its peak wind speeds between May and August (Weiß et al., 2022). Currently, there are two wind farms under construction in Ethiopia. Such as; the Ashegoda wind farm near Mekele with a capacity of 120 MW, and Adama Wind Park with a capacity of 153 MW (Matsiko, 2019).

Oda Bultum University relies on two sources of electricity. Such as the main utility grid power and diesel generators. While the main utility grid power is the primary source, generators powered by diesel are also used as backups in case of power outages or when the grid is unable to meet the energy demands of the university. So, hybrid renewable energy systems are very important for reducing reliance on diesel generators and ensuring the continuity of reliable power by installing solar panels and wind to generate electricity from the sun and wind speed, managing energy properly, and developing microgrids to provide more reliable and affordable energy to their university.

Generally, Solar and wind energy are intermittent sources, with wind power being more variable compared to solar power. Standalone solar and standalone wind systems face challenges in meeting consistent electricity demand due to fluctuating output. To overcome this, hybrid systems combine both solar and wind power, along with energy storage help balance power supply and demand, stabilizing system output. Hybrid systems offer advantages such as enhanced reliability, environmental friendliness, and suitability for any areas with and without grid access. So for this study, I selected Oda Bultum University (library, data center, and registeral office) as a case study to design a hybrid solar/wind/microgrid system. By doing this, universities can guarantee their research output and student education remain high-quality.

1.2 Motivation of Study

Frequently power outages and unstable electricity significantly affect students' research, educational laboratories, and essential services in the university. So, my motivation is to contribute to the design of a sustainable backup power supply that ensures uninterrupted electricity, smooth academic operations and promotes environmental responsibility by reducing reliance on diesel generators and the main utility power grid.

1.3 Problem Statement

Ethiopia has numerous renewable energy sources that are reliable. Rising energy demand generates greenhouse gas emissions, causing issues for the power sector. Due to swings and outages, existing infrastructure is straining to meet demand, resulting in voltage and frequency inconsistencies and an unstable power supply. This is particularly evident at Oda Bultum University (library, data center, and registeral office), which relies on expensive generators to supplement grid power. The absence of reliable electricity makes it impossible for students to conduct research, run educational laboratories, and perform other services efficiently. Microgrids appear to be a potential remedy for the difficulty of providing reliable, affordable electricity to universities, where the main electricity grid is unreliable.

The problem of fluctuating and unreliable power was a common challenge encountered during my studies and work at Oda Bultum University. To address this, a fuzzy logic-based microgrid energy management system was selected as the solution that can use wind and solar power to generate electricity for Oda Bultum University. This system was more reliable and affordable than the diesel or fuel generators that the university was currently using. It reduced the university's reliance on the main electricity grid, which was unreliable in the area. Fuzzy logic can effectively handle the uncertainty in renewable generation, using flexible linguistic variables to adaptively balance supply and demand. This fuzzy logic approach is preferred over traditional methods, as it can better manage the complexities and nonlinearities of the microgrid system, leading to improved efficiency, reliability, and balance.

1.4 Research Question

The following questions have often served as a guide for the investigation and analysis;

1. Does the study area have adequate potential for solar and wind?
2. How much energy and power is required in the selected site?
3. How are intelligent controllers used to monitor and regulate energy consumption?

1.5 Objective of the Study

1.5.1 General objectives

The primary goal of this thesis was a fuzzy logic-based microgrid energy management system that utilizes non-conventional energy resources (solar and wind power) for Oda Bultum universities.

1.5.2 Specific objective

The thesis aims to achieve specific objectives, which are as follows:

- Asses the potential of wind, and solar energy sources around Oda Bultum University.
- Analyze the energy, and power needs of Oda Bultum University (library, data center, and registeral office).
- Select suitable solar panels, wind turbines, and batteries for Oda Bultum University (library, data center, and registeral office) based on its energy needs.
- Design and analysis of a hybrid solar/wind/battery system using MATLAB/Simulink software.
- Simulate fuzzy logic-based energy management system.

1.6 Site Identification

The selected sites have challenges of intermittent and unstable power supplies during my studies and work. It also has a high potential for solar radiation. The identification of the case study area involved a direct visit to the site. Furthermore, obtain from google maps was used.

Figure 1. 1 Site of location (Source: Google maps)

1.7 Significance of the Study

Designing a microgrid system using solar panels, wind turbines, and battery storage can help to provide uninterrupted and high-efficiency energy to the library, data center, and registeral office at Oda Bultum University. This also gives users more reliable and balanced power. This research can be helpful to other universities that have similar lack of electricity access issues.

1.8 Scope of Study

This thesis investigates the challenges of providing electricity to the library, data center, and registeral office at Oda Bultum University using renewable energy sources. Designs a microgrid energy management system using solar, wind, and battery storage to provide the energy requirements for the specific location.

1.9 Limitations of the Study

There is a limitation that may apply when writing research papers. First, employees in the chosen area and other offices might not cooperate, making it challenging to obtain necessary information and recorded data on wind speed and load demand. Second, it might not be possible to model every part of the suggested hybrid system in Matlab/Simulink because of the study's width. Thirdly, when solar and wind with battery backup and main power were not available select sites didn't get energy, and batteries were used as a backup for only priority loads. Cost analysis was also not considered in this study. Finally, the system was restricted to simulation because it would necessitate more time, resources, and budget to be implemented.

1.10 Thesis Outline

This section provides a brief description of each chapter of our thesis report. It has a total of five chapters.

Chapter 1: Introductions- This chapter covers the background of the study, description of the site identification, statement problem, the object of the study, research question, motivation of the study, scope of the study, significance of study, and limitation of the study.

Chapter 2: Literature Reviews- Provides an overview of microgrids and green energy resources, including photovoltaic, wind, and energy storage, as well as related works.

Chapter 3: Materials and Methods- This chapter focused on assessing the potential of solar and wind sources at the select site, data analysis, system designing, and modeling each component capacity.

Chapter 4: Result and Discussion- This chapter analyzes simulation results with a discussion of each component and monitoring energy management by using fuzzy logic.

Chapter 5: Conclusion and Recommendations- This final chapter, covers conclusions and recommendations.

CHAPTER TWO

2. LITERATURE REVIEW AND RELATED WORKS

2.1 Introduction

This chapter explores into the fundamentals of renewable energy (solar and wind) sources and microgrid systems. Furthermore, different classifications of microgrids and relevant studies are examined.

2.2 Overview of Microgrid System

A microgrid consists of a collection of linked loads and dispersed energy resources that provide electricity to specific areas, such as university campuses, cities, communities, hospitals, commercial centers, and residential neighborhoods. It's generates power using one or more widely distributed energy sources, such as solar, wind turbines, diesel engines, or fuel cells. Depending on the financial and environmental circumstances, the microgrid may or may not link to the main grid. It has two modes of operation, where it is operating as synchronous with the grid and isolated from the main electrical grid. Many modern microgrids include energy storage, usually in the form of batteries (Asian Development Bank, 2020). Figure 2.1 depicts a microgrid's structure.

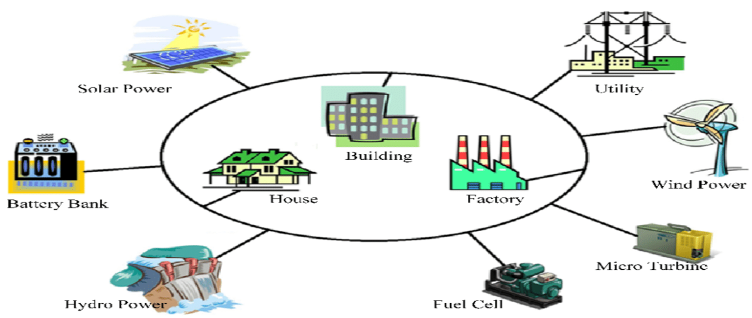

Figure 2. 1 Microgrid structure (Kuo & Lu, 2013)

2.2.1 Classifications of microgrids

Microgrids can be categorized in several ways based on their purpose. Some common categories are: -

Institutional microgrids: These microgrids are used on university campuses or other institutional campuses. They are typically interconnected with the public utility grid, but they can also operate independently. Institutional microgrids often have a variety of loads, such as lighting, heating, cooling, and research equipment.

Remote microgrids: These microgrids are situated in rural places that are not linked to the public utility network. Renewable energy sources, such as wind and solar electricity, are frequently used to run them. Remote microgrids are typically self-sufficient, but they can also be interconnected with the public utility grid if desired.

Commercial and industrial microgrids: These microgrids are used by businesses and industries. They can be interconnected with the public utility grid or they can operate independently. Commercial and industrial microgrids often have high-powered loads, such as manufacturing equipment and data centers.

Microgrids can operate in a variety of modes, depending on their specific needs. The most common modes are:

Grid-connected mode: Grid-connected mode: In this setup, the microgrid is linked to the main electrical distribution network. Because of this, the microgrid may import and export electricity from the grid according to its requirements.

Island mode: In this mode, the microgrid is disconnected from the main power grid and operates independently. This can be necessary during power outages or for other reasons.

Hybrid mode: In this mode, the microgrid may function in both island and grid-connected modes. This allows the microgrid to take advantage of the benefits of both modes.

Advantages and disadvantages of microgrid

Microgrids are small, localized power grids that offer many advantages over traditional power grids, including:

- Increased efficiency: Microgrids can reduce energy losses by generating and distributing power closer to consumers.
- Increased flexibility: Microgrids are self-sufficient electricity systems that may be customized to meet the unique requirements of their users.
- Improved environmental performance: Microgrids can assist in incorporating solar and wind power into the grid, reducing emissions and promoting sustainability.
- Reduced vulnerability: Microgrids are less vulnerable to power outages than traditional power grids because they can continue to operate even if the main grid is down.

- Easier control: Microgrids are easier to control than traditional power grids because they are smaller and more localized.

There are also some disadvantages to using microgrids, such as:

- High initial cost: Microgrids can be expensive to install and operate, especially in the early stages of development.
- Complexity: Microgrids are complex systems that require careful planning and management.
- Technical challenges: Microgrids can face many technical challenges, such as integrating renewable energy sources and managing energy storage.

2.3 Hybrid Energy Source

Hybrid energy sources can be broken down into different components, each playing an essential part in ensuring a stable and efficient energy supply. These components include wind, solar, energy storage systems, power converters, and control systems. The task of storing energy from various sources, such as solar or wind power, and making it available for use when needed falls to energy storage systems. Energy may be changed from one form to another using power converters, including DC to AC, DC to DC, AC to AC, and AC to DC. To make sure that energy is distributed properly and efficiently, a control system is employed to monitor the energy flow.

2.4 Wind Energy System and Its Essential Elements

Wind energy is a form of solar energy that is generated by the sun's uneven heating of the atmosphere, surface fluctuations, and the earth's rotation. It is characterized by the air's movement from areas of higher atmospheric pressure to areas of lower atmospheric pressure. Across the span of human civilization, individuals have harnessed and leveraged the energy of wind for a variety of purposes, such as sailing, flying kites, and generating electricity. Wind turbines effectively capture this environmentally friendly and renewable energy to generate mechanical power or electricity (Reddy et al., 2015). Wind power has emerged as a crucial component of human life globally, and has witnessed substantial advancements across numerous domains in recent years. The rising prominence of wind energy can be attributed to the persistent decline in fossil fuel supplies, fears of an impending energy crisis, price instability, and increased public consciousness about the importance of cleaner, greener energy options. Wind power is widely considered to be the renewable energy technology undergoing the fastest growth and deployment globally (Bangga, 2022).

2.4.1 Wind turbine

The purpose of wind turbines is to capture the kinetic energy present in wind and convert it into mechanical power. This mechanical energy can be applied directly for specific tasks, like grinding grain or pumping water. Conversely, it can also be transformed into electricity by employing a generator. In contrast to a fan that necessitates electricity to create wind, a wind turbine leverages the inherent power of wind to generate electricity. The functioning of a wind turbine is based on a straightforward principle: as the wind blows, it causes the rotation of two or three blade-like structures attached to a rotor. This rotational motion, in turn, drives a generator that produces electricity (Reddy et al., 2015).

a) Vertical axis wind turbine

When the principal wind turbine components are located at the base and the main rotor shaft is vertically oriented, it is considered an asymmetric wind turbine design with a vertical axis. As the Savonius is a drag-type VAWT, it cannot rotate faster than the wind speed itself. This results in a tip speed ratio of one or less, rendering it unsuitable for power generation applications. Furthermore, due to its relatively poor efficiency compared to other wind turbine types, the Savonius is better suited for purposes like water pumping or grain milling. The lower wind speeds nearer to the ground mean that a substantial portion of the swept area is near the earth, thereby reducing the overall energy harvesting effectiveness of this design. A vertical-axis wind turbine doesn't have to face the breeze, and the power transition mechanisms can be installed at ground level for simple access (Reddy et al., 2015).

b) Horizontal axis wind turbine

HAWT is distinguished by the orientation of its rotor blades connected to the horizontal axis. These turbines are commonly used for commercial purposes and consist of several essential components. The rotating shaft, gearbox, wind speed measurement device, generator, controls, turbine orientation, control system, and footing are all integral parts of HAWTs. These elements collaborate to efficiently harness the wind's power and generate electricity (Sumit S. Chaudhari et al., 2017). HWAT is classified into two types.

Upwind turbine: In an upwind turbine, the rotor is placed facing the direction of the wind. The primary advantage of this upwind design is that it avoids the wind shadow that forms behind the tower. This helps to minimize the impact of tower shading. As the airflow reaches the tower, it will begin to curve to pass around the structure. This results in some power loss from the interference, but not to the same degree as what would be seen in a downwind turbine configuration (Reddy et al., 2015).

Downwind turbine: In a downwind turbine design, the rotor is placed on the side of the turbine that faces away from the incoming wind. The nacelle is often designed to try to find the wind, reducing the requirement for a separate yaw mechanism. The blades of the rotor may be versatile since there is no threat of tower assault. The downwind configuration typically results in lower manufacturing costs, and the ability of this design to channel some of the wind force directly to the blades rather than just loading the tower can serve to reduce the structural stress on the tower when facing strong wind conditions (Reddy et al., 2015).

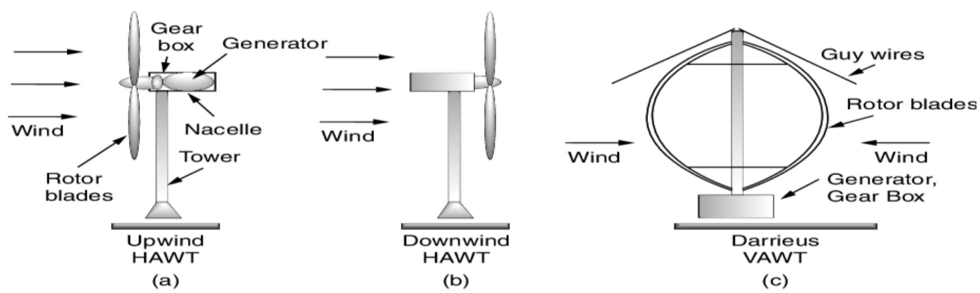

Figure 2. 2 Type of wind turbines (Nomandela et al., 2023)

2.4.2 Wind turbine components

The integral components that make up the design of a HAWT are: (Reddy et al., 2015);

Nacelle: A nacelle is a structure that contains every component required to operate a turbine efficiently.

Anemometer: Determines the wind speed and sends information about it to the controller. An anemometer for measuring wind speed and a wind vane are installed in the nacelle.

Hub: The Hub is where the low-speed shaft and rotor blades link.

Gearbox: The gearbox serves the purpose of connecting the low-speed main shaft to the high-speed shaft that leads to the generator. This gearbox mechanism allows the rotational speed to be increased from around 30-60 revolutions per minute up to approximately 1200-1500 rpm, which is the necessary speed range for most generators to efficiently produce electrical energy.

However, the gearbox is a costly and heavy component within a wind turbine system. As a result, researchers are exploring "direct drive" generator designs that can operate at slower rotational speeds and do not require a gearbox, particularly for smaller-scale wind turbine applications.

Generator: The generator is the key system component attached to the high-speed shaft that converts the rotational mechanical energy into electrical output. Common generator types used in wind turbines include induction generators (IGs), doubly-fed induction generators (DFIGs), and permanent magnet synchronous generators (PMSGs), each with its advantages. PMSGs are commonly used in wind turbines because they are highly efficient, enhanced partial load performance, and are compact and lightweight. The core purpose of the generator is to transform the rotational power from the turbine blades into usable electrical energy.

High-speed shaft: A High-speed shaft takes the rotational mechanical energy and transfers it directly to the generator to power the generator's electrical output.

Low-speed shaft: The rotor turns the low-speed shaft at about 30 to 60 rpm.

Pitch: The pitch system adjusts the angle of the turbine blades to prevent the rotor from spinning in wind conditions that are either too strong or too weak to efficiently generate power.

Rotor: The rotor is the assembly of the wind turbine blades attached to a central hub.

Foundation: A well-built foundation is necessary to hold the tower, and the various sections of a wind turbine weigh in tons.

Tower: An assembly that supports the hub's nacelle and rotor. These are made of steel lattice or concrete.

Yaw drive: This is an essential component for upwind turbines, allowing the entire turbine to turn and continuously face the wind as conditions change. Downwind turbines, on the other hand, can passively orient themselves without the need for a powered yaw system.

Yaw motor: The yaw motor is responsible for powering the yaw drive component that maintains the turbine's alignment with the wind direction.

Electronic equipment: Electronic equipment for wind turbines includes controllers and connectivity equipment. This encompasses electrical components such as cables, ground support equipment, and other peripherals necessary for the turbine's operation.

Blades: Wind turbine blades collect and convert wind energy from its kinetic form into mechanical energy. These blades are composed of wood epoxy or fiberglass-reinforced polyester. Wind turbines can have one, two, three, or more blades, depending on their construction. The vast majority of horizontal-axis wind turbines (HAWTs) feature three blades. These blades are connected to the rotor hub through three connection points or attachment points. (Reddy et al., 2015). The main parts of a wind turbine have a horizontal axis(Madvar et al., 2019).

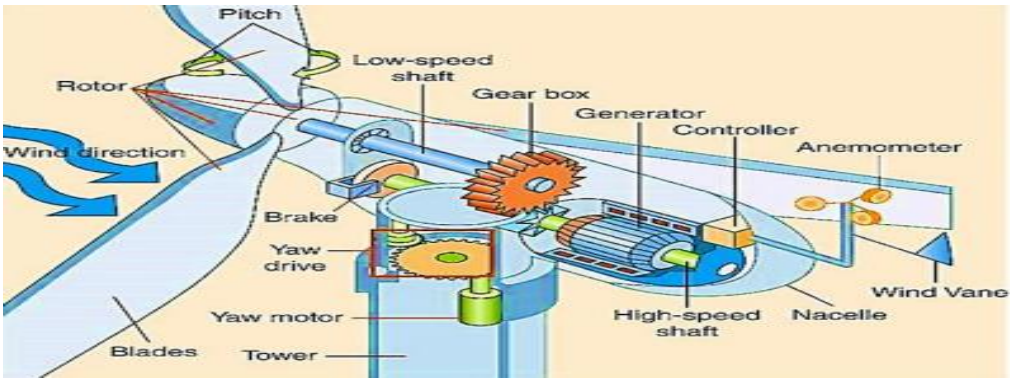

Figure 2. 3 Wind turbine components (Madvar et al., 2019).

2.4.3 Wind turbine's operating principle

The wind turbine has a big rotor with long blades that are attached to the top of a tall tower structure. The rotor blades' design and arrangement cause the turbine to revolve when the wind blows against them. The wind turbine's rotor blades are connected to a shaft. As the wind causes the rotor blades to spin, the shaft also starts to rotate. This spinning shaft is linked to a gearbox, which is responsible for increasing the rotational speed. The high-speed output shaft from the gearbox is then connected to an electrical generator. So as the gearbox speeds up the shaft's rotation, it in turn causes the generator's rotor to spin faster as well. This generator converts the mechanical energy from the spinning rotor into electrical energy. Electrical cables are then used to collect and transmit the electrical power generated by the wind turbine. The generator requires an exciter component to properly stimulate the magnetic coil in the generating field system, enabling it to produce the desired electrical power output. The voltage generated at the alternator's output terminals is directly proportional to both the alternator's rotational speed and the strength of its magnetic field flux, which are ultimately driven by uncontrolled wind power. To maintain the homogeneity of the alternator's output power, excitation must be adjusted by the availability of natural wind power. A turbine controller measures the wind speed and controls the exciter current. The output voltage of the electrical generator (alternator) is then sent into a rectifier, where it is rectified to DC. The rectified DC output is then sent to a line converter unit, which converts it into stabilized AC output, which is then delivered to either an electrical transmission network or the transmission grid via a step converter.

2.4.4 Wind energy converters and regulations

The wind turbine's unique physical design creates uneven forces on the passing airflow, causing it to rotate and oscillate. This allows the system to harness the kinetic energy of the wind and use it to power an electrical generator. It's generate electricity by leveraging the energy contained in wind. They collect the kinetic energy from the wind passing over the swept area of the turbine blades, generating pressure differences that drive the rotation of the blades and, in turn, the connected electrical generator. The generator converts this mechanical rotational energy into usable electrical power. The wind turbine are begin to produce electricity once the wind speed reaches a minimum threshold, and its power output was increase with stronger winds up to the rated maximum. Because of the installation of safety systems that might prevent the turbine from producing power above the cut-off wind speed. To safeguard both the load and the turbine during high wind speeds power control systems are required.

Pitch regulation:- Pitch regulation is a form of wind turbine control system that employs an electronic control system or active control mechanism to lower the wind turbine's aerodynamic efficiency. When the wind velocity exceeds the rated wind speed, the regulatory system alters the blade pitch automatically. The rotor's capabilities would be reduced if the angle of attack was changed. To avoid operating wind turbine blades outside of their viable range, the regulating system should respond faster to changes in wind speed. When wind speeds are moderate, pitch-regulated turbines convert wind speed more effectively because the blades are turned to the optimum angle of attack.

Stall regulation:- This energy management method has no active control and uses aerodynamic adjustment of the blade profile along its longitudinal axis to raise the angle of attack. Blade stall arises from the air sticking to the upper side of the blade due to an increase in the angle of attack. This turbulence prevents the lift force from acting on the blades. The rotor blades are specially designed to guarantee that when wind speed increases, turbulence forms on the side of the turbine blades, reducing the turbine’s aerodynamic efficiency and controlling the power output.

Active stall regulation:- Active stall regulation in wind turbines automatically adjusts the blade angles to limit power output in high winds. This protects the turbine components from excess stress and prevents damage. It works by deliberately stalling the putting a brake on the wind to keep the turbine safe and operating smoothly.

2.4.5 Power of wind turbine

The utilization of wind as a source to generate mechanical force or electrical energy is known as wind power. Wind energy is becoming an increasingly appealing energy source, owing to rising global energy demand and environmental concerns. Because of the differing working speed ranges of the wind into mechanical energy via a shaft and gearbox configuration (Manyonge et al., 2012). The wind turbine's rotor, composed of blades, captures the wind energy and converts it into low-speed rotational motion. This mechanical rotation is then fed into the generator component, which primarily consists of an electrical generator, control electronics, and a gearbox. The gearbox increases the rotational speed to drive the generator, which in turn converts the mechanical energy into usable electrical energy (El-Ahmar et al., 2017). The power that can be extracted from the wind is directly related to the amount of kinetic energy contained within the flowing air as it passes through the wind turbine.

$$P_w = \frac{1}{2}(air\ mass\ per\ unit\ time)(wind\ speed)^2 \quad (2.1)$$

$$= \frac{1}{2}(\rho A v_o)v_o^2 \ = \ \frac{1}{2}\rho A v_o^3 \quad (2.2)$$

The power available in the wind is not equivalent to the actual power generated by the wind turbine. A power coefficient factor accounts for the efficiency of the power transformation process. Specifically, the aerodynamic power produced by the wind turbine is determined by:

$$P_W = \frac{1}{2}\rho A v_0^3 C_p \quad (2.3)$$

Where, P_W is wind power.

V_o = Speed of free wind in the unperturbed state of the rotor blades of the turbine

A = Rotor swept area

C_p = Power coefficient

Factors that influence wind turbine output power

Numerous aerodynamic elements, including temperature, wind speed, height, air density, air pressure, and area swept, have an impact on the production of electricity from wind turbines (El-Ahmar et al., 2017).

a) Wind speed

The link between the wind speed at the hub height and the anticipated active power to generate is shown by the wind turbine power curve based in part on the wind speed ranges, one may observe from the power curve that wind turbines run in several operational modes. In the following figure 2.4, the wind turbine's mode of operation is based on wind speed (Bilendo et al., 2023).

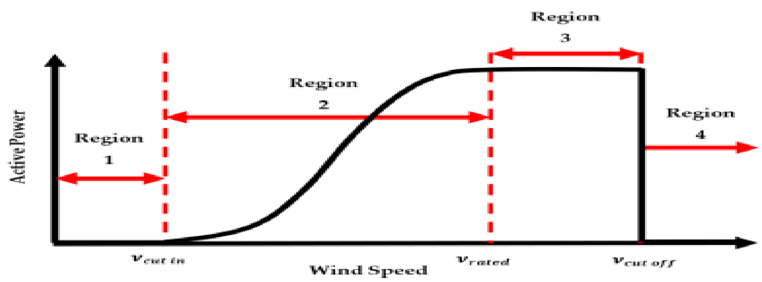

Figure 2. 4 Wind turbine power curve against wind speed (Bilendo et al., 2023).

The characteristic curve of wind speed and output power has three key points.

Cut-in speed:- At low wind speeds power generation begins at the cut-in speed ($V_{cut_{in}}$) the wind turbine is not producing any energy (Bilendo et al., 2023).

Rated speed:- The wind turbine produces electricity at an increasing rate up to the rated speed (V_{rated}) when the wind speed level climbs above the " cut in speed" (Bilendo et al., 2023).

Cut-out speed:- The wind turbine produces power at a steady rate after reaching the rated speed. This power is the maximum rated power up to the "cut-off speed" $V_{cut_{off}}$. In $V_{cut_{off}}$ the wind turbine from greater speeds that might reveal danger and significantly harm the wind turbine, it is often shut off from the "cut off" speed limit (Bilendo et al., 2023). The following represents how wind velocity and energy are related (El-Ahmar et al., 2017);

$$P_e = \begin{cases} 0 & v < v_{ci} \text{ or } v > v_{co} \\ P_{nl} & v_{ci} \leq v < v_r \\ P_r & v_r \leq v < v_{co} \end{cases} \tag{2.4}$$

Where, P_e is electric power in W, v_{ci} is the cut in wind speed in m/s, v_{co} is the cut out speed in m/s, v_r is the rated wind speed in m/s, P_r is the rated power in W and P_{nl} is the non-linear relationship among power and wind speed.

b) Rotor-swept area

Power available in wind per unit area;

$$\frac{P_w}{A} = \frac{1}{2}\rho v_o^3 \tag{2.5}$$

The power that can be extracted from the wind is directly proportional to the cube of the wind speed and the swept area of the wind turbine's rotor.

$$A = \frac{\pi}{4} D^2 \tag{2.6}$$

Where, D is the diameter of the rotor.

c) Air density

The performance and power output of a wind turbine are directly influenced by the air density. The energy that can be extracted from the wind is proportional to the air density (El-Ahmar et al., 2017). The relationship between air pressure and air density (ρ) is inversely related to temperature.

$$P = \frac{P_a}{R*T} = \frac{1.0132*10^5}{287*288} = 1.226 JK/kg/m^3$$

Where; $\mathrm{P_a}$ is standard air pressure (1.013×10^5 Pa)and at 15 °C

T is air temperature in kelvin and R is the gas constant, $\left(\mathrm{R} = 287 \frac{\mathrm{JK}}{\mathrm{kg}}\right)$

d) Height effect of wind power

Any little increase in wind velocity will have a big effect on the economic component since it is widely known that the power available in the wind is proportionate to the cube of the wind's velocity. Turbines mounted atop taller towers are an effective way to harness greater winds. The air's friction as it moves across the earth's surface has a significant impact on wind velocity in the first few meters above the surface. There is little resistance from frictionless surfaces, such as a calm sea, and there is very little variation in velocity with height below the surface. However, winds are much longer over uneven surfaces, such as those found in woods and buildings (El-Ahmar et al., 2017). To show how the roughness of the earth's surface affects wind speed, the following equation is commonly used;

$$V(H_{agh}) = V(H_{ref}) \frac{\ln\left(\frac{H_{agh}}{H_o}\right)}{\ln\left(\frac{H_{ref}}{H_o}\right)} \quad (2.7)$$

Where $V(H_{agh})$; Wind speed at the above ground height (H_{agh})

$V(H_{ref})$; Wind speed at reference height (H_{ref})

H_o ; Measure of surface roughness

The relationship between wind speed and height above the ground is described by the wind speed power law, often referred to as the wind speed profile. It is predicated on the finding that, as altitude increases, wind speeds often rise as a result of a decrease in surface roughness and ground friction. The power law for wind speed is stated as ("Green Energy Technol.," 2006):

$$V(h_{esti}) = V(h_{ref})(\frac{h_{esti}}{h_{ref}})^a \quad (2.8)$$

Where, $V(h_{ref})$ is wind speed measured at h_{ref}, $V(h_{esti})$ is wind speed at h_{esti} and a is the ground surface friction coefficient.

Different values of ground surface friction coefficient (a) are listed in the below table.

Table 2. 1 Type of terrain and value of (a) (Aziz et al., 2022).

Type of environment elevation	Ground surface coefficient friction (a)
Lake, sea, flat or undulating terrain	0.1
Grass on level ground	0.15
Hedges, shrubs, and tall crops	0.20
A forested area with plenty of trees	0.25
Some trees and bushes in a little city	0.30
Town with high-construction	0.40

2.5 Solar Energy and its Classifications

The heat and radiation that the sun emits is known as solar power, and it may be harvested utilizing several cutting-edge technologies, including solar thermal energy, PV systems , and solar heating. Although sunlight generates enormous amounts of radiation, only a small portion of it reaches Earth. The sun is the source of fossil fuels, as they come from organisms that use solar energy to grow and survive (Nandakumar & Sekar, 2022).

i) Photovoltaic systems

The photovoltaic system is a desirable alternative source of energy for distributed electrical power generation due to its compact size and silent operation. It has witnessed significant growth worldwide. The PV system is made up of different parts that work together to convert, regulate, distribute, conduct, and store the energy produced by the photovoltaic array (Rajashekar Reddy Palle, Jens Schuster, Yousuf Pasha Shaik, 2018). The key structures of a photovoltaic system are simplified:

a) PV Array: A PV array refers to a group of PV modules operating together as one unitary system. To achieve the required power needs for a given application, additional modules can be linked in parallel or series when the power provided by a single module is inadequate. A PV array comprises multiple PV modules, and each module is made up of individual PV cells.

b) PV Cell: The basic elements of a photovoltaic system are PV cells. A photovoltaic cell's semiconductors absorb light from the sun's rays and release electrons that are collected by metal contacts attached to the cell.

c) PV module: PV modules are composed of many PV cells. These cells are frequently connected in series to increase the panel's voltage rating. A single cell can only produce a limited amount of electricity; thus, multiple cells are linked in series to provide a greater total power output. Figure 2.5 depicts the architecture of solar cells, modules, or arrays.

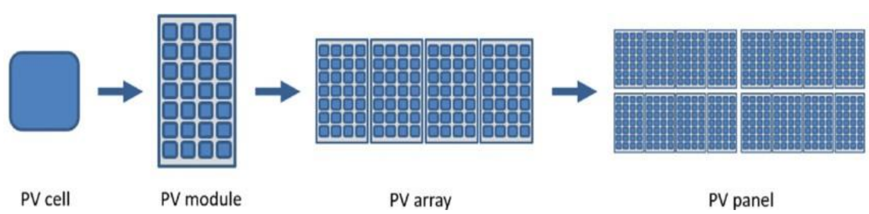

Figure 2. 5 Photovoltaic cells, module, array (Rajashekar Reddy Palle, Jens Schuster, 2018).

ii) Type of photovoltaic cell

Solar cell advances in technology have resulted in the availability of numerous types of photovoltaic (PV) technology on the market today. The conversion performance and module cost of these methods differ. The following are the primary types of photovoltaic cell technology;

a) Single-Crystalline Silicon: Single-crystalline silicon cells consist of a continuous and unbroken crystal lattice structure. They are made of highly pure silicon and can be either intrinsic or doped with small amounts of other elements to modify their semiconducting properties (Ali McBride, 2021).

b) Poly-crystalline and Semi-Crystalline: Poly-crystalline and semi-crystalline cells are produced using a faster and more cost-effective manufacturing process. These cells have a lower conversion efficiency but offer a noteworthy decline in cost per watt of power, making them more affordable (Ali McBride, 2021).

c) Thin Films: Thin film PV technologies are relatively new and gaining popularity in the market. Compounds like gallium arsenide, copper indium diselenide, and cadmium telluride are used. The thin film technique necessitates less material per square area of the cell, resulting in a cheaper cost per watt of electricity produced (Ali McBride, 2021).

d) Amorphous Silicon: In photovoltaic cells, amorphous silicon is a kind of non-crystalline silicon. Unlike mono-crystalline and poly-crystalline silicon, amorphous silicon lacks a well-defined crystal structure and is made up of small grains or crystallites (Ali McBride, 2021).

Table 2. 2 The most popular and unique forms of solar panels (Online, Accessed 27 03 2024).

Type of cells	Efficiency	Advantages	Disadvantages
Single-Crystalline cell	20%	High efficiency, durable, and high life cycle	More complex and expensive
Poly-crystalline cell	15%	Less expensive, lower conversion efficiency	Sensitive to high temperature, lower life span, and slightly less space efficiency
Thin film (Amorphous)	7-10%	Comparatively cheap, simple to make, and adaptable	Less efficiency, lower guarantees, and short span

Generally, solar photovoltaic systems have several benefits, such as fast installation lead times, modular design, high power output, extended lifespan with minimal maintenance, and mobility. However, disadvantages include the upfront cost of installation, inefficiency during nighttime and cloudy weather, the use of polluting materials in solar panels, and larger installation area requirements for higher power output.

iii. Working Principles of Solar Photovoltaic System

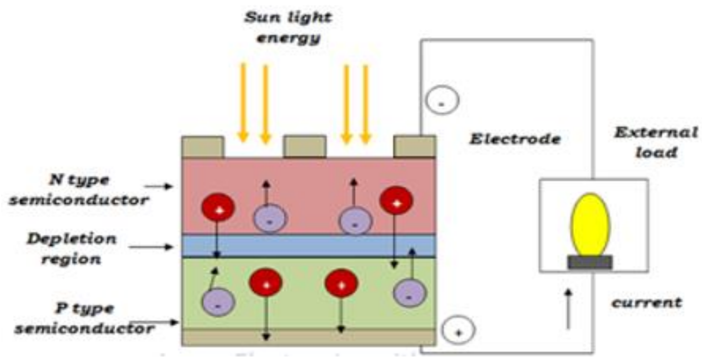

Figure 2. 6 Working Principles of Solar Photovoltaic (Al-Ezzi & Ansari, 2022).

Sunlight is converted into electrical energy by solar PV cells using the photovoltaic effect. When photons, or light particles, collide with a semiconductor material, electrons are liberated from their atoms. These liberated electrons can then travel through the semiconductor, resulting in an electric current. The semiconductor material of a solar photovoltaic cell is commonly silicon. The band gap, sometimes referred to as bandwidth, is the amount of energy needed in silicon to free an electron from its atom. When a photon of light strikes the silicon, it can provide the electron with enough energy to cross the band gap and become free. The liberated electrons then travel to the N side of the solar cell, while the holes move to the P side. This generates a voltage across the cell and can be used to power electronics (Al-Ezzi & Ansari, 2022).

Solar photovoltaic systems have several benefits, such as fast installation lead times, modular design, high power output, extended lifespan with minimal maintenance, and mobility. However, disadvantages include the upfront cost of installation, inefficiency during night time and cloudy weather, the use of polluting materials in solar panels, and larger installation area requirements for higher power output.

2.6 Energy Storage

Electricity is highly versatile and efficient in converting to other forms of energy. However, heat energy cannot be efficiently converted back into electricity. In most cases, the total heat-to-electrical transition performance of fossil heat power plants is below fifty percent. The drawback of electricity is its limited large-scale storage capability. Wind and PV systems, as intermittent power sources, require energy storage to meet continuous load demand. Since electricity generally energy storage cannot be stored immediately, it must first be transformed into other forms before it may occasionally be turned back to electricity (Das et al., 2018).

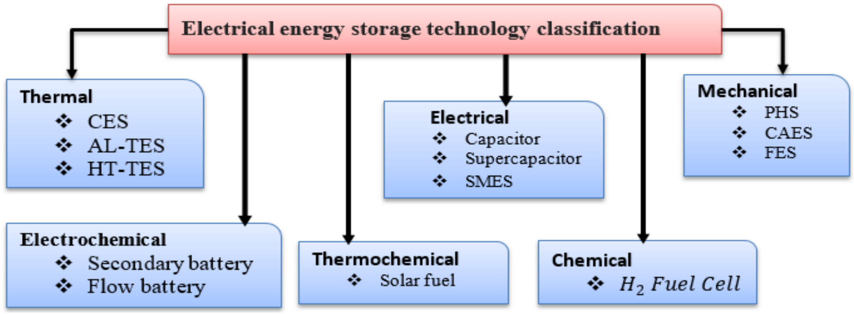

Figure 2. 7 Categories of energy storage system (Das et al., 2018)

Battery energy storage system

An electrochemical device that stores chemical energy and transforms it into electrical energy when required is a battery. This conversion occurs through a process called an electrochemical reaction, which involves the transfer of electrons between two or more substances. Batteries are one form of energy-storing equipment, that works through electrochemical processes. There are two kinds of batteries (Stephie, 2023).

Non-rechargeable batteries: Primary cells are capable of producing electricity right away. These are mostly utilized in low-power portable devices that are used seldom or distance from another power source, including communication and alarm circuits in situations where other electric power is only available intermittently. Reusable rechargeability is impossible for disposable primary cells because of the non-reversible nature of chemical reactions and the potential for non-return of active ingredients to their initial configurations (Stephie, 2023).

Rechargeable batteries: Also known as secondary batteries, secondary cells often contain depleted active components and must be charged before use. The chemical changes that occur during discharge are reversed by electric current in rechargeable batteries. The gadgets that supply the required current are called chargers (Stephie, 2023).

Characteristic of the battery

Capacity of Battery (CB): - This shows the amount of energy that a battery can hold. A battery's usable energy is determined by several variables, including its kind, age, temperature, and speed of discharge.

Voltage of Battery: When a battery is completely charged, its voltage is as follows. The quantity and voltage of the battery's cells determines the particular voltage.

Depth of Cycle: - Batteries that have been entirely drained may experience damage or lose their capacity to perform sooner than expected. A deep-cycle battery has a depth of discharge (DOD) of 80% – 85% and is intended to discharge up to 15%–20% of its capacity (Fissaha, 2017).

Autonomy: - The maximum amount of time that a system may discharge energy continuously. This is the restorable power capability to maximum power discharge ratio, and it depends on the type of application and storage capacity (Fissaha, 2017).

$$A = \frac{P_{restore}}{P_{disp}} \tag{2.9}$$

Capacity for cycling: - It shows how many instances a battery may discharge to its intended energy level following a recharge. The amount of cycles (Ncycles) determines the cycle's capacity. The depth of discharge has a significant influence on cycle capacity. The quantity of cycles about the discharge depth is plotted in Figure 2.8 below.

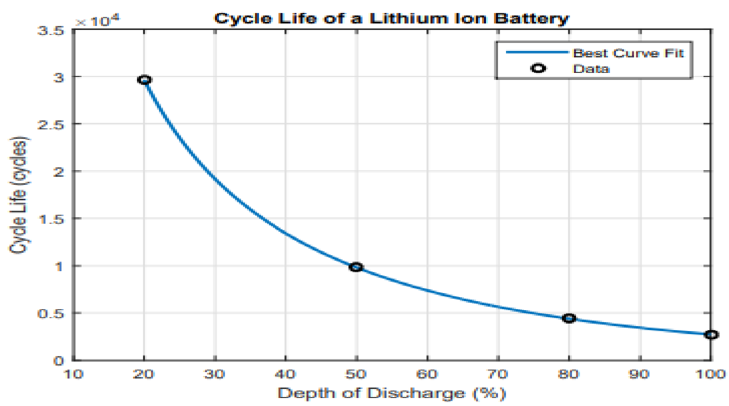

Figure 2. 8 Lead acid battery cycle life versus depth of discharge (Mallon et al., 2017).

2.7 Electronic Power Converters

Electrical power converters are devices that change the voltage or current of an electrical signal. They are a crucial part of the hybrid clean energy systems, which generate electricity through the incorporation of numerous sources of renewable energy, such as solar and wind sources.

DC-to-DC converter: A converter device used to regulate the magnitude of a DC voltage or current. These have to be used because the DC voltage cannot easily be raised or lowered using transformers. In hybrid renewable energy systems, DC-to-DC converters are used to convert the voltage that results from the output of solar panels and wind turbines to a single voltage level.

DC-to-AC converter: These are electrical devices that transform voltage into an alternating current from a direct current. This is crucial since the majority of equipment and appliances run on alternating current voltage. In non-conventional energy combination systems, inverters are used to convert direct current electricity from solar panels and batteries to alternating current voltage.

AC–to–DC converter: Used to convert alternating current voltage to direct current voltage. This is necessary to charge the battery bank in a hybrid renewable energy system. Rectifiers are also used to convert AC voltage to DC voltage for use in certain appliances and devices.

Bi-directional converters: It is employed to change an alternating current voltage from a direct current voltage and vice versa.

2.8 Maximum Power Point Tracking

A method used in PV systems to maximize the power output of solar panels is called Maximum Power Point Tracking. It entails tracking and modifying the system's operating point continually to ensure that it operates at its maximum power point (MPP) in response to shifting environmental circumstances. By dynamically adjusting the voltage or current, MPPT algorithms ensure that the PV system operates at its peak efficiency, maximizing energy production and overall system performance. The choice of the MPPT algorithm plays a significant role, with the incremental conductance and P&O algorithms being commonly used due to their simplicity, ease of use, and minimal hardware requirements (Babaa et al., 2014).

2.8.1 Perturbation and observation (P&O) method

This algorithm adjusts voltage based on the change in power, with a positive change leading to a rightward voltage adjustment and a negative change resulting in a leftward adjustment. The control signal for PWM is calculated accordingly, gradually reducing overshoot until a stable steady state is reached. Control continues until maximum output power is achieved. According to the flow chart, if both the change in power (dp) and the change in voltage (dv) are positive, the algorithm recommends increasing the voltage as the power is on the left side of the maximum power track point. Conversely, if both dp and dv are negative, the algorithm suggests decreasing the voltage as the power is on the right side of the maximum power track point (Babaa et al., 2014).

2.8.2 Incremental conductance method

The perturbation and observation approach's shortcomings are addressed by the IC algorithm, which makes use of photovoltaic conductance. When the conductance reaches the incremental conductance, it looks for the voltage operation point and stops adjusting the operating point at that moment. The IC algorithm offers advantages such as determining the distance to the maximum power point (MPP), precise tracking in variable weather conditions, and reduced oscillatory behavior compared to the P&O method (Babaa et al., 2014). Generally, MPPT uses both the perturb and observe and incremental conductance approaches. The P&O algorithm is simple and requires less hardware, but it incurs slightly high power loss as the output of the PV array oscillates around the MPP. On the other hand, the IncCond method provides better control and smaller oscillations, but it demands more hardware. Additionally, the IncCond method achieves its steady state value faster compared to the P&O method (Babaa et al., 2014).

2.9 Fuzzy Logic

Fuzzy logic is a versatile tool for establishing a connection between an input space and an output space. Fuzzy logic utilizes several basic fuzzy rules to make complex decisions even though it maps inputs to outputs. Fuzzy reasoning can be interpreted in two ways. In simple terms, Multi-valued logic is extended by fuzzy reasoning. It’s generates an output depending on the degree of membership, as opposed to discrete logic, which has discrete and exact points (i.e., either 1 or 0, HIGH or LOW). For example, rather than only having HIGH and LOW states, it will also include VERY HIGH, HIGH, LOW, and VERY LOW states, which represent the range of potential values between 0 and 1 (POPESCU & PİSTOL, 2021), (Makkar & Renu Makkar, 2018), (Chitra & Jackson, 2022).

2.9.1 Matlab fuzzy logic toolbox system

The MATLAB Fuzzy Logic Toolbox is a collection of tools for designing, assessing, and generating fuzzy logic algorithms. This toolbox contains utilities for developing and altering FIS, as well as fuzzy association and adaptive neuro-fuzzy training. A Simulink block is also included in the Fuzzy Logic Toolbox for modeling fuzzy systems inside a larger model of the entire dynamic environment (POPESCU & PİSTOL, 2021), (MathWorks, 2014). The Fuzzy Logic Toolbox has several essential characteristics include (MathWorks, 2014):

- A Fuzzy Logic Design program for developing a Fuzzy inference system and visualizing and evaluating results.
- Membership tools that generate a Fuzzy inference system.
- Support OR, AND, and NOT logic in user-defined procedures.
- Sugeno-type and Standard Madman-type FIS.
- Ability to incorporate an FIS model created with Simulink.

2.9.2 Fuzzy logic control system

Fuzzy logic models are designed and evaluated within the Simulink environment, which provides a simulation-based platform for developing and testing these controllers. The FLC systems in Simulink allow users to create, configure, and simulate the behavior of fuzzy logic-based control systems. This approach enables engineers and researchers to observe the performance of the fuzzy logic model, analyze its characteristics, and draw insights that can inform the final implementation. The simulation-based workflow facilitates the iterative development and refinement of fuzzy logic controllers before deploying them in real-world applications (Dumitrescu et al., 2021).

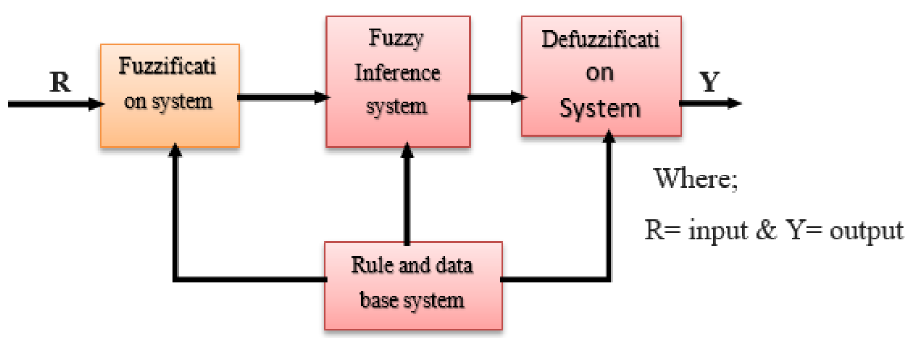

Figure 2. 9 Overall architecture of FLC (Dumitrescu et al., 2021)

In this structure, the technique of transforming inputs into fuzzy sets based on supplied rules is known as fuzzification. The fuzzy inference block makes inferences based on the provided rules, and the defuzzification process produces the outputs. Consequently, using the given rules, the inputs are mapped to the outputs. In other words, the fuzzification process converts crisp inputs into fuzzy sets. This is done by assigning membership values to the inputs based on the defined membership functions. The fuzzy inference block then applies the fuzzy regulations to the fuzzy inputs to create fuzzy outputs and also defuzzification process converts the fuzzy outputs into crisp outputs. This procedure makes it possible for fuzzy logic control to handle ambiguous or inaccurate inputs. Fuzzy logic controls are capable of representing an interval of anticipated results for an input using fuzzy sets. Because of this, they can make better judgments even in situations where the inputs are not entirely understood. A useful tool for designing and managing complicated systems is fuzzy logic controls. By using fuzzy logic, it is possible to create controllers that are more robust to uncertainty and that can make more informed decisions (Jäkel & Bretthauer, n.d.).

2.10 Hybrid Solar/Wind Microgrid System

A microgrid is a localized power system that functions independently of the main utility power grid. It includes distributed power sources such as solar panels and wind turbines, and energy storage devices such as batteries. The microgrid works grid connected in this thesis, which means it is connected to the broader electrical network. Renewable energy is provided in the DC buses. The DC bus delivers power directly to the DC electrical demand and the DC bus stores energy in batteries. A DC-to-AC inverter transforms the voltage from the DC bus into the AC bus, which is then provided to the AC load.

The energy management system of the microgrid intelligently regulates the flow of power within the system, optimizing power generation, battery charging, and energy storage to achieve different operational objectives such as cost reduction, power availability, and customer demand. The figure depicts the overall design of the microgrid system.

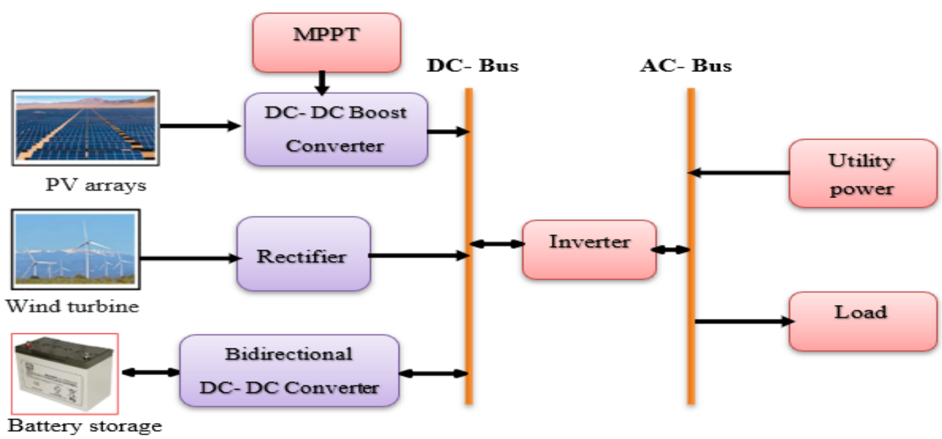

Figure 2. 10 Block diagram of the hybrid microgrid system

2.11 Related Works

Several scholars from throughout the world, including Ethiopia, have investigated energy management systems, particularly those based on sustainable energy resources. Numerous papers have published the findings of their study, some of which was examine as below.

Jain & Sen, 2020, The paper explores autonomous microgrid control using conventional and non-conventional energy sources and storage. It evaluates PID controllers' performance in load disturbance rejection and compares them to conventional methods. The analysis, using MATLAB/Simulink. I suggests fuzzy logic controllers are more suitable for managing complex systems, offering flexibility in handling uncertainties, and improving load disturbance rejection and energy management was also neeeded.

Saha et al., 2019, Authors of this paper focused on the design of a smart distributed stand-alone solar micro-grid system, specifically tailored for island regions where supplying electricity through conventional power systems was challenging and expensive. A gap of this paper only focused on using solar resources for island areas and doesn't consider other renewable resource to optimize energy.

Nebey, 2020, Authors of this paper investigate on the effectiveness of load sharing between solar, battery, and the national grid in Ethiopia's energy crisis. Gaps of this studied, it doesn't mention the integration with wind sources, which is another important renewable energy source for reducing dependency on the national grid.

Et al., 2018, The paper presents a PI-based control strategy for optimizing PV-Battery isolated DC systems in rural areas but notes challenges with non-linearities, variability, slow response, and parameter tuning. Fuzzy logic controllers offer better adaptability, handling of uncertainties, quicker response times, simplified tuning, and greater robustness, making them a superior alternative. Additionally, the paper lacks detailed discussion on energy management, which is crucial for maintaining power balance and optimizing performance.

Solomon Kirkos, 2014, Studied the economic performance of adopting a variety of independent PV/Wind hybrid systems to electrify Kutur hamlet in Ethiopia, which is 30 kilometers from the nearest national grid.

Fitwi, 2014, Investigation of the feasibility of a solar PV/Wind/Biogas hybrid system with the storage of batteries as a backup to electrify a community in Ethiopia's Adigrat province. Gap, the authors of this study do not consider energy management systems it was only optimize energy by homersoftware.

B. A. Taye, 2018, This study**,** investigates a DC microgrid system's viability for supplying electricity to small communities was illustrated by the authors through the creation of a simulation model using MATLAB/Simulink.

Borkute et al., n.d. , In this paper, explain how to use hybrid energy sources, such as diesel generators and solar electricity, to manage the power requirements of a DC microgrid. The objective is to boost the production of the microgrid dependably and efficiently. A gap in this study, a diesel generator was not cost-effective, so it makes sense to use unconventional resources and supplies.

Thirunavukkarasu & Sawle, 2020, This study proposes a method for designing, analyzing, and sizing a standalone hybrid power system consisting of photovoltaic (PV) panels, batteries, and diesel generators, using the HOMER software. A gap in this study, utilizing diesel generators was expensive and inefficient because, instead of utilizing diesel generators, it was preferable to optimize energy through the use of photovoltaic panels, wind turbines, and batteries as backup services recommended to maximize energy.

Teshale & Science, 2012, Author's of this paper to model and simulate a solar-wind-diesel hybrid energy system for irrigation. A gap in this research doesn't consider the environmental and economic damage caused by the diesel generator.

Pattanayak et al., 2015, Author's this papers investigate the study and design of a combination system consisting of solar and wind technologies for a limited region, with the combination system constructed using HOMER software.

Kefelegn, 2023, A feasibility assessment and optimal design of a hybrid renewable energy microgrid system for rural electrification in Ethiopia are proposed. The article explores various energy resource combinations, such as solar, hydro, energy storage devices, and diesel generators. Gaps, this paper does not consider the negative economic and environmental impact using of diesel generators, and mini-hydro energy is not available in all areas.

Roine et al., 2014, In this paper explore energy management in a microgrid using fuzzy logic rules to optimize load consumption during summer days. It aims to ensure grid reliability and minimize financial costs but the gap of this paper doesn't consider atmospheric pollution and battery storage and optimizes load consumption during summer days only.

Papageorgiou & Alexandridis, 2017, Author's this paper investigates the effective use of PI controllers for VSI control, it does not address the dynamic, nonlinear, and adaptive control needs of modern smart grids. So, for this, Fuzzy logic controllers present a promising alternative, offering enhanced adaptability, better handling of nonlinearities, and improved energy management of complex interactions and uncertainties.

Alhamrouni et al., 2019, Auhor's of this paper discusses the use of PID controllers in hybrid AC microgrids with Distributed Energy Resources (DERs). But, their was gaps in dealing with nonlinearity, uncertainty, and complex interactions between DERs and the main grid. So, Fuzzy logic control system address these issues by using linguistic rules and membership functions for control decisions, making them more effective in handling nonlinear systems and uncertainties. They are also more adaptable, able to handle complex interactions and are easier to maintain and modify than PID controllers. Therefore, fuzzy controllers are preferred for hybrid AC microgrids with DERs.

In general, a few papers that are relevant to this thesis work are evaluated. Additionally, an attempt was made to describe each study that was evaluated. The use of diesel generators was not cost-effective and had negative environmental impacts, but energy management strategies were not adequately discussed in the reviewed studies. Many studies utilized PI and PID controllers, but these struggled to effectively handle nonlinearity, uncertainty, and complex system interactions. The reviewed studies lacked the use of bidirectional converters, which are important for managing the flow of power between renewable sources, storage, and the load. Perturbation and observation (P&O) algorithms for maximum power point tracking (MPPT) were found to have limitations compared to the incremental conductance (IC) approach, which can more accurately track the maximum power point under varying conditions and has fewer oscillation. To address the limitations identified in the reviewed literature, this thesis work aims to provide a stable power system by selecting the most efficient combination of solar, wind, and battery storage, rather than relying on diesel generators and reduce dependence on the national grid. The thesis also intends to utilize the incremental conductance MPPT algorithm instead of the P&O approach. Additionally, the thesis incorporates fuzzy logic control instead of traditional PI or PID controllers to better manage the nonlinearity and uncertainty in the system.

Previous researcher also uses Homer software for modeling and optimizing the hybrid energy system design, and that the investigations were carried out in various locations with and without existing power infrastructure. This thesis was the design of a microgrid energy management system for Oda Bultum University using fuzzy logic control. The system was designed using MATLAB/Simulink software and energy was managed by using fuzzy logic.

CHAPTER THREE

3. MATERIALS AND METHODS

3.1 Overview of the Research Environment

Presently, microgrids have gained significant traction in developing countries, including Ethiopia, where they are used in a variety of settings, including industrial parks, universities, and residential areas to cater to the energy needs of local communities. The modeling of microgrid systems has been recognized for its reliability and has a positive impact on community well-being. This thesis designs a fuzzy logic-based microgrid energy management system for the University, which includes a library, data center, and registeral office.

3.2 Materials and Methods of the Study

3.2.1 Material and software tools

The material required preparation of the thesis includes the following:-

- Microsoft Word 2019: This word-processing software is used for writing, formatting, and structuring research documents.
- Microsoft Excel 2019: The spreadsheet application is employed for data analysis, organization, and visualization.
- MathType: This tool is utilized for the seamless integration and formatting of mathematical equations within the research documents.
- Mendeley: A reference management software that assists in organizing citations, generating bibliographies, and managing the research literature.
- MATLAB/Simulink: This computational software suite is leveraged for modeling, simulation, and analysis tasks associated with the research work.

3.2.2 Research methods

This thesis provides a survey of the literature on microgrid systems with energy management systems. Design, analysis, and mathematical formulation are based on data obtained from the Chiro station as well as NASA and PVGIS-SARAH2. The simulation results and conclusions was discussed. Generally, to accomplish the general and the specific object of study the following approaches and procedures were followed.

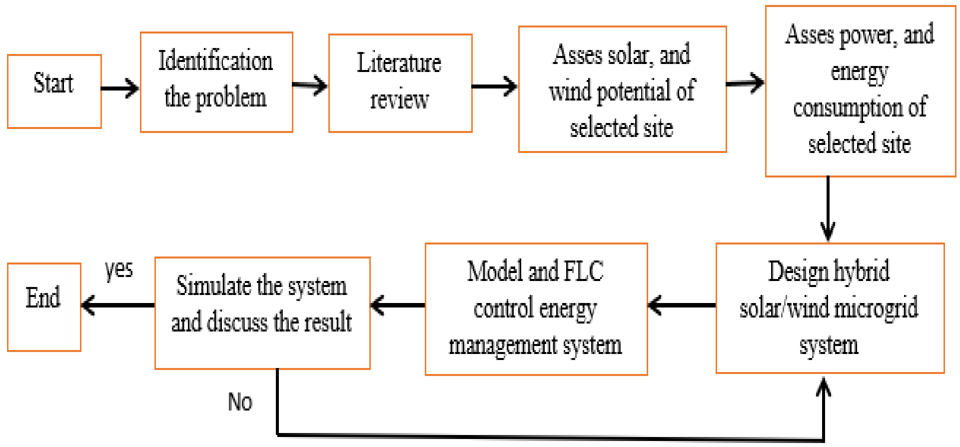

Figure 3. 1 Block diagram of research methodology

3.3 Techniques of Gathering and Analyzing Data

In this thesis, data taken from the chiro station, NASA, PVGIS-SARAH2, and Oda Bultum University are used to estimate the power needs of the library, data center, and registeral office. Following that, appropriate materials are chosen to satisfy these needs. The obtained data was utilized to develop hybrid solar/wind systems with battery backup for these sites, to build efficient and dependable systems. The main goal of this thesis was to design a microgrid energy management system using fuzzy logic control.

3.4 Gathering and Evaluation of Primary Data and Secondary Data

Primary data are those obtained directly from the source, without the use of any intermediaries. The primary data in this thesis was collected by a field survey and direct data collection from the library, data center, and registeral office at Oda Bultum University. This data includes a total load of each facility. Secondary data for this thesis was collected at various height levels in terms of wind direction, speed, and solar radiation provided data. The potential of Oda Bultum University's solar and wind resources was assessed based on these factors. Wind direction, average wind speed over 10-years, and 10-year average solar radiation and clarity index were all included in the data.

3.4.1 Solar radiation estimations

When designing a solar system, several factors play a critical role in maximizing its efficiency and performance. The sun's location in the sky is quite significant. Understanding the sun's angle of elevation and azimuth throughout the day, as well as seasonal variations, helps determine the optimal orientation and tilt angle of the collecting surface. By aligning the surface properly, it can receive the maximum amount of sunlight, increasing energy generation potential (Bunting, 2010).

The collecting surface's direction and slope are important factors to take into account. The slope, or tilt angle, determines how well the surface captures solar radiation. The ideal tilt angle varies depending on factors such as geographical location and the intended use of the system. The orientation, or azimuth angle, defines the direction the surface faces. By aligning it towards the path of the sun, the collecting surface can receive sunlight more effectively, enhancing energy output. Obstructions and reflections from neighboring structures can significantly impact the efficiency of a solar-based system. Shadows cast by nearby buildings or trees can reduce the amount of sunlight reaching the collecting surface. Reflections from surrounding structures can affect the quality and quantity of sunlight received. To maximize system performance and guarantee reliable energy generation, it is essential to assess and mitigate these barriers and reflections. The geometry characterizing the orientation of a collector and the sun's location in the sky is shown in Figure 3.2. Latitude and longitude coordinates are often used to describe a point's position on the surface of the Earth (Bunting, 2010).

Slope or Tilt Angle(β): The slope, also known as the tilt angle (β), is the angle formed between the collector's inclined planar surface and the horizontal. When sloping southward, it is +ve. The slope of a surface facing the equator is 0° to 90° ($0° < \beta < 90°$). Conversely, the slope of a surface pointing away from the equator varies from 90° to 180° ($90° < \beta < 180°$).

Surface azimuth angle(γ): It is the angle formed in the horizontal plane between the normal's horizontal projection on the inclined plane surface and the line due south. When calculating from south to west, it is +ve. In the northern hemisphere, γs is expressed in degrees and can take on values ranging from 0° to 180° for surfaces facing westward, 180° for surfaces facing straight north, and 0° for surfaces facing due south. γs has the same values in the southern hemisphere, but for a surface facing east, it may also vary from 0° to -180°. Since a horizontal surface is flat on the horizontal plane and lacks orientation, its γs value is always 0° (Bunting, 2010).

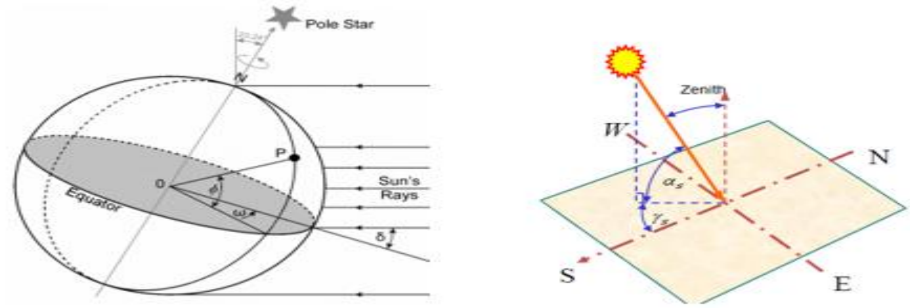

Figure 3. 2 Solar collector geometry and the sun's relative position to the earth (Bunting, 2010).

Latitude or Angle of Latitude (φ):- Is the angle formed by a line traced from the equatorial plane to the center of the earth from a point on its surface.

Decline angle (δ): The angle formed by a line drawn from the sun to the earth's center and the earth's equatorial plane is known as the declination angle (δ).

$$\delta = 23.45 \sin\left[\left(\frac{72}{73}\right)(284 + k_d)\right] \deg rees \quad (3.1)$$

Hour angle (ω): The angle between the observer's meridian and the sun-containing meridian. The hour angle is the angle at which the earth must rotate at any particular moment to line up the observer's meridian with the sun's rays.

Solar altitude angle (αs): The angle between the sun's core beam and its projection on the horizontal plane, which includes the observer.

Solar zenith angle (θz): This is the angle between the sun's rays and the horizontal plane's.

Solar azimuth angle (γs): Is the angle measured clockwise on the horizontal plane between due south and the sun's center ray projection

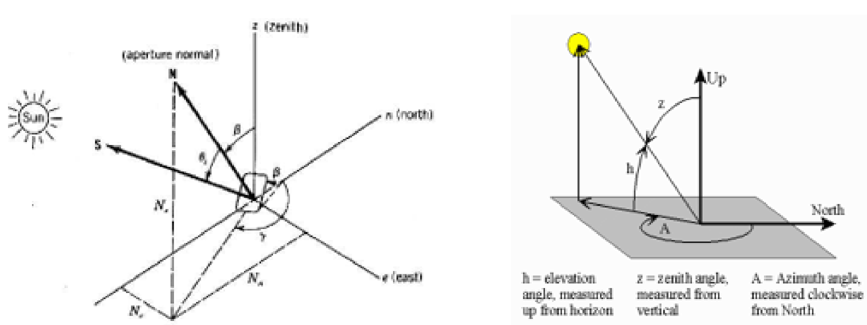

Figure 3. 3 Solar radiation geometry (Bunting, 2010).

Length of the solar day

At sunrise, the beams are parallel to the horizontal surface. The appropriate hour angle (ω_s) is;

$$\omega_s = cos^{-1}(-tan\varphi tan\delta) \tag{3.2}$$

The daylight hours (T_d) is given by,

$$T_d = \left(\frac{2}{15}\right) cos^{-1}(-tan\varphi tan\delta) \tag{3.3}$$

The whole daily extraterrestrial radiation (Ho) from sunrise to sunset can be calculated as Follows (Duffie & Beckman, 2006), (Kharseh, 2015);

$$H_o = I_{sc}\left(1 + 0.033\cos(\frac{72 * k_d}{73})\right)\left(\frac{\pi\omega_s}{180}\sin\varphi\sin\delta + \cos\delta\cos\varphi\sin\omega_s\right) \tag{3.4}$$

Where; $I_{sc} = \frac{24*3600*G_{sc}}{\pi}$

$G_{sc} = 1367\,\frac{W}{m^2}$

φ = Latitude of the location (9.0607º)

δ = Declination angle (º)

ω_s= Sunset hour angle

k_d= Day of the year

Ideally, it would take several years of observations of the specific irradiance on the planned collector plane to estimate the solar potential of a given area. However, such detailed data is often not readily available. As a result, alternative methods must be employed to estimate the required data using meteorological information. There are three primary approaches to estimating the necessary solar data. The first involves utilizing meteorological data collected directly from the site itself. The second approach involves utilizing data from a nearby location that experiences similar irradiance conditions. Lastly, an official solar atlas or database can be utilized for estimation purposes. One popular technique is to use sunlight duration data from the nearest meteorological station to determine the monthly average solar radiation. This data is then applied in an Angstrom-type equation, which provides an estimation of the solar radiation.

$$H = H_0\left(a + b\frac{n}{T_d}\right) \tag{3.5}$$

Where, H = Monthly average daily radiation on a horizontal surface (MJ/m2).

H_0 = Monthly average daily extraterrestrial radiation on a horizontal surface (MJ/m2).

T_d = The maximum possible daily hours of bright sunshine given by the equation.

n = Monthly average daily hours of bright sunshine a and b are regression coefficients which are a= 0.3 and b= 0.5.

To normalize the monthly mean of daily global solar radiation (H) was divided by the monthly mean of daily extraterrestrial solar radiation (H_0). The clearness index (CI) is defined as the ratio of measured or observed horizontal solar radiation (H) to expected horizontal /extraterrestrial solar radiation (H_0). The fraction of solar energy deflected by the sky reveals the availability of solar radiation and variations in atmospheric conditions in a certain location.

$$CI = \frac{H}{H_0} \tag{3.6}$$

Where; CI is the clearness index.

The following relation is used to get the value of H_0 and H in kWh (to convert MJ to kWh).

$$1J = 2.78*10^{-7} kWh \tag{3.7}$$

Table 3. 1 Suggest a month's average day and the monthly value of N (Ahmad & Tiwari, 2016).

Month	kd for Nth day of the month	For the average day of the month		
		Date(N)	kd, day of year	δ(degree)
Jan	N	17	17	-20.9
Feb	31+N	16	47	-13.0
Mar	59+N	16	75	-2.4
Apr	90+N	15	105	9.4
May	120+N	15	135	18.8
Jun	151+N	11	162	23.1
Jul	181+N	17	198	21.2
Aug	212+N	16	228	13.15
Sep	243+N	15	258	2.2
Oct	273+N	15	288	-9.6
Nov	304+N	14	318	-18.9
Dec	334+N	10	344	-23.0

3.4.2 Solar energy assessment of Oda Bultum University

Oda Bultum University is located in Chiro City, Oromia, Ethiopia at geographic coordinates of 9°0607' North latitude and 40°8665' East longitude. The university is situated at an elevation of 1,540.12 meters above sea level. To assess the potential of solar radiation in the chosen area, data is gathered from three main sources which are, Chiro station, PVGIS-SARAH2, and

NASA. The first approach involves utilizing data obtained from the chiro station. A mathematical analysis is conducted using the sunshine duration data collected over ten years, specifically from 2014 to 2023. To convert this sunshine duration data into actual solar radiation values, researchers use the Angstrom Radiation-Sunshine Relation. This is a mathematical formula that establishes a correlation between the measured sunshine duration and the corresponding solar radiation intensity. To calculate the solar radiation in kilowatt-hours per square meter per day (kWh/m^2/d) based on sunshine duration, regression coefficients α and β are utilized. In this case, the values for α and β are determined as 0.3 and 0.5, respectively. Upon applying these coefficients, the estimated annual average solar radiation obtained from Chiro station, NASA, and PVGIS-SARAH2 is found to be 6.234 kWh/m^2 d, 6.32kWh/m^2/d, and 5.72kWh/m^2/d while the data obtained from yields an average. Table 3.2 provides the sunshine duration data obtained from the Chiro station, while Table 3.3 shows the analysis of the monthly average solar radiation (in kWh/m^2/d) for the year 2022. These Tables serve as references for the study. To model the hybrid system, the calculated monthly average daily radiation summarized in Table 3.4 is employed. Table 3.4 and Table 3.5 present the monthly average solar radiation data for the Oda Bultum University area based on the data gathered from the Chiro station and NASA. Additionally, Table 3.6 contains the corresponding data obtained from PVGIS-SARAH2.

Table 3. 2 Sunshine duration (n) of the selected site from Chiro station.

Year	2014	2015	2016	2017	2018	2019	2020	2021	2022	2023	Mon Ave.
Jan	9.7	9.5	7.22	10.3	10.5	10.38	6.99	9.88	9.65	10.1	9.42
Feb	8.5	10.5	9.38	8.18	8.48	9.33	8.31	8.23	9.39	10.6	9.09
Mar	7.27	8.32	8.42	8.58	6.89	8.31	7.58	9.79	9.33	9.6	8.41
Apr	7.42	8.96	8.5	7.91	6.36	6.63	6.08	6.75	7.32	7.47	7.34
May	8.09	7.02	7.88	6.12	7.27	7.6	8,32	7.89	9.84	7.73	7.72
Jun	8.6	7.2	7.54	6.97	6.02	7.19	7.62	7.16	6.89	8.95	7.41
July	7.42	8.39	8	6.37	6.91	6.99	5.79	4.3	6.17	8.5	6.88
Aug	6.83	7.87	6.76	5.61	6.64	6.11	6.73	-----	6.8	8.47	6.87
Sept	6.96	7.03	6.71	5.59	7.65	6.1	5.97	------	6.59	6.61	6.58
Oct	8.05	8.45	8.51	8.5	8.13	6.92	9.13	9.25	7.62	----	8.28
Nov	8.97	8.92	8.19	9.61	7.85	7.82	8.97	9.58	8.79	-----	8.74
Dec	9.82	8.1	9.38	9.96	9.82	7.83	9.25	9.86	9.25	-----	9.25
Ann Ave.											**8.00**

Table 3. 3 Analysis of the monthly average solar radiation in (kWh/ m^2 /d) 2022 year.

Month	Nth day of the month	Date (N)	kd	δ	ω_s	Td	n	Ho(kWh/ m^2 /d)	n/ Td	H(kWh/ m^2 /d)
Jan	N	17	17	-20.9	86.5	11.53	9.65	9.01	0.84	6.48
Fer	31+N	16	47	-13.0	87.9	11.72	9.39	9.69	0.80	6.78
Mar	59+N	16	75	-2.4	89.6	11.95	9.33	10.29	0.78	7.1
April	90+N	15	105	9.4	91.5	12.2	7.32	10.52	0.6	6.31
May	120+N	15	135	18.8	93.1	12.41	9.84	10.37	0.79	7.21
June	151+N	11	162	23.1	93.8	12.52	6.89	10.2	0.55	5.86
July	181+N	17	198	21.2	93.5	12.47	6.17	10.23	0.49	5.58
Aug	212+N	16	228	13.2	92.1	12.28	6.8	10.39	0.55	5.97
Sept	243+N	15	258	2.2	90.5	12.05	6.59	10.32	0.55	5.93
Oct	273+N	15	288	-9.6	88.5	11.79	7.62	9.83	0.65	6.14
Nov	304+N	14	318	-18.9	86.7	11.58	8.79	9.14	0.76	6.22
Dec	334+N	10	344	-23.0	86.1	11.48	9.25	8.77	0.81	6.18

Table 3. 4 Solar radiation of selected site in kWh/ m^2 /d from chiro station 2014 to 2023 year

Date Month	kd, day of year	δ	ω_s	Td	n	Ho(kWh/ m^2 /d)	n/Td	H(kWh / m^2 /d)	Clear index
Jan,17	17	-20.9	86.51	11.53	9.42	9.01	0.82	6.397	0.71
Feb,16	47	-13	87.89	11.72	9.09	9.69	0.78	6.686	0.69
Mar,16	75	-2.4	89.62	11.95	8.41	10.29	0.7	6.689	0.65
Apr,15	105	9.4	91.51	12.2	7.34	10.52	0.6	6.312	0.60
May,15	135	18.8	93.11	12.41	7.72	10.37	0.62	6.326	0.61
Jun,11	162	23.1	93.89	12.52	7.41	10.2	0.59	6.069	0.595
July,17	198	21.2	93.54	12.47	6.88	10.23	0.55	5.882	0.575
Aug,16	228	13.2	92.13	12.28	6.87	10.39	0.56	6.026	0.58
Sept,15	258	2.2	90.47	12.05	6.58	10.32	0.546	5.913	0.573
Oct,15	288	-9.6	88.46	11.79	8.28	9.83	0.7	6.389	0.65
Nov,14	318	-18.9	86.7	11.58	8.74	9.14	0.7	5.941	0.65
Dec,10	344	-23	86.12	11.48	9.25	8.77	0.81	6.183	0.705
Ann Ave.								**6.234**	

Table 3. 5 Daily solar radiation(kWh/ m^2 /d) selected site 2013-2022 year (Source: NASA)

Year	2013	2014	2015	2016	2017	2018	2019	2020	2021	2022	Mon Ave.
Jan	6.08	6.31	6.28	5.33	6.81	6.33	6.67	5.37	6.53	5.94	6.165
Feb	6.95	6.18	7.08	6.81	6.16	6.58	6.71	6.39	6.3	6.76	6.592
Mar	6.57	6.46	7.04	7.05	7.09	6.38	7.08	6.62	7.44	7.05	6.878
Apr	6.71	6.43	7.13	5.64	6.91	6.21	6.5	6.14	6.67	6.73	6.507
May	6.5	6.5	6.39	6.7	6.3	6.54	6.71	6.91	6.72	7.14	6.641
Jun	6.34	6.74	6.2	6.46	6.68	6.14	6.44	6.55	6.65	6.4	6.46
Jul	5.37	6.18	6.59	5.99	6.04	6.11	5.99	5.69	5.03	5.53	5.852
Aug	5.9	6.12	6.45	6.39	5.72	6.01	5.85	6.02	6.29	5.88	6.063
Sep	6.25	5.86	6.21	6.23	5.95	6.64	5.98	6.04	6.13	6.18	6.147
Oct	6.19	6.3	6.45	6.61	6.32	6.28	6.06	6.7	6.26	6.19	6.336
Nov	5.9	6.18	6.09	6.04	6.37	5.9	5.73	6.27	6.39	6.16	6.103
Dec	6.27	6.23	5.65	6.21	6.43	6.11	5.74	6.11	6.2	5.85	6.08
Ann Ave.											**6.317**

Table 3. 6 Daily solar radiation (kWh/ m^2 /d) Selected site 2010-2020 year (Source: PVGIS)

Year	2010	2011	2012	2013	2014	2015	2016	2017	2018	2019	2020	Mon Ave.
Jan	5.91	5.91	6.21	5.59	6.06	6.26	4.87	6.78	6.4	6.66	4.99	5.97
Feb	4.5	6.62	7.01	6.77	5.64	7.02	6.59	5.46	6.1	6.37	6.02	6.19
Mar	5.35	6.45	7.08	5.72	5.69	6.39	6.19	6.7	5.4	6.58	6.11	6.15
Apr	5.82	6.49	5.58	5.36	6.32	6.66	5.1	6.13	5.19	6.07	5.26	5.82
May	5.18	5.12	5.67	5.48	5.53	5.13	5.68	5.19	5.86	5.62	5.58	5.46
Jun	6.16	6.15	5.48	5.58	6.1	5.66	6.02	6.16	5.7	5.22	5.7	5.81
July	5.32	5.94	5.55	5.14	5.79	6.45	5.49	5.94	5.77	5.66	5.05	5.64
Aug	5.55	5.29	5.61	5.22	5.49	5.85	5.81	5.2	5.42	5.11	5.34	5.44
Sep	5.34	5.3	5.43	5.47	5.12	5.78	5.48	5.2	5.83	5.16	5.04	5.38
Oct	5.61	6.22	6.04	5.18	5.17	5.45	4.88	5.54	5.48	5.28	5.96	5.53
Nov	5.39	5.02	5.73	4.98	5.29	5.25	5.42	5.83	5.31	4.72	5.62	5.32
Dec	5.66	6.18	5.76	6.34	5.87	5.36	5.89	6.48	6.07	5.35	5.8	5.89
Ann Ave.												**5.72**

Table 3.4 shows that the minimum average solar radiation is 5.88 kWh/ m^2 /d in July and the maximum average radiation is 6.69 kWh/ m^2 /d in February and March from the Chiro station. Table 3.5 shows that the minimum average solar radiation is 5.85 kWh/ m^2 /d in July and the maximum average radiation is 6.88 kWh/ m^2 /d in March from NASA. Table 3.6 indicates that the minimum average radiation was 5.32 kWh/ m^2 /day in November and the maximum average

radiation was 6.19 kWh/ m^2 /d in February from the PVGIS- SARAH2. Generally average solar radiation from Chiro station was 6.23kWh/ m^2 /d, the average solar radiation from NASA was 6.32kWh/ m^2 /d and the average solar radiation from PVGIS- SARAH2 was 5.72kWh/ m^2 /d.

3.4.3 Data compression of global solar radiation from Chiro station, NASA and PVGIS-SARAH2

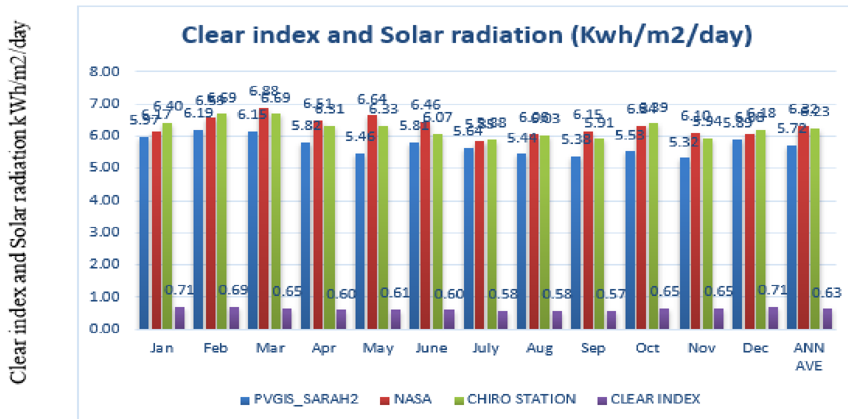

Figure 3. 4 Data comparison of Chiro station, NASA, and PVGIS

Figure 3.4 above makes it clear that the data obtained from the Chiro Station is trustworthy and shows adequate quantities of sun radiation. This is enough solar energy available to generate power for the university. So around Oda Bultum University receives adequate sunlight excellent for an energy-producing system. The selected site location is Oda Bultum University, which is seen in Figure 3.5.

Figure 3. 5 Google map of Oda Bultum University (Source: Google map)

3.5 Wind Energy Source

Wind source is the most essential factor of assessing a turbine's efficiency since the energy recovered from the flow of wind is related to the cube its speed. Wind, on the other hand, is variable, altering with the season, the time of day, height, and topography. Choosing a location with constant high winds and little obstacles provides for free wind passage to the turbine, optimizing power output. By analyzing historical wind data and selecting the appropriate turbine technology for the specific wind resource.

3.5.1 Measurement of wind speed

Wind speed is measured with a device known as an anemometer. There are several sorts of these devices. The most popular variety is a cup anemometer, which consists of 3 or 4 cups coupled to a revolving shaft. The anemometer converts the physical motion of the wind into a rotational speed that can be calibrated to measure the linear wind speed. The wind vane determines the direction the wind is blowing from. Together, the anemometer and wind vane, connected to a data logger, provide the necessary information to fully characterize the wind resources at a specific location.

To accurately assess wind energy potential, wind speed measurements must be taken at the proposed turbine hub height, avoiding interference from nearby obstacles. If the data is not collected at hub height (in this case 10 meters), it can be adjusted using the logarithmic or power law models. Higher hub heights capture stronger wind speeds, increasing power generation, but also raising construction and maintenance costs. Thus, there is a balance to be struck between the benefits of higher hubs and the associated economic impacts. Wind speed and height are by nature exactly proportionate. The wind speed increases at any height in tandem with height. As a result, the wind speed at any height may be calculated using the wind speed distribution or by applying the power law method.

3.5.2 Distributions of wind speed

Wind dispersion is expressed as a Weibull distribution across a certain period and place. For K=2, the wind distribution is given by the Weibull distribution, often known as the Raleigh distribution. It is described by the equation below.

$$w(v) = \frac{\pi v}{(2\breve{v})} exp[-\frac{\pi}{4}(\frac{v}{\breve{v}})^2] \tag{3.8}$$

$$prob(v \le V) = 1 - exp[-\frac{\pi}{4}(\frac{v}{\breve{v}})^2] \text{ and } prob(v \ge V) = exp[-\frac{\pi}{4}(\frac{v}{\breve{v}})^2] \quad (3.9)$$

Where $w(v)$; Weibull PDF of wind distribution

$\breve{v}$; Wind speed mean (m/s) and v = Wind speed at any given moment (m/s)

$prob(v \le V)$; Probability of sudden wind speed is smaller than V

$prob(v \ge V)$; Probability of sudden wind speed is smaller than V

3.5.3 Analyzing the potential of wind power of a selected site

Assessing the viability of a region for wind energy development requires gathering comprehensive data on the local wind characteristics. This includes collecting information on both the wind speed and the wind direction at the site. To conduct the assessment, it is necessary to install a network but it's time-consuming and expensive. Many wind researchers utilize previously recorded data sets, which can be obtained from various sources like NASA. In the case of Oda Bultum University, the average wind speed data was obtained from NASA and the Chiro station. It is common practice to measure wind speeds at an elevation of 10 meters above the ground level. This standard height is widely used as a reference point for collecting wind data. However, due to limitations in technology, sometimes only data at 2 meters is available. Fortunately, this 2-meter data can still be used to estimate wind speeds at other heights, including 10 meters and 35 meters, through mathematical calculations. In this case, have wind speed data collected every 15 minutes for nine years (2014-2023 except 2015) at a height of 2 meters for a specific site in Chiro. This data was obtained from the chiro station. The wind speed at 10 meters has been obtained from NASA using the site's geographic coordinates as the same location. By applying the power law equation to the 2-meter wind speed measurements, it is possible to derive an estimate of the wind speed at the 35-meter level. This calculation takes into account the relationship between wind speed and height above the ground. The power law equation incorporates factors such as surface roughness and atmospheric stability to determine the appropriate wind speed adjustment. This allows for a more accurate estimation of the wind speed at the desired 35-meter height, which is often more representative of the actual wind turbine hub height. It is typically expressed as follows;

$$V(h_{esti}) = V(h_{ref})(\frac{h_{esti}}{h_{ref}})^a \quad (3.10)$$

Where; $V(h_{ref})$ is wind speed measured at h_{ref}, $V(h_{esti})$ is wind speed at h_{esti} and a is the ground surface coefficient friction and $a = 0.4$ for tall buildings in city or university

Table 3. 7 Wind speed measured at 2 meters from the Chiro station

Year	2014 m/s	2016 m/s	2017 m/s	2018 m/s	2019 m/s	2020 m/s	2021 m/s	2022 m/s	2023 m/s	Monthly Ave.
Jan	1.63	1.53	1.37	1.23	1.66	1.26	1.04	1.35	1.29	1.37
Feb	1.77	1.54	1.68	1.29	1.72	1.62	1.31	1.22	1.4	1.51
March	1.56	1.75	2.21	1.48	1.79	1.82	1.38	1.45	1.05	1.61
April	1.45	1.21	1.99	1.33	1.92	1.75	1.21	1.51	1.07	1.49
May	1.59	1.42	1.59	1.54	1.77	1.09	1.01	1.84	0.97	1.42
June	1.9	2.51	2.13	2.33	2.13	2.12	2.03	2.43	1.51	2.12
July	2.89	2.39	3.66	3.14	3.18	2.32	2.41	2.14	2.37	2.72
Aug	2.05	1.89	3.22	2.55	2.14	2.21	1.39	1.57	1.81	2.09
Sept	1.35	1.14	1.46	1.23	1.72	1.04	1.18	1.09	1.35	1.28
Oct	1.1	1.43	1.24	1.46	1.16	1.07	1.11	1.17	---	1.22
Nov	1.42	1.67	1.27	1.23	1.39	1.14	0.96	1.01	---	1.26
Dec	1.45	1.37	1.32	1.42	1.33	1.21	1.06	1.31	----	1.31
Ann Ave.										**1.62**

Table 3. 8 Wind speed selected site at 10 meters (Source: NASA)

Year	2013 m/s	2014 m/s	2015 m/s	2016 m/s	2017 m/s	2018 m/s	2019 m/s	2020 m/s	2021 m/s	2022 m/s	Monthly average
Jan	2.54	2.46	3.13	2.59	2.87	3.17	2.73	2.7	2.66	2.71	2.76
Feb	2.63	2.41	2.77	2.96	2.61	2.63	2.56	2.87	2.94	3.19	2.76
Mar	3.31	2.78	3.02	2.72	2.74	2.45	2.88	2.7	2.85	2.91	2.84
Apr	2.62	3.02	2.97	3.18	2.62	2.66	2.51	2.32	2.71	3.11	2.77
May	4.23	3.02	3.32	2.99	2.88	3.12	3.2	2.62	2.93	3.82	3.21
Jun	4.62	4.2	3.58	4.27	4.57	4.06	3.68	3.57	4.96	4.62	4.21
Jul	4.2	4.12	4.43	3.61	4.05	4.48	3.84	3.7	3.98	3.84	4.03
Aug	3.37	3.23	4.3	3.8	3.96	3.82	3.4	3.39	3.55	3.73	3.66
Sep	3.26	3.1	3.36	3.75	3.04	3.56	3.42	3.22	3.45	3.42	3.36
Oct	2.5	2.24	2.61	2.62	2.51	2.64	2.2	2.43	2.38	2.65	2.48
Nov	1.91	2.36	2.77	2.42	2.52	2.06	2.23	2.64	2.42	2.42	2.38
Dec	2.23	2.62	2.76	2.93	2.87	2.65	2.54	2.76	2.13	2.47	2.6
Ann Ave.											**3.09**

Table 3. 9 Average wind speed and wind direction selected site (Source: NASA)

Month	Wind speed at 10m from NASA (m/s)	Wind speed at 50m from NASA (m/s)	Wind direction at 10m (degree)	Wind direction at 50m (degree)
Jan	2.76	3.85	20.29	25.87
Feb	2.76	3.83	41.26	47.24
March	2.84	4.03	90.43	92.43
April	2.77	4.03	116.89	119.43
May	3.21	4.63	131.36	133.06
June	4.21	5.69	148.52	148.1
July	4.03	5.48	165.31	163.97
Aug	3.66	5.25	163.29	161.09
Sept	3.36	5.01	143.59	143.27
Oct	2.48	3.61	68.63	73.17
Nov	2.38	3.46	43.17	47.40
Dec	2.6	3.70	22.09	27.26
Ann Ave.	**3.09**	**4.38**	------------	-----------

3.5.4 Measured and estimated average monthly wind speed (m/s) at different heights

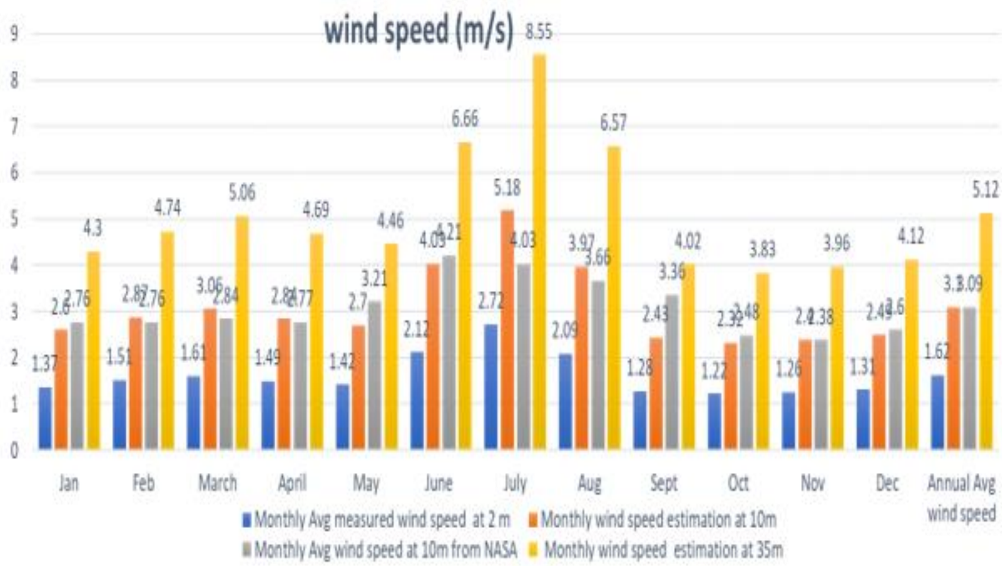

Figure 3. 6 Measured and estimated average monthly wind speed (m/s)

According to NASA's data, around Oda Bultum University's monthly average wind speed for 10 years ranges from 4.21m/s in June to 2.38m/s in November at a height of 10 meters, and the Estimated average wind speed is 8.55 m/s in July to 3.83 m/s in October at a height of 35 meter from estimated based measured data at 2 meter from Chiro station. The average wind speeds for the university are 3.09m/s at 10 meters from NASA and 5.12m/s at 35 meters estimated based on recorded data from Chiro station. Given that the selected site is characterized by different-height buildings, and construction around 15 meters from the university, a friction coefficient of 0.4 is utilized to account for the impact of wind flow surrounding the university. Using this coefficient, the wind speed at a height of 35 meters can be estimated, as mentioned earlier. Based on the collected wind speed data and the resulting estimation at 35 meters, it is inferred that the wind conditions in the area are conducive to the construction of a little wind turbine. This turbine is specifically intended to operate efficiently at lower wind speeds with the accessibility of wind speed data it is feasible to develop a small wind turbine capable of harnessing energy from these lower wind speeds.

3.6 Electrical Load Estimation and Energy Demand of the Three-Site

Estimating the electrical load was done for the three sites at Oda Bultum University which are, the library, data center, and registeral to size the solar, wind, and battery storage system. The predicted electrical loads are shown in Tables 3.10-3.12.

3.6.1 Electrical load estimation at the data center

The evaluation of the electrical load carried out at the data center is displayed in Table 3.10. electrical load ratings are based on their nameplates.

Table 3. 10 Data center electrical load estimation

Load	Rating (W)	Quantity	Adjusted Power in (W)	Operating time(Hrs)	Energy (kWh)
Dell Desktop	80	50	4000	8	32
Lighting (Fluorescent lamp)	15	100	1500	4	6
LCD projector (EPSON PowerLite)	292	1	292	2	0.584
Printer (HP laser jet enterprise M608dn)	340	2	680	1	0.68
Photocopier (Canon Image Runner advance C3525i III)	300	3	900	1	0.9
Network switches	370	2	740	24	17.76
Cooling and servers	500	2	1000	24	24
Air conditioner	1900	6	11400	2	22.8
Refrigerator	100	2	200	2	0.4
Total load			Pt1=20.7kW		Et1=103.12kWh

3.6.2 Electrical load estimation at the library

Table 3.11 displays the results of the electrical load calculation at the Library.

Table 3. 11 Library electrical load estimation has high-priority loads

Load	Rating (W)	Quantity	Adjusted Power in (W)	Operated time (hours)	Energy (kWh)
Dell Desktop	80	80	6400	20	128
Lighting (Fluorescent lamp)	15	150	2250	11	24.75
Printer (HP laser jet enterprise M608dn)	340	1	340	0.5	0.17
Photocopier (Canon Image Runer advance C3525i III)	300	1	300	1	0.3
Network switches	370	1	370	24	8.88
Cooling and servers	500	1	500	24	12
Air conditioner	1900	6	11400	3	22.8
Refrigerator	100	1	100	2	0.2
Total load			Pt= 21.66 kW		Et2=197 kWh

3.6.3 Electrical load estimation at the registeral office

Lastly, the electrical load calculation at the registeral office is shown in Table 3.12.

Table 3. 12 Registeral office electrical load estimation

Load	Rating (W)	Quantity	Adjusted Power in (W)	Operating time(Hrs)	Energy (kWh)
Dell Desktop	80	10	800	8	6.4
Lighting (Fluorescent lamp)	15	50	750	6	4.5
LCD projector (EPSON PowerLite)	292	1	292	2	0.584
Printer (HP laser jet enterorise M608dn)	340	3	1020	1	1.02
Photocopier (Canon Image Runner advance C3525i III)	300	3	900	1	0.9
Network switches	370	2	740	24	17.76
Cooling and servers	500	2	1000	24	24
Air conditioner	1900	3	5700	2	11.4
Refrigerator	100	1	100	2	0.2
Total load			Pt3=11.3 kW		Et3=66.7 6kWh

3.6.4 Total electrical load estimation of the selected site at Oda Bultum University

The electrical load estimate assesses the present electrical loads (kW) placed in all areas. So, Figure 3.7 Summarizes the electrical demand estimation across all areas selected.

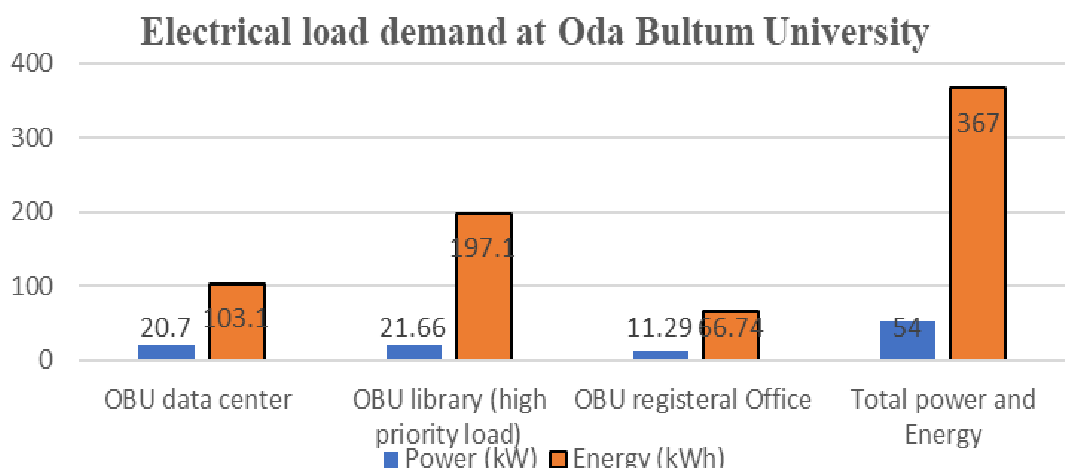

Figure 3. 7 Total electrical estimation load.

3.7 System Modelling of Energy Management System

The system uses wind, solar, and battery as backup power sources. A fuzzy inference system regulates how much energy is generated from these renewable energy sources. So, the system first determines whether the main utility power is available. If it is, the current load was supplied by the main utility power; otherwise, if the main utility power is unavailable, the fuzzy inference system intelligently decides which multiport switch to use to switch the required load demand output based on the load amount.

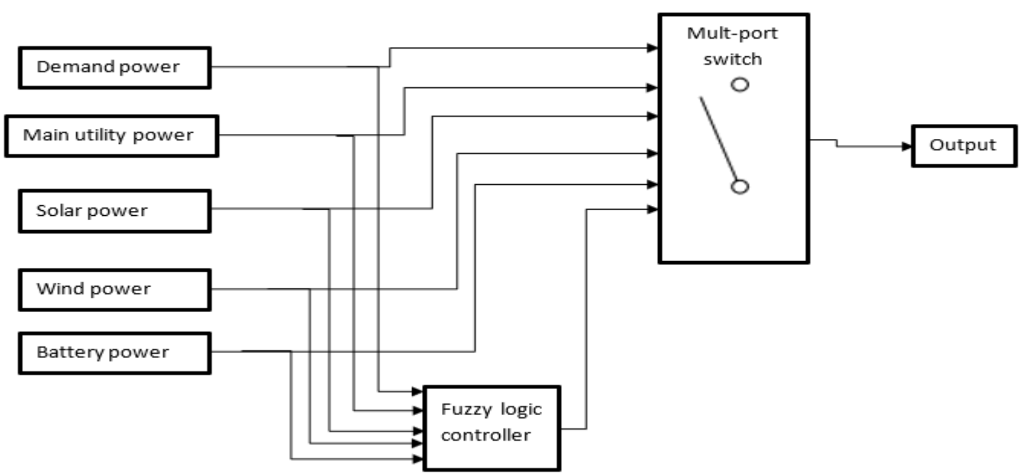

Figure 3. 8 Overall energy management system

3.8 Design and Sizing of Hybrid Solar/Wind System

This research focused on the design of a system that meets the daily energy demand assessment of a specific selected site at Oda Bultum University. The peak load, which represents the power required in a day is estimated to be 54kW. The total energy consumption for the specific selected site in the university is calculated to be 367 kWh/day. In this research paper, it is taken that 76% of the daily energy consumption for a specific selected site in the university, which amounts to approximately 278.92 kWh/day, was generated from solar panels. Additionally, 24% of the daily energy requirement for the same area, equivalent to 88.1 kWh/day, was supplied by wind energy. This assumption aims to achieve a balanced energy supply by using sustainable energy sources, like wind and solar energy. Solar panels contributed the majority share of the energy demand, while wind energy provided a significant portion as well.

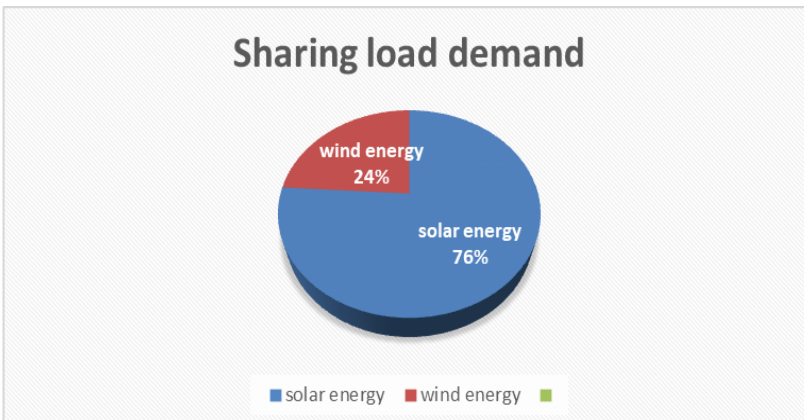

Figure 3. 9 Load demand sharing

3.8.1 Design of photovoltaic system

Before designing a PV system, find the suitable size for the photovoltaic array. It is necessary to calculate the average daily energy consumption in Watt-hours. This calculation involves assessing the power requirements of all appliances and determining the number of hours each appliance is utilized throughout the day. By evaluating the power consumption of various appliances and considering the duration of their usage, the total energy consumed by these appliances daily can be determined. This information is then expressed in terms of Watt-hours, which provides a measure of the energy consumed over 24 hours (Algburi & Saadoon Al-Juboori, 2017). Constant parameters taken for sizing the photovoltaic system are; Battery efficiency between 0.8 and 0.85, Temperature losses 0.9, Wire losses 0.9, Inverter efficiency 0.9, Depth of charge 0.85, Output efficiency 0.765, Combined efficiency 0.68.

Sizing of PV Array

Based on the above data, it is assumed that 76% of the daily energy consumption for a specific area selected in the university, which amounts to approximately 278.92 kWh/day, will be generated from solar panels. The selection of the PV module and electrical data specification used to design the PV array are listed in Table 3.13.

Table 3. 13 Electrical data specification of SPR-305E-WHT-D modules (SunPower, 2007).

Electrical data sheet/specifications	
Parameters	Specfication
Module name	SPR-305E-WHT-D
Nominal power(Pnom)	305 W
Power Tolerance	+/-5%
Panel efficiency	18.7%
Rated voltage (Vmp)	54.7V
Rated current (Imp)	5.58A
Open circuit Voltage (Voc)	64.2V
Short circuit current (Isc)	5.96A
Series fuse rate	15A
Coefficient of power temperature	-0.386%C
Coefficient of voltage temperature	-276.6mV%C
Coefficient of current temperature	3.5mA%C
Series solar cell	5
Parallel solar cell	46

So, to adjust the size PV array based on the above specification, the following steps can be followed:-

1. Calculate the total daily energy consumption in Watt-hours

Total energy requirement for the specific area selected in OBU =278.92kWh/day

$$E_{pvs} = \frac{Energy \text{ requirement}}{efficiencies} \tag{3.11}$$

$$= \frac{279.92kWh/day}{0.68} = 410kWh/day$$

2. Determine the total Watt-peak rating required for the PV modules.

The minimum average daily solar radiation (Smin) is calculated as 5.88kWh/ m^2 /day from the Chiro station.

$$P_{pvs} = \frac{E_{pvs}}{S_{min}} * 1000 w / m^2 \qquad (3.12)$$

$$= \frac{410 kWh / day}{5.88 kWh / m^2 / day} * 1000 w / m^2 = 70 kW$$

Where, E_{pvs} is total energy required from PV system.

P_{pvs} is total peak power required from PV system.

S_{min} is minimium solar radiation monthly occurs in the years

3. To calculate the total PV current, divide peak power by the system's stated DC voltage.

$$I_{pvs} = \frac{P_{pvs}}{V_{dc} system} \qquad (3.13)$$

$$= \frac{70000}{273} = 256.6 A$$

PV module for design are selected (SPR-305E-WHT-D)

4. The following formula may be used to determine the total number of modules connected in parallel and series.

$$N_s = \frac{System \text{ Vdc}}{Module \text{ rated Voltage}} = \frac{273}{54.7} = 5$$

$$N_p = \frac{Module \text{ rated Current}}{Rate\ current\ of\ one\ module} = \frac{256.6}{5.58} = 46$$

$$N_T = N_p * N_s = 46 * 5 = 230 \text{mod} ules$$

5. Determine parallel and series resistance for PV modules

$$R_s = \frac{V_{oc} - V_{mp}}{I_{mp}} = \frac{(64.2 - 54.7)V}{5.58 A} = 1.7025 \Omega$$

$$R_{par} = \frac{I_{sc} * R_s - V_{oc}}{I_{mp} - I_{sc}} = \frac{5.96 * 1.7025 - 64.2}{5.58 - 5.96} = 142.245 \Omega$$

The total area of solar panel design

When designing a photovoltaic system, it is crucial to determine the total covered by the solar panels. This involves considering the length and width of each solar module (SunPower, 2007). L=1559mm, W= 1046mm. The total area of solar panels is; N_T*L*W=230*1559*1046 = 375.064m^2. The area that the solar modules cover is critical for improving the system's power production and guaranteeing optimal use of available space. By properly determining the structure and positioning of solar panels to maximize solar energy capture and overall system performance.

3.8.2 Design of wind energy generator system

Table 3. 14 Specifications of a 15KW wind turbine (Maegaard & Krenz, 2016)

Model	H15 class II
Rated power	15000W
Starting wind speed	3.5m/s
Rated wind speed	12m/s
Security wind speed	20.5m/s
Rated DC voltage	220/240/380V
Rotor diameter	11000mm
Protection	Electromagnetic torque control and electricity brake
Type	3phase permanent magnetism synchronization generator
Number of blades	3
Blade material	GPR composite
Head weight (kg)	1450kg

The wind turbine's electrical energy outputs can be stated as follows;

$$P_{Wout} = \frac{1}{2} A v_o^3 C_p \eta_{overall} \tag{3.14}$$

The power rating and rotor size for wind energy generation can be determined using the following parameters and calculations; Coefficient of Performance (Cp) = 0.4, Density of air (ρ) = 1.225 kg/m^3, Wind speed at 35m height = 5.12 m/s, Capacity factor = 0.30, Transmission losses = 0.90, Generator losses = 0.90, Energy from wind (Ew) = 88.1kWh/day. Power density is power available in wind per unit area.

$$\frac{P_{Wout}}{A} = \frac{1}{2} v_o^3 C_p \eta_{overall} \tag{3.15}$$

Calculate the actual power density

$$Actual\ power\ density = 0.5*1.225*5.12^3*0.9*0.9*0.41 = 27.3W/m^2$$

Calculate the daily energy density

$$Daily\ energy\ density = 27.293W/m^2*24hours = 0.655kWh/m^2$$

Calculate the real daily energy density

$$Real\ daily\ energy\ density = 0.655kWh/m^2*0.30 = 0.1965kWh/m^2$$

Calculate the rotor-swept area

$$Rotor\ swept\ area(A) = \frac{E_{wind}}{real\ daily\ energydensity} = \frac{88.1}{0.1965} = 450m^2$$

$$Rotor\ swept\ area\ (A) = \frac{\pi}{4}*D^2$$

The radius of the rotor blade covered area, (R)= 11.9m.

Calculate the Actual power rating of the turbine

$$Actual\ power\ rating\ of\ turbine = 27.293W/m^2*450m^2 = 12.3kW$$

Therefore, based on the given situation, a wind turbine with a rated power of around 15 kW was suitable to achieve the desired energy output.

3.8.3 Sizing of battery bank system

To size of the battery bank system depends on the capacity of each battery (CB) in the bank. To satisfy the chosen battery voltage rating and system requirements, the battery bank is made up of batteries that are connected in series and parallel. By dividing the battery bank's ampere-hour capacity by the capacity of a single chosen battery, the total number of batteries may be calculated. The maximum permitted depth of discharge that battery manufacturers specify should be taken into account. The percentage of the battery's overall capacity that has been used is indicated by the DOD. The maximum permitted DOD for most batteries is approximately 85%. The select a battery capacity that is at least three times larger than the calculated value due to climate conditions, such as those experienced in solar PV and low wind speed cases. In thesis research Battery bank was used for only high-priority loads (E_{hl}) is 200kWh/day.

$$CB_n = \frac{E_{hl}}{V_{n,bat}} = \frac{200kWh}{400} = 500Ah/day$$

$$CB = \frac{CB_n}{DOD * efficiency} = \frac{500}{0.765 * 0.85} = 768.935Ah/day$$

$\mathrm{So, CB} * 3 = 768.935 * 3 = 2307\mathrm{Ah/day},$ for lead acid batteries.

Therefore, the Capacity of the battery taken = 2307Ah/day, and also selected battery Ah rating = 200Ah with nominal 12V. To determine how many batteries must be connected in series and parallel to provide the system with the necessary Ampere-hours (Ah).

$$B_{pb} = \frac{CB}{Battery\ \mathrm{rating}\ Ah} = \frac{2307}{200} = 12\ batteries$$

$$B_{ps} = \frac{V_{n,batt}}{V_{batt}} = \frac{400}{12} = 34\ batteries$$

$$B_t = B_{ps} * B_{pb} = 12 * 34 = 408\ batteries$$

3.8.4 Charge controller size

In a solar PV system, the charge controller's main job is to manage the current flow. The maximum current produced by the solar array and the maximum load current should both be able to be handled by an efficient charge controller.

$$\text{Total Current control rating (I)} = \text{Short circuit current * Safety factor * parallel modules}$$

$$= Isc * Fsafe * Np = 5.58 * 1.3 * 46 = 333.684A$$

As a result of calculating the current controller rating, a 12V, 60Ah MPPT-based solar charge controller has been selected based on the provided specifications.

$$Number\ \text{of charger controller} = \frac{Total\ current\ controller\ rating}{Current\ controller\ rating}$$

$$= \frac{333.684}{60} = 5.56 \simeq 6$$

Adding a safety factor serves the objective of guaranting that the charge controller can manage the maximum current generated by the solar array, even if it exceeds the set value. It allows for the accommodation of increased load currents resulting from the addition of equipment or potential system expansions. In essence, the safety factor provides a margin of safety and flexibility for the system's operation, allowing for a slight expansion in capacity if needed.

3.8.5 Inverter sizing

An inverter's capacity is defined by the power needs of the AC load to which it will be connected, including the need for surge power. It chooses an inverter that is 25-30% larger than the total power of the loads to accommodate any unexpected spikes in power demand. The maximum AC load is 85kW and the inverter rating would be calculated as follows; 85kW*1.3=110.5kW. In this particular case, the available inverter sizes were 100kW, 150kW, 200kWand 250kW. The chosen inverter size for this thesis was 150kW, which met the power requirements of the AC load. Additionally, it was noted that the full load efficiency of the selected inverter was greater than 90%.

3.9 Modeling of Hybrid Solar/Wind System

3.9.1 Wind turbine modeling

Wind has kinetic energy due to its motion. This kinetic energy can be given by;

$$KE = \frac{1}{2} m v_o^2 \tag{3.16}$$

The power P(W) that the wind can provide is equal to the mass of moving air times the kinetic energy rate.

$$P_W = \frac{1}{2}\frac{dm}{dt} v_o^2 = \frac{1}{2}(\rho A v_o) v_o^2 = \frac{1}{2}\rho A v_o^3 \tag{3.17}$$

$$= \frac{1}{2}\rho A v_0^3 C_p(\beta, \lambda) \tag{3.18}$$

Where; m= Mass of air passing through an area A per unit time

v_o = Speed of wind or average speed at exit and entry of rotor blades turbine

A = The rotor swept area

ρ = The air density which is equal to $1.225 kg/m^3$

C_p = Performance coefficient of wind turbine (0.41)

λ= Tip speed ration

β = Blade pitch angle(degree)

The following is the typical function that defines the power coefficient in relation to the blade pitch angle and tip speed ratio (Aslam Husain & Tariq, 2014);

$$C_p(\beta,\lambda) = c_1(c_2 \frac{1}{\lambda i} - c_3\beta - c_4\beta^x - c_6)e^{-c_5/\lambda i} \quad (3.19)$$

Because this function is dependent on the kind of wind turbine rotor, different turbine designs may have different coefficients $c_1 - c_6$ and x. The coefficient values are; $c_1 = 0.5, c_2 = 116, c_3 = 0.4, c_4 = 0, c_5 = 5\ and\ c_6 = 21$ and the parameter is further specified as follows:

$$\frac{1}{\lambda i} = \frac{1}{\lambda + 0.08\beta} - \frac{0.035}{1+\beta^3} \quad (3.20)$$

Tip speed ratio of the wind turbine.

$$\lambda = \frac{Angular\ \text{speed of turbine}(\omega)}{wind\ speed(V_w)} \quad (3.21)$$

According to (Aslam Husain & Tariq, 2014), the ratio of the power taken from the wind to the turbine rotor speed (V_W) in rad/s yields the quantity of aerodynamic torque (T_W) in N-m.

$$T_w = \frac{P_w}{V_w} \quad (3.22)$$

Due to the absence of a gearbox, the mechanical torque applied to the generator is equal to the aerodynamic torque (Aslam Husain & Tariq, 2014). Based on the wind turbine system's equation, a mathematical model of a wind turbine is created using the MATLAB/Simulink program. This model incorporates various parameters such as wind speed, performance coefficient of wind turbine, radius, pitch angle (beta), and angular rotor speed. These parameters are obtained from the calculation.

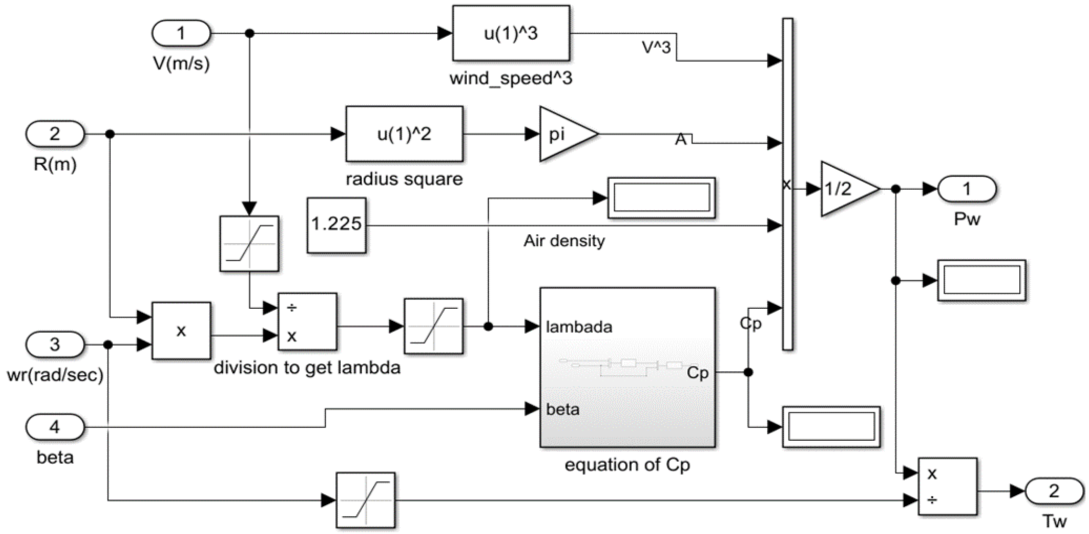

Figure 3. 10 Mathematical modeling of a wind turbine by Simulink

3.9.2 Modeling of photovoltaic module

A Photovoltaic (PV) model is a mathematical representation or simulation of a photovoltaic system that describes the behavior and performance of the system under various conditions. It can be used to predict the electrical output of the PV array, assess its performance, and optimize its design. One commonly used model for a PV array is the equivalent circuit model, which represents the electrical characteristics of the entire PV module or array. When solar cells are connected in series to generate maximum output voltage or in parallel to increase current within an array, the equivalent circuit model expands upon the basic single-diode model of a PV cell to account for the behavior of multiple cells connected in series and parallel.

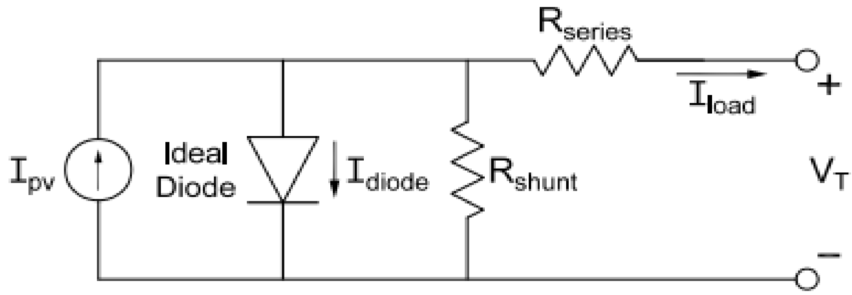

Figure 3. 11 Photovoltaic system equivalent circuit (Mallon et al., 2017).

Mathematical modeling of photovoltaic model is derived from the above equivalent circuit;

Photovoltaic module's photocurrent;

$$I_{pv} = \frac{S}{S_{on}}(I_{scr} + K_i(T - T_{ref})) \tag{3.23}$$

PV module's reverse saturation current;

$$I_{rsc} = \frac{I_{scr}}{\exp\left(\frac{q*E_{go}}{N_s*B_k*A*T}\right) - 1} \tag{3.24}$$

PV module saturation current;

$$I_S = I_{rsc}[\frac{T}{T_{ref}}]^3 exp[\frac{q*E_{g0}}{A*B_k}(\frac{1}{T_{ref}} - \frac{1}{T})] \tag{3.25}$$

PV module parallel current:-

$$I_{par} = \frac{\frac{N_p}{N_s}*V_L + I_L*R_s}{R_{par}} \tag{3.26}$$

PV module's output current;

$$I_L = N_p I_{pv} - N_p I_s \left\{ \exp\left[\frac{q*(\frac{V_L}{N_s}*V_L + I_L*\frac{R_s}{N_p})}{N_s*A*B_k*T} \right] - 1 \right\} \tag{3.27}$$

where, $\mathrm{I_{par}}$ = Parallel current (amperes)

$\mathrm{I_{pv}}$ = Photo current

$\mathrm{I_{rsc}}$ = Reverse saturation current

$\mathrm{I_L}$ = Output current

V_L = Output voltage

V_{oc} = open circuit voltage

$\mathrm{I_{rsc}}$ = Reverse saturation current (amperes)

A = Diode ideality factor (1 for an ideal diode)

q = Elementary charge ($1.6 * 10^{-19}$C)

B_k = Boltzmann's constant $\left(1.38 * 10^{-23}\ {}^{j}/_{k}\right)$

T_{ref} = Nominal temperature, at 25°C, *which equal to* 298 *kelvin*

N_s = The number of cells connected in series

N_p = The number of cells connected in parallel

$\mathrm{E_{go}}$ = Band energy gap (1.11)

S = The actual irradiance in W/m^2

S_{on} = The irradiance at the nominal condition

The modeling of a photovoltaic (PV) array is carried out using MATLAB/Simulink blocks, utilizing the mathematical equation of the solar system. To accurately represent the PV array, various parameters are required, which are obtained from the PV array's specifications. These parameters include Voc (open-circuit voltage), Iscr (short-circuit current), Ns (number of series-connected cells), Np (number of parallel-connected cell strings), Ki (temperature coefficient), Tref (reference temperature), and S (solar irradiance). These parameters are essential for accurately modeling the behavior and characteristics of the PV array in the simulation environment.

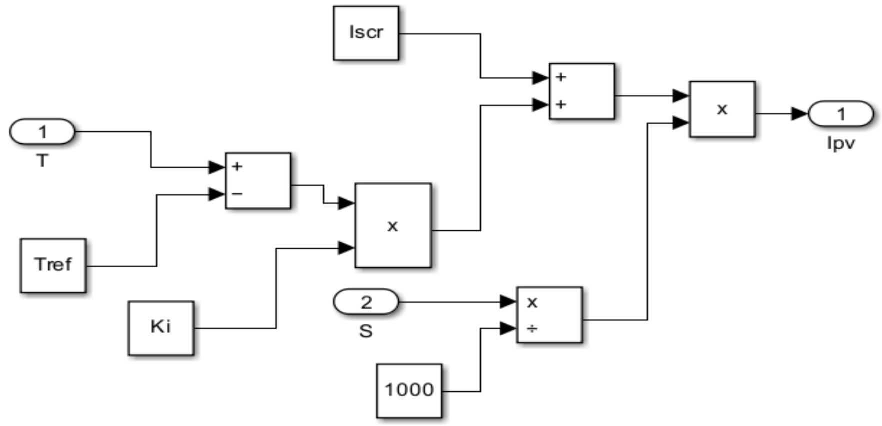

Figure 3. 12 Photo current of the PV

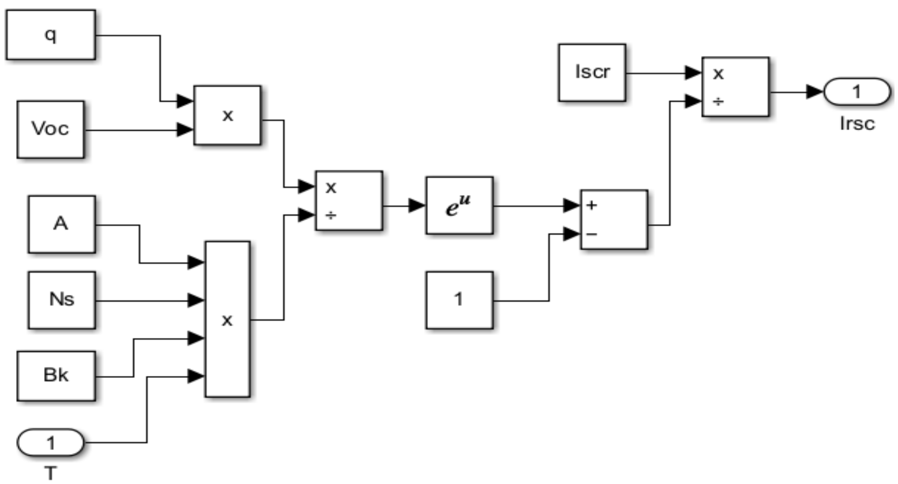

Figure 3. 13 Reverse saturation current of the PV

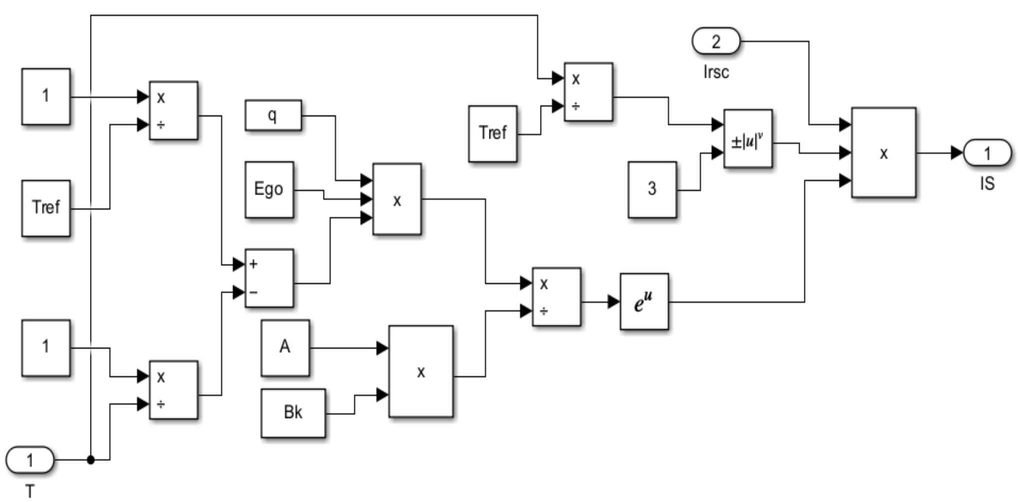

Figure 3. 14 Saturation current of the PV

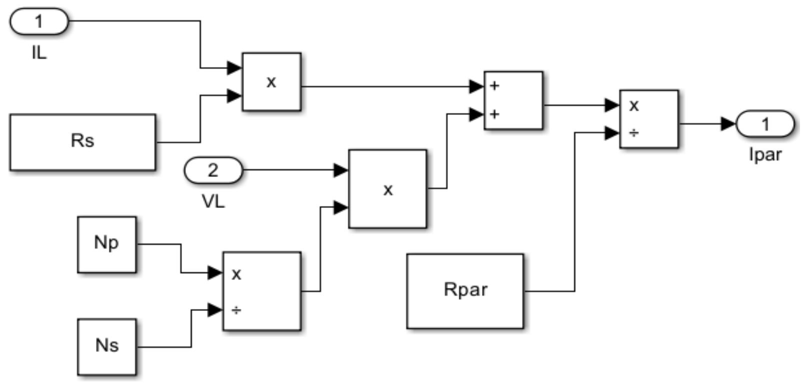

Figure 3. 15 Shunt current of the PV

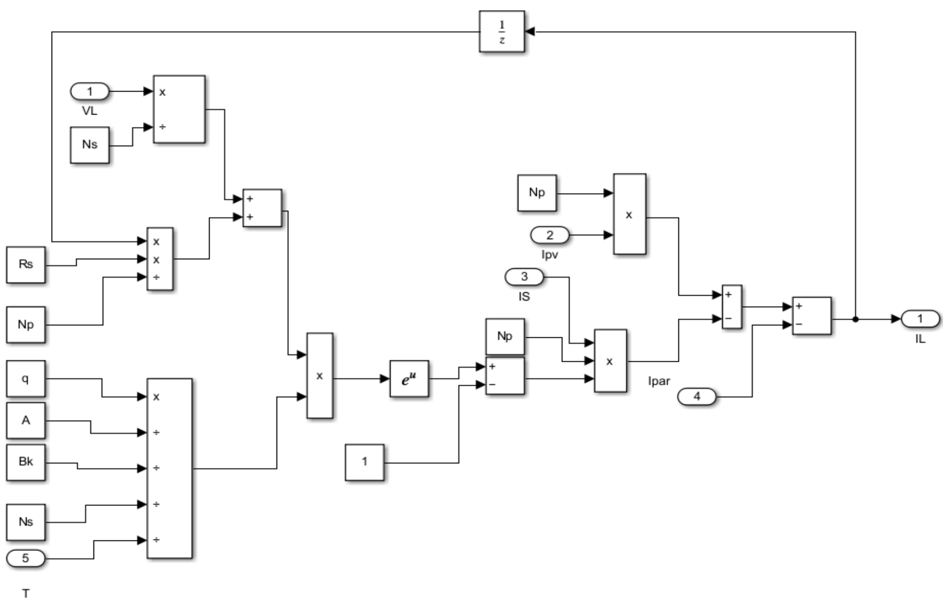

Figure 3. 16 Output current of PV

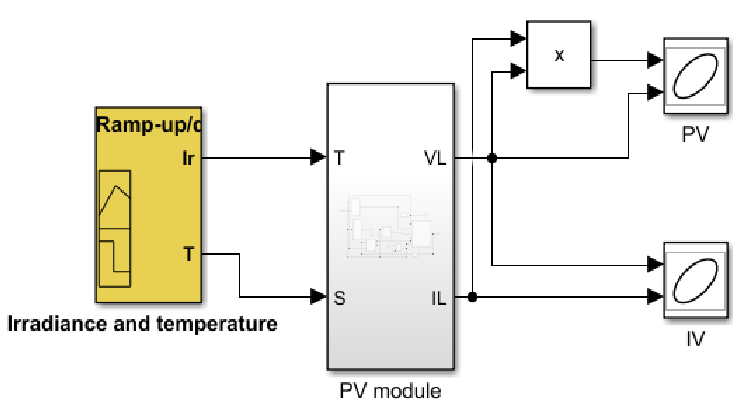

Figure 3. 17 PV module system

The relationship between the current and power output of photovoltaic modules can be determined under varying temperatures and irradiance levels. Keeping the temperature fixed at 25°C, the characteristic I-V and P-V curves are plotted for irradiance values of 400 W/m^2 , 600 W/m^2 , 800 W/m^2 , and 1000 W/m^2 , respectively. The curves exhibit a non-linear behavior, as they are dependent on both temperature and solar radiation. As the irradiance increases, the current increases at a greater rate than the voltage, and the maximum power point also increases accordingly, as illustrated in Figure 3.18

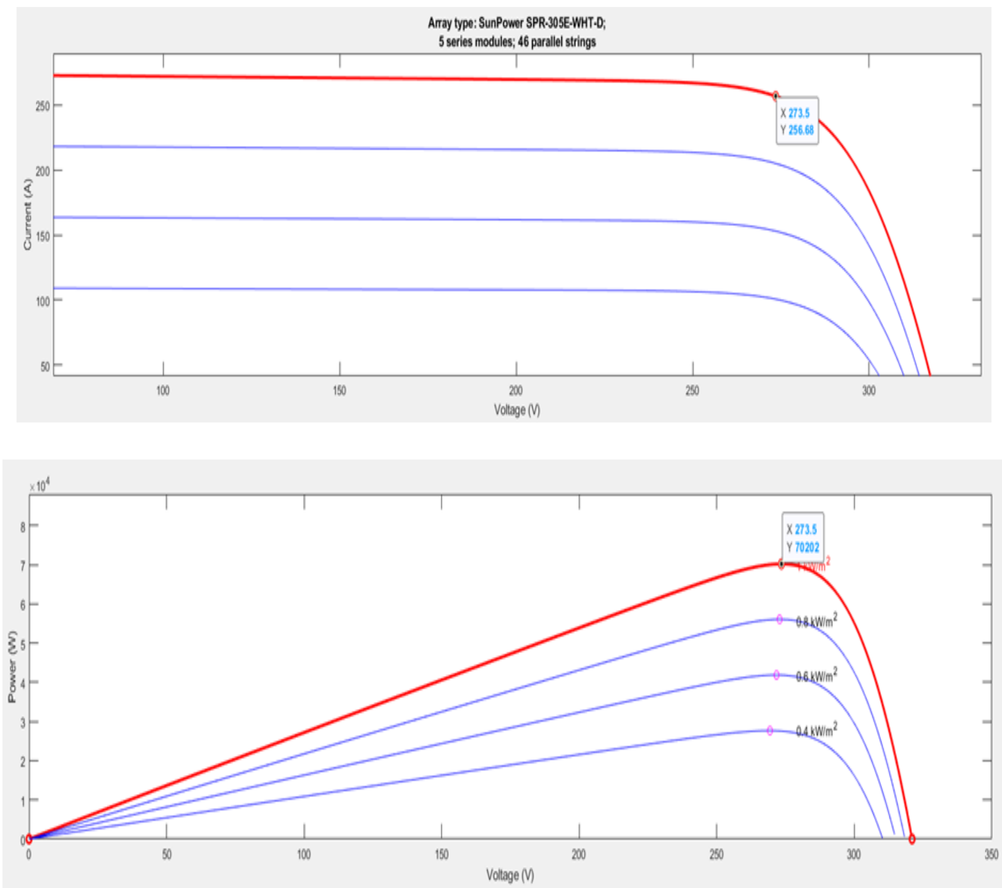

Figure 3. 18 I-V and P-V characteristics curve of the solar power generation system

3.9.3 Incremental conductance MPPT control

The incremental conductance algorithm adjusts the PV panel's terminal Voltage to track the maximum power point. When the IC algorithm determines the MPP has been reached, it stops adjusting the operating point. The MPP is found by comparing the instantaneous conductance (I/V) to incremental conductance (dI/dV). This is possible because the power derivative (dP/dV) is negative when the operating point is to the right of the MPP, and positive when it's to the left. Where the value of dP/dV=0 then the algorithm knows that the extreme power point is reached. This method is better than other tracking methods and this method is used when the solar radiation is varies frequently (Babaa et al., 2014). For the IC flow chart shown in Figure 3.19, the following equations are applicable.

$$\frac{dP}{dV} = 0 \text{ for V=V}_{mp} \tag{3.28}$$

$$\frac{dI}{dV} = -\frac{I}{V} \tag{3.29}$$

$$\frac{dP}{dV} < 0 \text{ for V > V}_{mp} \tag{3.30}$$

The fact that; P =IV, the derivative of the products yields

$$\frac{dP}{dV} = \frac{dIV}{dV} = I\frac{dV}{dV} + V\frac{dI}{dV} = \text{I+V}\frac{dI}{dV} \tag{3.31}$$

As, $\frac{\mathrm{dP}}{\mathrm{dV}} = 0$ for $\mathrm{V} = \mathrm{V_{mp}}$;

$$\frac{dI}{dV} = -\frac{I}{V} \tag{3.32}$$

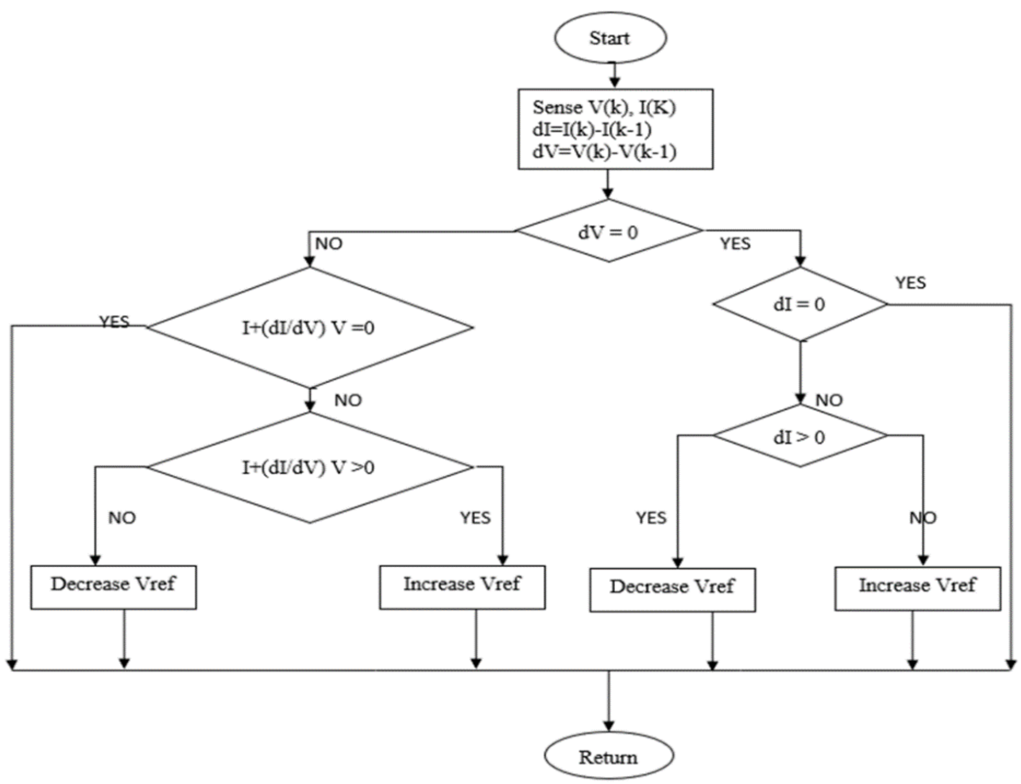

Figure 3. 19 Flow chart for incremental conductance method (Babaa et al., 2014).

The MPPT algorithm shown in Figure 3.19 produces a duty cycle as its output, which is then delivered to the boost converter switch to maximize solar panel energy and maintain a steady voltage even in the face of fluctuating solar radiation. The maximal power point is reached when the value of dP/dV equals zero. So in this thesis used, incremental conductance and integeral regulator MPPT controller.

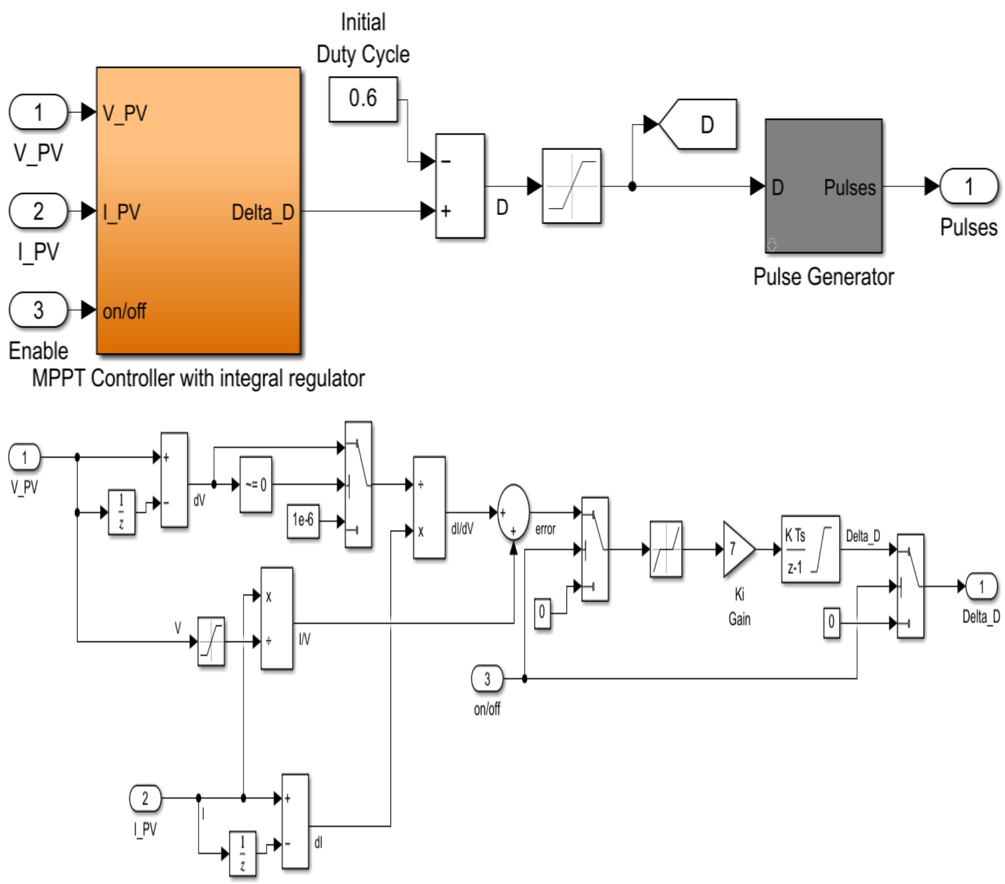

Figure 3. 20 Simulink model of Inc cond with integral regulator MPPT control

3.9.4 DC-DC boost converter modeling

Three different types of DC-DC converters exist: the Buck, Boost, and Buck-Boost converters. Periodically opening and shutting a switch is how these converters work. Whereas the Boost converter raises the input voltage, the Buck converter lowers it. The Buck-Boost converter has the unique capability to either increase or decrease the input voltage, but with a reversal in polarity. The mathematical equations governing the parameters of the Boost, Buck, and Buck-Boost converters were derived using the following equations.

$$V_{out} = \frac{V_{in}}{1-D} \quad (3.33)$$

$$V_{out} = V_{in} * D \quad (3.34)$$

$$V_{out} = \frac{-(V_{in} * D)}{1-D} \quad (3.35)$$

This thesis analyzes the boost converter and its design parameters. The input DC voltage (Vin) is defined as 250V-300V and the output DC voltage (Vout) is 400V, with a DC link voltage ripple of 1% and a current ripple of 5%. This ripple value is critical for maintaining a consistent output voltage. The converter's switching frequency is set at 5kHz. This frequency governs how often the switch in the converter circuit opens and shuts. By carefully setting the switching frequency, the converter can convert the input voltage to the required output voltage effectively. So to determine the parameter of the boost converter as follows.

$$I_{dcboost} = \frac{P}{V_{dcboost}} = \frac{70000}{400} = 175A$$

$$\Delta I = I_r * I_{dcboost} * \frac{V_{dcboost}}{V_{in}} = 0.05*175*1.465 = 12.82A$$

$$\Delta V = V_r * V_{dcboost} = 0.01*400 = 4V$$

$$L_{mn} = \frac{V_{in}(V_{dcboost} - V_{in})}{\Delta I * f_s * V_{dcboost}} = \frac{273(400-273)}{12.82*5000*400} = 1.34mH$$

$$C_{mn} = \frac{I_{dcboost}(V_{dcboost} - V_{in})}{\Delta V * f_s * V_{dcboost}} = \frac{175(400-273)}{4*5000*400} = 2.78mF$$

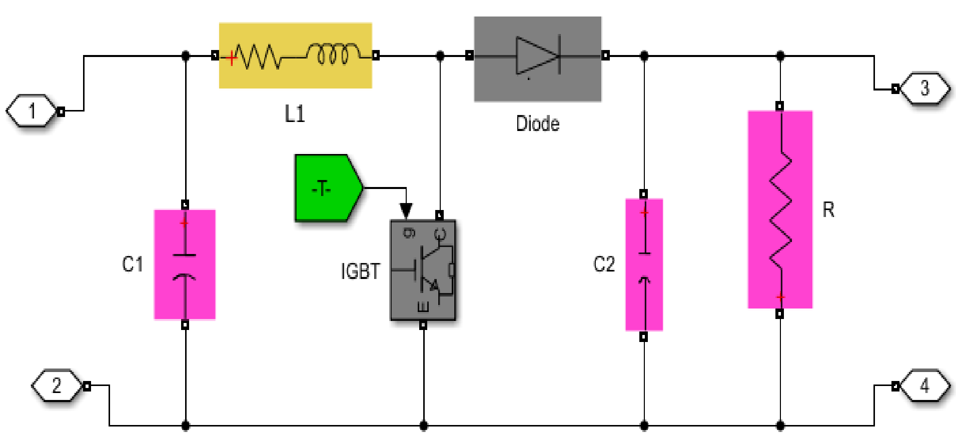

Figure 2. 21 Models of the boost converter

3.9.5 Bidirectional DC-DC converter modeling

A bidirectional DC-DC converter with battery discharging and charging capabilities transfers power between a DC voltage source (such as a battery) and an external load or another voltage source. It allows bidirectional power flow, meaning it can charge the battery from an external source (photovoltaic and wind energy source) or discharge the battery to power the load. A bidirectional DC-DC converter with battery charging and discharging typically operates in two modes.

Charging mode/buck mode

During the charging phase, the bidirectional DC-DC converter transfers power from an external voltage source (photovoltaic and wind energy source) to the battery for charging. The input voltage (Vin) is typically higher than the battery voltage (Vbat). In this mode, the converter operates as a buck converter.

Discharging mode/boost mode

The bidirectional DC-DC converter moves electricity from the battery to the load or another voltage source while it is in the discharging mode. The battery voltage (Vbat) is typically higher than the output voltage (Vout). In this mode of operation, the converter functions as a boost converter. In these two modes, the photovoltaic and wind systems transfer energy to the battery and vice versa. A bidirectional DC-DC converter consists of two switches with an inductor and capacitor. The switch is responsible for monitoring the charging and discharging modes. The following equations are used to determine the parameters of the bidirectional DC-DC converter.

$$D = \frac{V_{out}}{V_{out} + V_{in}} = \frac{433}{433 + 400} = 0.52$$

$$I_{oconv} = \frac{I_{dcboost(1-D_2)}}{D_1} = \frac{175(1-0.52)}{0.52} = 161.54A,\ where\ D = D_1 = D_2$$

To determine the critical value of inductance and capacitance safety converters are considered, so the ripple current rate is 200% and ripple voltage 5% as switch frequency 10kHz.

$$L_{ctrl} = (\frac{V_{dcboost}}{I_r * f_s * I_{dcboost}}) * D = \frac{400}{200*10000*175} * 0.52 = 59.43\mu H$$

$$L_{ctrl} = \frac{D}{V_r * f_s * R} = \frac{0.52}{0.05*10000*0.312} = 3.33mF$$

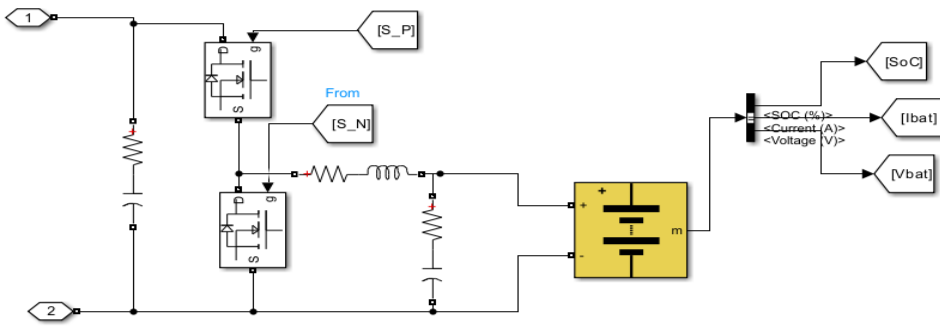

Figure 3. 22 Models of battery with bidirectional DC to DC converter

3.9.6 Filter design

In grid synchronization, the presence of ripple current from a PWM inverter requires an LC filter to counteract the effect. The inductor is designed to account for the current ripple magnitude, which can range from 10% to 15% of the rated value. Selecting an inductor value corresponding to 10% of the rated current is a common approach for effective performance (Kahlane et al., 2014).

$$L_f = \frac{Vdc}{16 * f_{sw} * \Delta I_{1\max}} = \frac{400}{16*10000*30} = 83\mu H$$

Where, $\Delta I_{lmax} = \frac{10\%*S*\sqrt{2}}{V_{inv}}$, L_f, is filter inductor, L_g, grid side inductor V_{dc} is dc link voltage, f_{sw} is switch frequency, ΔI_{lmax} is 10% ripple current, C_f is filter capacitor, f_{nom}, nominal frequency, ω_n is natural frequency and S is active rate power.

The inductance of the grid side is as follows;

$$L_g = r * L_f = 0.6*83\mu H = 50\mu H$$

A capacitor is designed based on the reactive power absorbed at the rated conditions. Reactive power (Q) absorbed by the capacitor is limited to 5% of active rated power(S) (Kahlane et al., 2014).

$$C_f = \frac{0.05*S}{V_o *2* pi * f_{nom}} = 84.5\mu F$$

The resonant frequency for the LCL (inductor-capacitor-inductor) filter can be calculated using the following formula (Kahlane et al., 2014)

$$f_{res} = \frac{\pi}{2}\sqrt{\frac{L_f + L_g}{L_f * L_g * C_f}} = 19.5kHz$$

The natural frequency of the LCL filter;

$$\omega_n = \frac{1}{\sqrt{L_f * C_f}} = \frac{1}{\sqrt{83*10^{-6}*84.5*10^{-6}}} = 11.94 krad/s$$

3.9.7 Three-phase voltage source inverter

A three-phase voltage inverter is primarily used to convert a constant DC voltage into an AC voltage with variable amplitude and frequency.

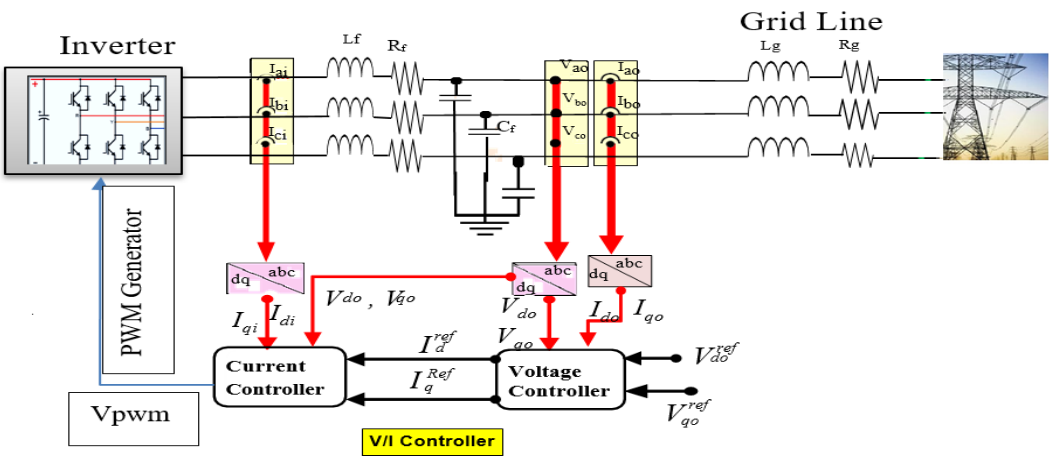

Figure 3. 23 Three-phase voltage and current control diagram(Kumar & Bhimasingu, 2021).

Phase locked loop

The voltage and current controller employs a phase-locked loop to determine the phase angle and frequency of the input voltage waveform, which are then used to perform the abc-to-dq transformation and obtain the q-axis and d-axis voltage components Vqo and Vdo (Kahlane et al., 2014).

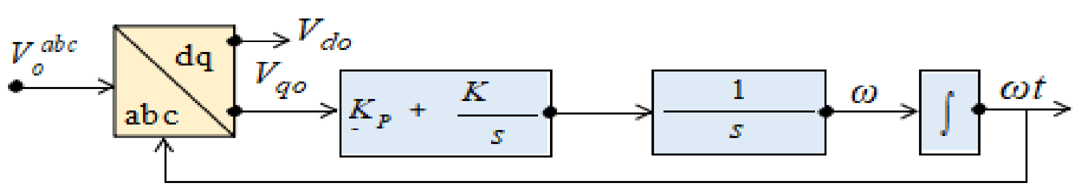

Figure 3. 24 Phase locked loop model (Kumar & Bhimasingu, 2021).

$$V_0^a = V_o sin(\omega t) \quad (3.36)$$

$$V_0^b = V_o sin(\omega t - \frac{2\pi}{3}) \quad (3.37)$$

$$V_0^c = V_o sin(\omega t + \frac{2\pi}{3}) \quad (3.38)$$

The abc to dq transform is defined as below;

$$\begin{bmatrix} V_{do} \\ V_{qo} \end{bmatrix} = \frac{2}{3}\begin{bmatrix} \cos(\theta) & \cos(\theta - \frac{2\pi}{3}) & \cos(\theta + \frac{2\pi}{3}) \\ -\sin(\theta) & -\sin(\theta - \frac{2\pi}{3}) & -\sin(\theta + \frac{2\pi}{3}) \\ 0 & & 0 \\ & & \end{bmatrix}\begin{bmatrix} V_o^a \\ V_o^b \\ V_o^c \end{bmatrix} \tag{3.39}$$

To design the control loop $\zeta = 0.707$ and natural frequency 100Hz taken.

$$Ki = \frac{\omega_n^2}{V_o} = \frac{(2*3.14*100)^2}{400} = 985.96 \tag{3.40}$$

$$Ki = \frac{\omega_n^2}{V_o} = \frac{(2*3.14*100)^2}{400} = 985.96$$

$$Kp = \frac{2\zeta * \omega_n}{V_o} = \frac{2*0.707*2*3.148100}{400} = 2.22$$

Operation of the voltage and current controller

The voltage and current controller generates a three-phase reference signal using the inverse Park that control the power converter's switches, ultimately regulating the converter's electronics output (Kumar & Bhimasingu, 2021).

A voltage control module is;

$$I_d^{ref} = I_{d0} + (V_{do}{}^{ref} - V_{d0})(\frac{Kp_V s + Ki_V}{s}) - V_{q0} C_f \omega \tag{3.41}$$

$$I_q^{ref} = I_{q0} + (V_{qo}{}^{ref} - V_{q0})(\frac{Kp_V s + Ki_V}{s}) + V_{d0} C_f \omega \tag{3.42}$$

A current control module is;

$$E_d = V_{d0} + I_{di} R_f + (I_d{}^{ref} - I_{di})(\frac{Kp_a s + Ki_a}{s}) - I_{qi} L_f \omega \tag{3.43}$$

$$E_q = V_{q0} + I_{qi} R_f + (I_q{}^{ref} - I_{qi})(\frac{Kp_a s + Ki_a}{s}) - I_{di} L_f \omega \tag{3.44}$$

$$V_{PWM} = \begin{bmatrix} V_a^{ref} \\ V_b^{ref} \\ V_c^{ref} \end{bmatrix} = \begin{bmatrix} \sin(\omega t) & \cos(\omega t) & 1 \\ \sin(\omega t - 120^o) & \cos(\omega t - 120^o) & 1 \\ \sin(\omega t + 120^o) & \cos(\omega t + 120^o) & 1 \end{bmatrix}\begin{bmatrix} E_d \\ E_q \\ E_0 \end{bmatrix} \tag{3.45}$$

Where, Vpwm is reference input voltage to PWM generator

Iqref, Idref, Vdoref and Vqoref is reference input current to current and voltage controller

Iqo, Ido, Vqo and Vdo is dq equivalent of Ioabc, Voabc

Idi, Iqi is dq component of Iiabc

Ed, Eq is dq component of Vpwm

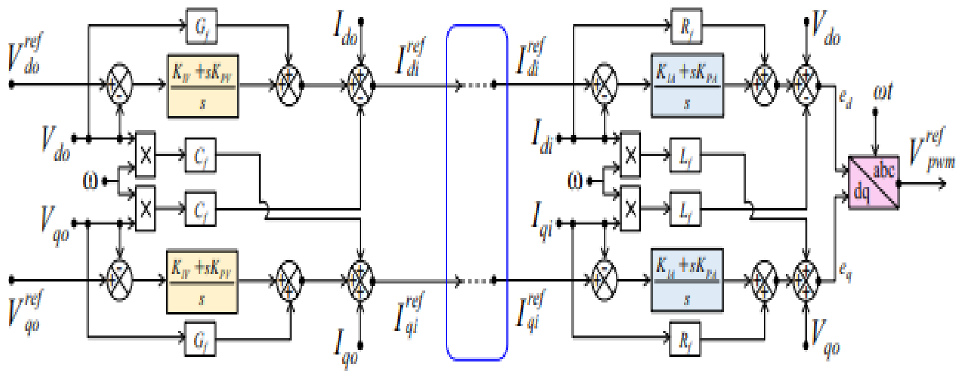

Figure 3. 25 Diagram of voltage and current control(Kumar & Bhimasingu, 2021).

$$I_{il}(s) = I_{og}(s) + I_c(s) \text{ and } I_c(s) = I_{il}(s) - I_{og}(s) \quad (3.46)$$

$$V_{og}(s) = \frac{V_{\sin}(s) - (R_f + sL_f) I_{og}(s)}{1 + sC_f(sL_f + R_f)} \quad (3.47)$$

$$I_{il}(s) = I_{og}(s) + I_c(s) \text{ and } I_c(s) = I_{il}(s) - I_{og}(s) \quad (3.48)$$

$$V_{og}(s) = \frac{V_{\sin}(s) - (R_f + sL_f) I_{og}(s)}{1 + sC_f(sL_f + R_f)} \quad (3.49)$$

Where, Vsin, Vog, Vil is single phase equivalent of Vsinabc, Vogabc, Vilabc.

Iil, Iog,Ic is single phase equivalent of Iilabc, Iogabc, Icabc.

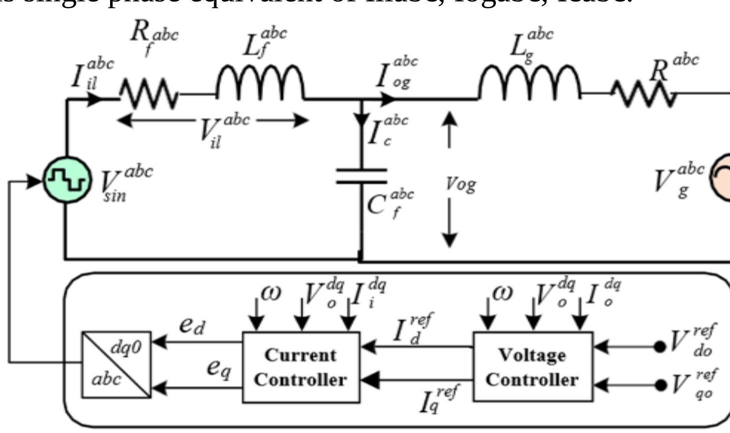

Figure 3. 26 Equivalent Circuit of voltage and current control (Kumar & Bhimasingu, 2021).

Internal current and outer voltage controller transfer function

The current controllers the system current drawn by modeling the inner current control loop and ignoring the voltage control outer loop(Kumar & Bhimasingu, 2021). Conversely, the voltage controller regulates the voltage by modeling the control loop and disregarding the inner control loop.

$$\frac{I_{il}(s)}{I_{il}^{ref}(s)} = \frac{Kp_a s + Ki_a}{s^2 L_f + s(R_f + Kp_a) + Ki_a} \tag{3.50}$$

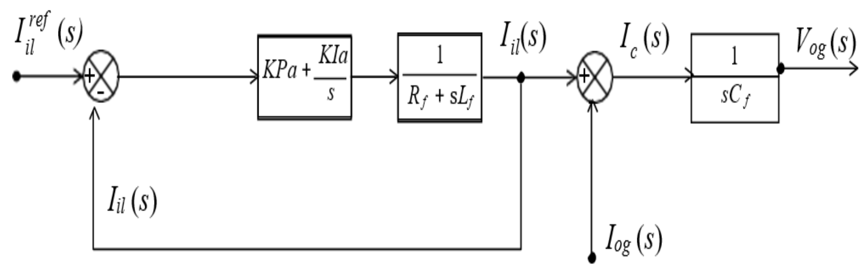

Figure 3. 27 Diagram of the current control (Kumar & Bhimasingu, 2021).

To calculate the values of the proportional gain and the integral gain for the current controller. The characteristic equation of the closed-loop current control system with second-order dynamic characteristic equation is;

$$s^2 + 2\zeta\omega_n s + \omega_n^2 = 0 \tag{3.51}$$

$$s^2 L_f + s(R_f + Kp_a) + Ki_a = 0 \tag{3.52}$$

Choose a desired damping ratio (ζ) for the closed-loop system was 0.707 for a good dynamic response and transient stability.

Proportional gain Kp_acalculated as;

$$Kp_a = 2\zeta\omega_n - R_f = 1*0.707*11.94*10^3 - 1.2 = 8.44*10^3$$

The integral gain Ki_a Calculated as;

$$Ki_a = \omega_n^2 * L_f = (11.94*10^3)^2 * 83*10^{-6} = 11.83*10^3$$

$$\frac{V_{og}(s)}{V_o^{ref}(s)} = \frac{sKp_v + Ki_v}{s^2 C_f + Kp_v s + Ki_v} \tag{3.53}$$

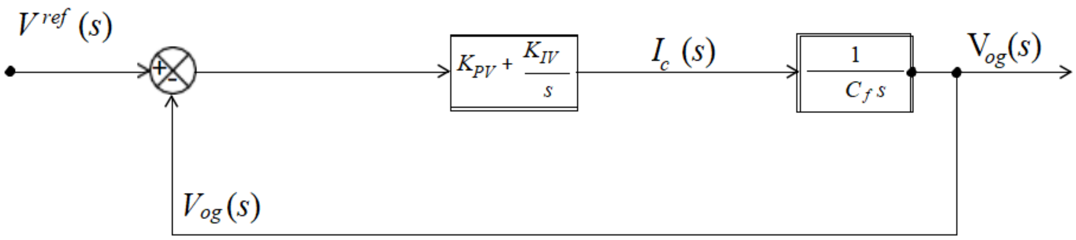

Figure 3. 28 Diagram of voltage control (Kumar & Bhimasingu, 2021).

The values of the proportional gain Kp_v and the integral gain Ki_v for the voltage controller.

$$s^2C_f + sKp_v + Ki_v = 0 \tag{3.54}$$

$$s^2 + 2\zeta\omega_n s + \omega_n{}^2 = 0 \tag{3.55}$$

Calculate the integral gain Ki_v;

$$Ki_v = \omega_n^2 * C_f = (11.94*10^3)^2 * 84.5*10^{-6} = 12*10^3$$

Calculate the proportional gain Kp_v;

$$Kp_v = 2*\zeta*\omega_n = 2*0.707*11.94*10^3 = 16.9*10^3$$

Table 3. 15 Parameter of inverter and filter design components.

Parameter	Value
Voltage inverter output(Vo)	400V
Rated power(S)	85kW
DC voltage(Vdc)	400V
Nominal frequency(fnom)	50Hz
Switching frequency (fsw)	10000Hz
Resistance (r)	1.2 ohm
Conductance(Gf)	0
Damping ratio	0.707
Primary Voltage	33kV
Secondary Voltage	0.400kV
Nominal power (KVA)	112.5KVA

3.10 Transformer

The transformer consists of two wound coils, which are the primary coil and the secondary coil. The primary coil receives the input electrical power from the AC source. The secondary coil takes the energy from the primary coil and delivers it to the load. Transformers can be designed to either increase or decrease the voltage level between the primary and secondary sides. A step-up transformer increases the voltage while decreasing the current, while a step-down transformer decreases the voltage and increases the current. The ratio of the number of turns in the secondary winding to the number of turns in the primary winding determines whether the transformer is step-up or step-down.

$$V_{t1}I_{t1} = V_{t2}I_{t2} \tag{3.57}$$

$$I_{t1} = \left(\frac{N_{t1}}{N_{t2}}\right)I_{t2} \tag{3.58}$$

Where, V_{t1}, V_{t2}, I_{t2} and I_{t2} primary and secondary voltage and current.

N_{t1} and N_{t1} primary turn and secondary

CHAPTER 4

4. RESULT AND DISCUSSION

4.1 Introduction

This section discusses the simulation and analysis of an energy management system that combines solar and wind power generation systems. The solar power system was designed and tested through simulations to have an expected output of approximately 70 kilowatts (kW). The wind turbine system was designed to generate 15 kW of power. Additionally, a battery system with a capacity of 10 kW was included as a backup power source, intended to be used only for the most critical electrical loads when needed. An intelligent fuzzy logic system was designed and simulated to efficiently manage the energy management system. Overall, the simulations showed that the combination of power components and the fuzzy logic controls could be successfully integrated to form an effective energy management system.

4.2 Solar Power Generation System

The solar panels are expected to generate approximately 70KW of power. Considering the solar radiation statistics of the selected site, a solar panel with an open circuit voltage of 64.2V and a short circuit current of 5.96A is selected to achieve this goal. These technical specifications indicate that to produce about 70KW of power, a solar panel with 5 solar cells linked in series and 46 solar cells connected in parallel is required. Solar panels at university are subject to varying levels of solar radiation of 1000W, at other times, the solar radiation levels drop to around 800W and there are also occasions when solar panels receive a relatively lower solar radiation of 600W.

4.2.1 Results of a solar panel simulation

The Matlab simulation results indicate that the designed solar array generates an approximate power output of 70 kW. The output DC current was measured at 176.3A, with a DC voltage of 400V. After the boost conversion stage, the system delivers a DC output power of 70 kW. The solar array's power generation capability was a significant achievement, demonstrating the effectiveness of the system's design and implementation. The boost conversion stage plays a crucial role in optimizing the power output, ensuring that the 70 kW of DC power was available for further distribution or applications.

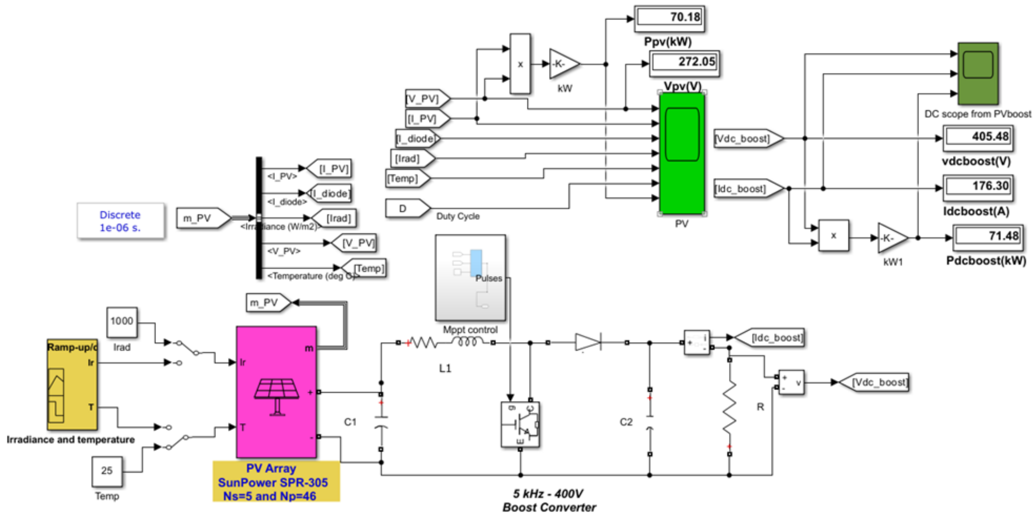

Figure 4. 1 Solar power generation Simulink simulation

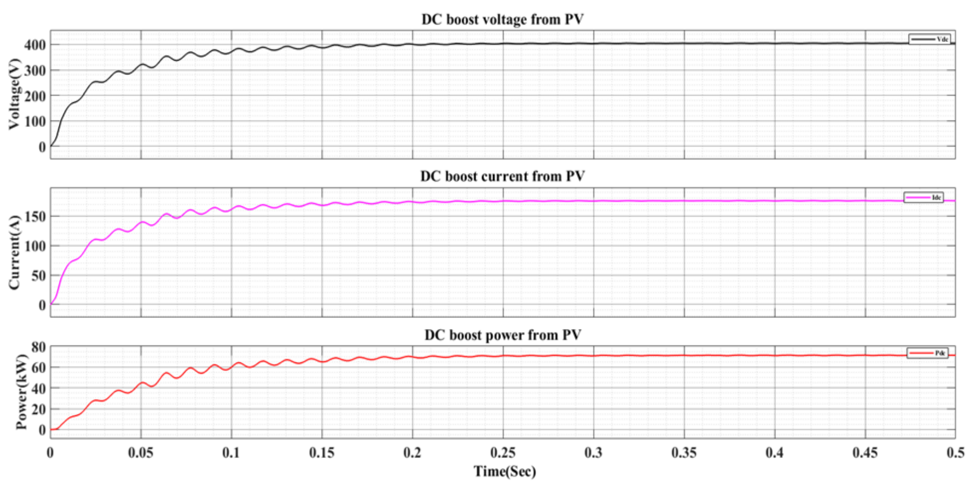

Figure 4. 2 DC voltage, current and power after boost from PV system

4.3 Wind Power Generation System

The MATLAB simulation has determined that the proposed wind turbines at Oda Bultum University can generate approximately 15 kW of power. The wind turbine system was designed using a specific model that is optimized for the average wind speed of 5.12 meters per second (m/s) measured at the university. This selected wind turbine model is capable of generating 15 kW of power given the typical wind conditions at the university. To optimize power generation in the specific wind conditions found at Oda Bultum University, PMSG was selected for the wind turbine system. This PMSG technology was chosen because it is well-suited to efficiently convert the available wind resources into electrical power given the unique wind characteristics at the university.

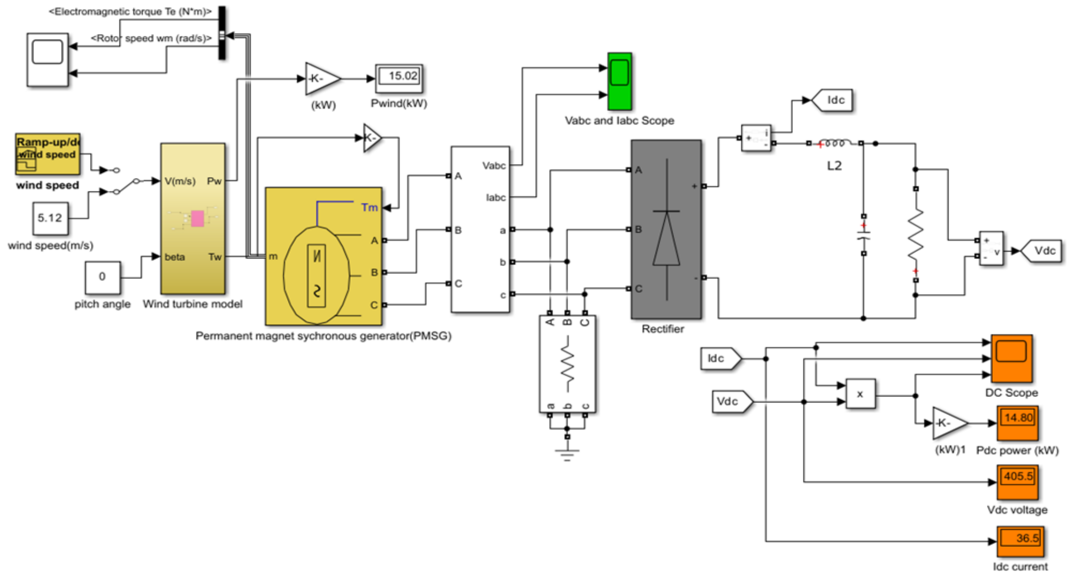

Figure 4. 3 Wind power generation Simulink simulation

4.3.1 Wind turbine simulation result

According to the results of the Matlab simulation, specifically Figure 4.4, it is evident that the proposed wind turbine is capable of generating approximately 15 kW of power. The simulation shows that the wind turbine can generate about 15 kW of output electricity at an average wind speed of 5.12 m/s.

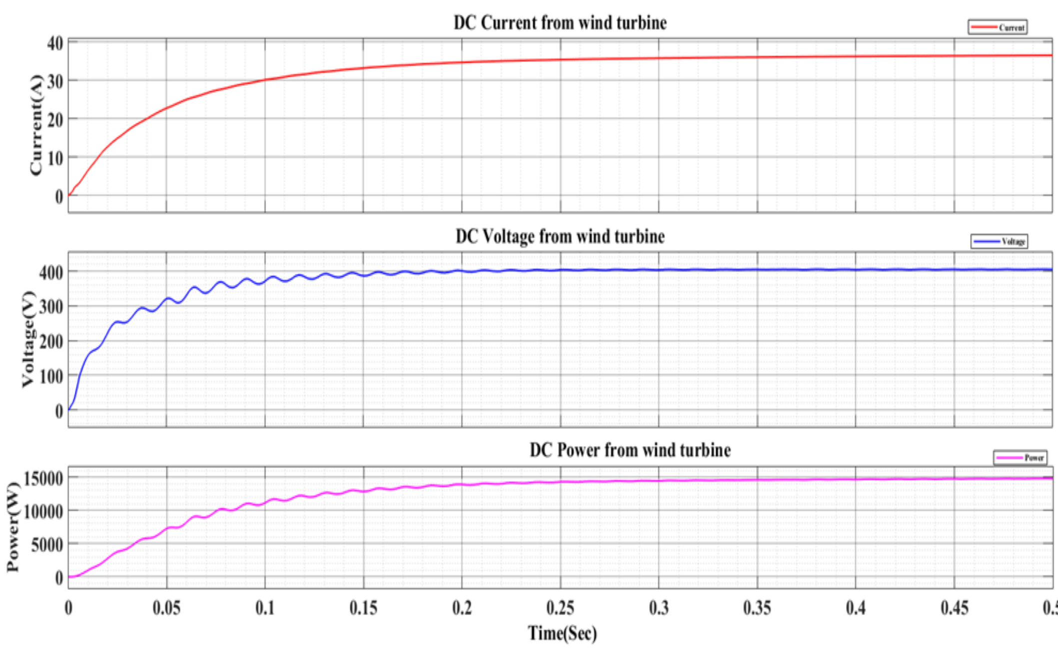

Figure 4. 4 DC voltage, current, and power simulation result from wind turbine

4.4 Battery Model and Simulation Result

In addition to the solar and wind power systems, a battery backup system with a capacity of 10 kW was designed. Through modeling and simulation, this battery system was determined to be sufficient to provide backup power for high-priority electrical at the university.

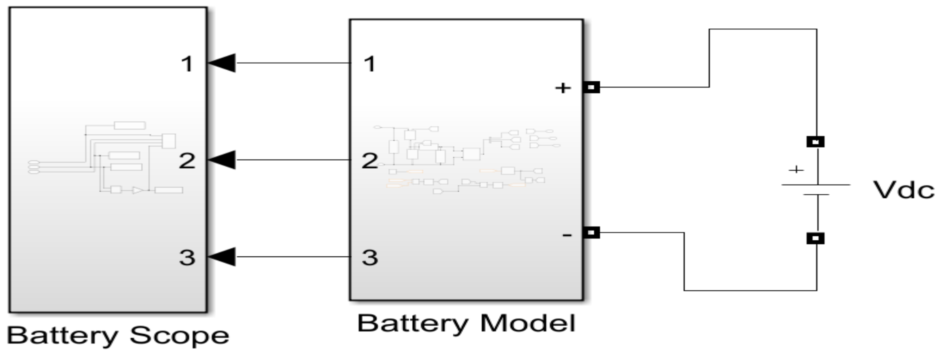

Figure 4. 5 Simulink battery model

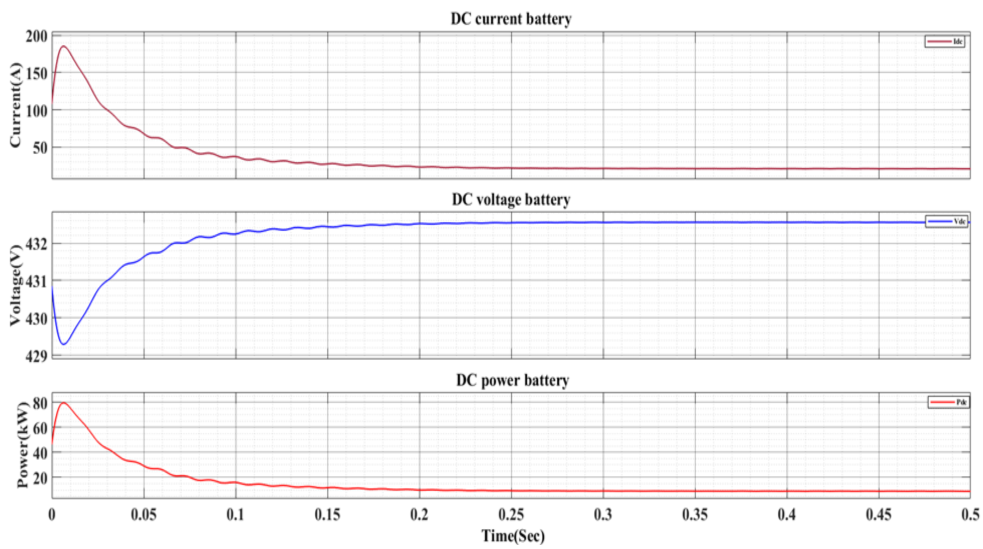

Figure 4. 6 Battery voltage, current and power simulation result

4.5 Overall Hybrid System

The hybrid system proposed combines two different renewable energy sources; solar power, and wind power with a battery as backup service. It was generate energy using these sustainable resources. The system has been modeled using Matlab/Simulink, as depicted in Figure 4.7. The model encompasses the overall functioning and interconnections of the system components.

The designed overall system generates AC voltage and current waveforms, as indicated by the MATLAB simulation result. The output AC current was 125 A, and the AC voltage was 400

V, converted from a 400 V DC link using an inverter. This configuration generates an 85 kW AC output power. In this overall system, when solar and wind power are available, the circuit breaker was closed, providing power to the load. However, if solar and wind power are not available during that time, the main utility power was used to supply power to the load.

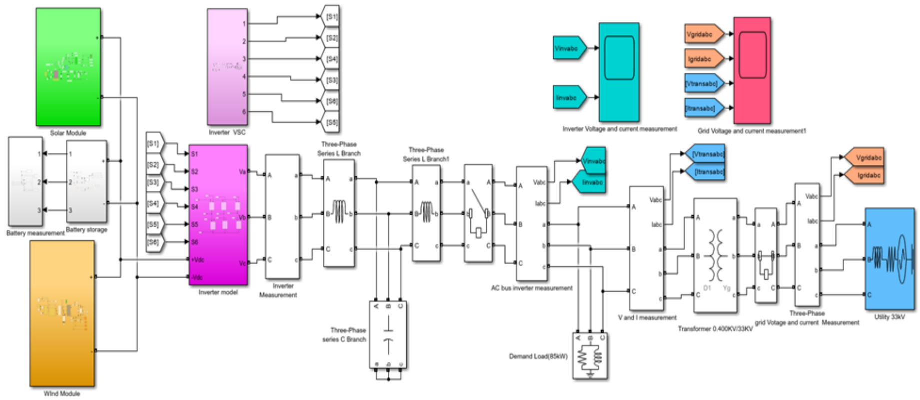

Figure 4. 7 Overall hybrid system

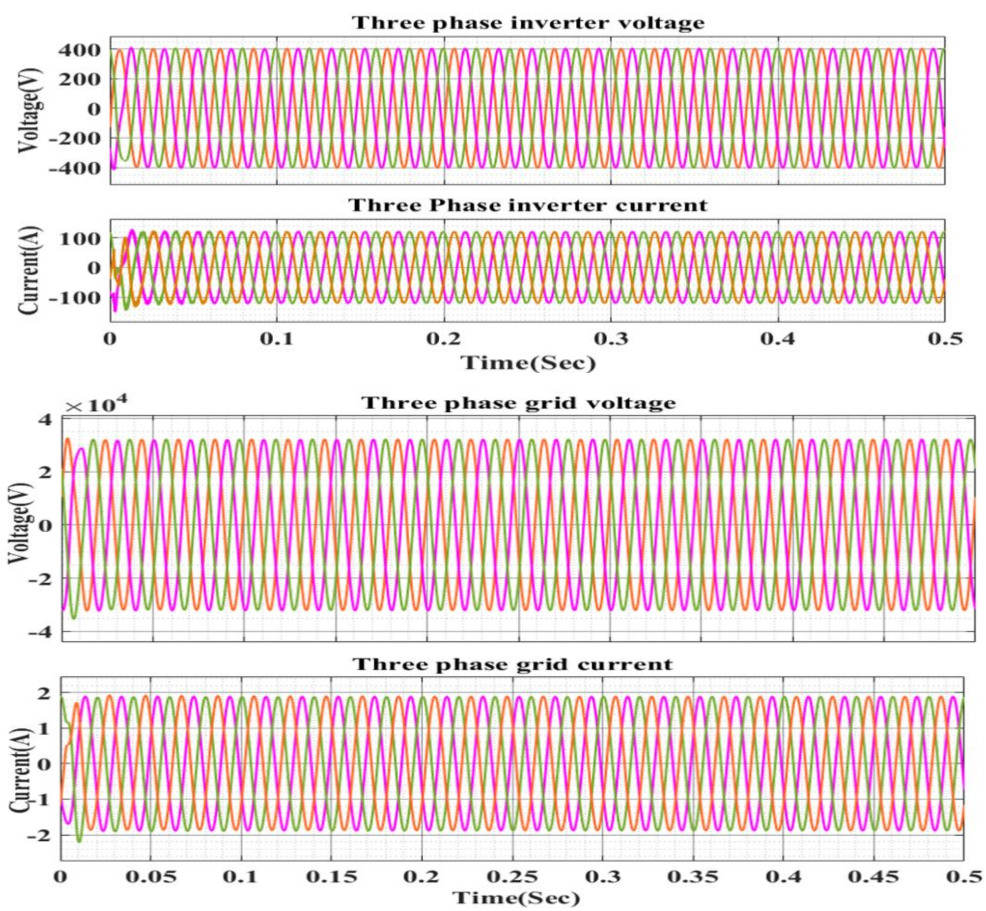

Figure 4. 8 Inverter and grid voltage and current simulation result

4.6 Fuzzy Logic Based Microgrid Energy Management System

The process of producing electricity was labor-intensive, expensive, resource-intensive, and time-consuming. However, producing energy was insufficient; instead, the electrical power produced must be used wisely and economically. In this thesis, the energy system was managed, and the fuzzy logic control managed the generated power from hybrid systems. The hybrid solar and wind-based microgrid system is designed with sufficient electric generation capacity to fully meet the power demand of the university. A fuzzy logic control system has been utilized to effectively manage electricity production and distribution to reliably satisfy the university's power requirements.

4.6.1 Fuzzy inference system

The intelligent tool known as a fuzzy logic control is used to regulate integrated energy sources to meet load requirements under a variety of load cases. Establishing the control rules, restrictions, and language variables are the steps involved in creating controller designs. The fuzzy logic system used in this thesis work has one output and five inputs. Solar power(Sp), wind power(Wp), main utility power(Mup), Battery power(Bp), and demand power (Dp) are the input language variables of FLC, while out power (Op) is the only output linguistic variable. The output linguistic variable contains the following linguistic values; Bp only, Sp only, Wp only, Mup only, and Sp+Wp. In this fuzzy logic system, each input linguistic variable has three linguistic values, except for the "battery" variable, which has three linguistic values: Low, Medium, and Large.

The fuzzy logic designer can select membership functions that accurately represent the input and output variables, align with the linguistic terms used in the fuzzy rules, and are optimized to deliver the desired control performance for the energy management system. The center of gravity method calculates the weighted average of the fuzzy output membership function, where the weights are the corresponding membership values. This results in a defuzzified output value that represents the "center of gravity" of the fuzzy output set. The Mamdani inference system for processing rules and the triangular membership function for justification are utilized. The components of a typical fuzzy system are the rule viewer, rule base, inference process, and membership functions, all of which are covered in the sections that follow. Following the creation of potential operational rules and assignment of a membership function to each input, and output linguistic value, the next stage is to assess the controller's rules for the input values to determine whether or not the output is acceptable to see the overall performance of the system.

4.7 Design of Fuzzy Inference

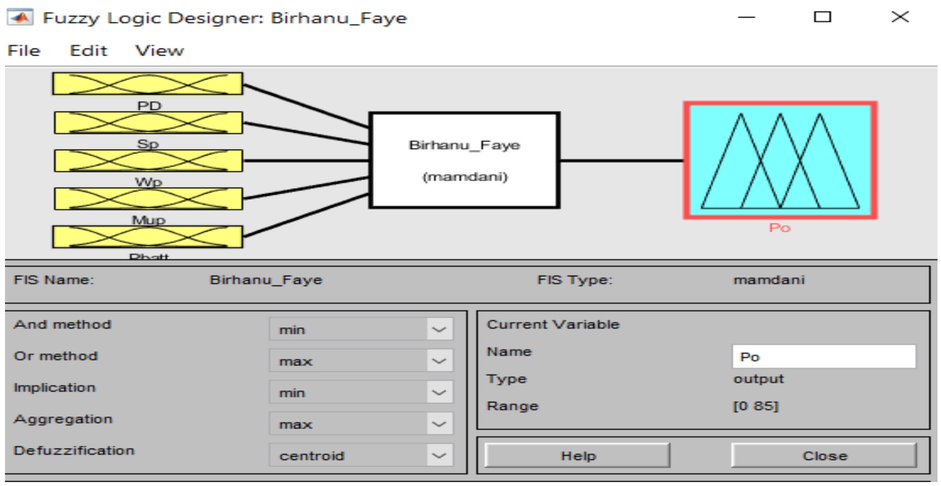

Figure 4. 9 Matlab implementation of fuzzy inference

4.7.1 Membership functions

1. Demand power membership functions (Dp)

The demand power, which is an input linguistic variable, is characterized by three membership functions: "Low," "Medium," and "Large". These membership functions can be defined as; Low (0 0 40), medium (0 40 85), Large (40 85 85).

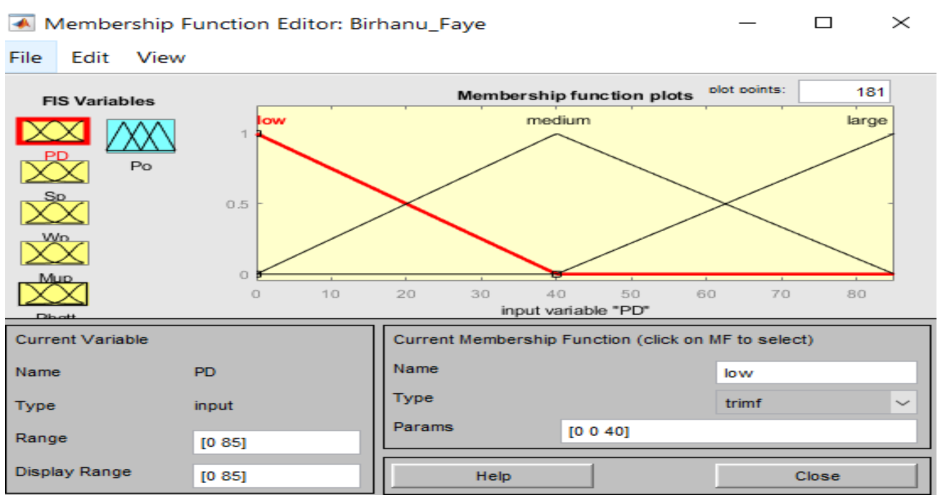

Figure 4. 10 Demand power membership function

2. Main utility power membership functions (Mup)

The main utility power, which is an input linguistic variable, is characterized by two membership functions: “OFF," and "ON". These membership functions can be defined as; OFF (0 0 20), and ON (10 85 85).

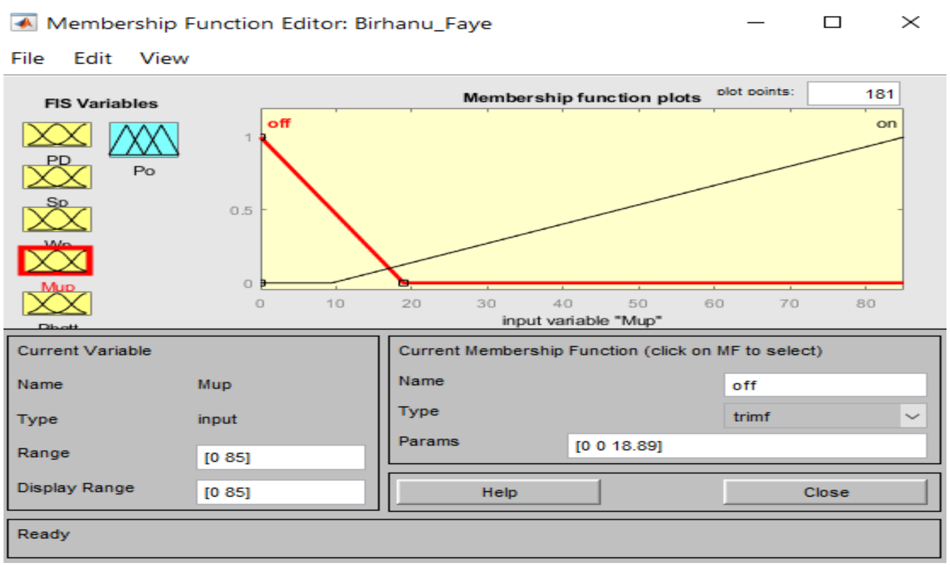

Figure 4. 11 Main utility power membership function

3. Solar power membership functions (Sp)

Solar power, which is an input linguistic variable, is characterized by three membership functions: "Low," "Medium," and "Large". These membership functions can be defined as; Low (0 0 35), medium (8 35 62), and large (35 70 70).

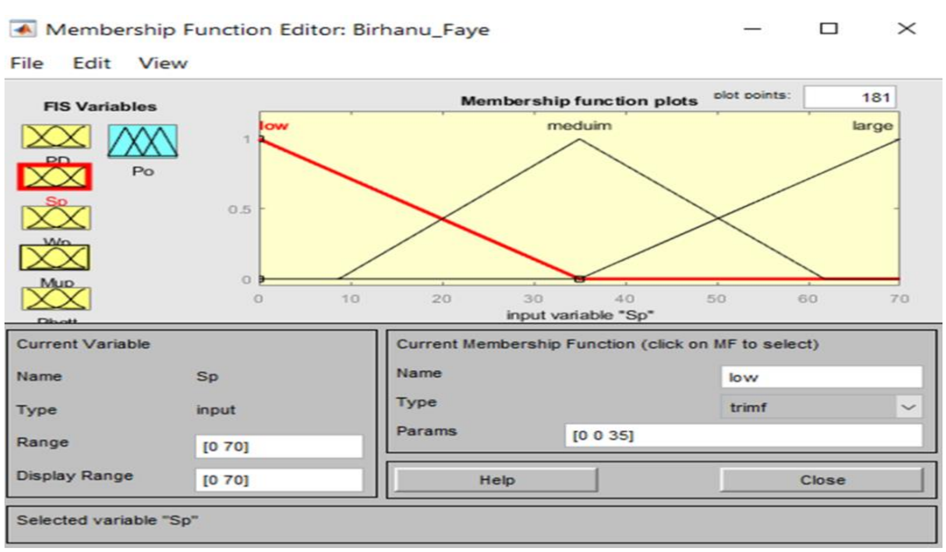

Figure 4. 12 Solar power membership function

4. Wind power membership functions (Wp)

The wind power, which is an input linguistic variable, is characterized by three membership functions: "Low," "Medium," and Large". These membership functions can be defined as; Low (0 0 7.5), medium (0 7.5 15), Large (7.5 15 15).

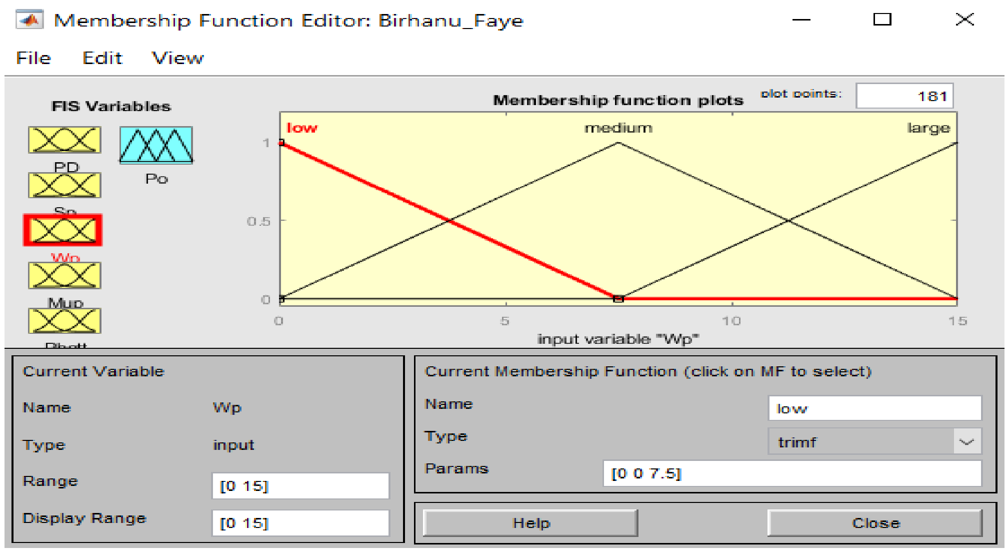

Figure 4. 13 Wind power membership function

5. Battery power membership functions (Bp)

The battery power, which is an input linguistic variable, is characterized by two membership functions: "low," and "high". These membership functions can be defined as low (0 0 5), and high (3 10 10).

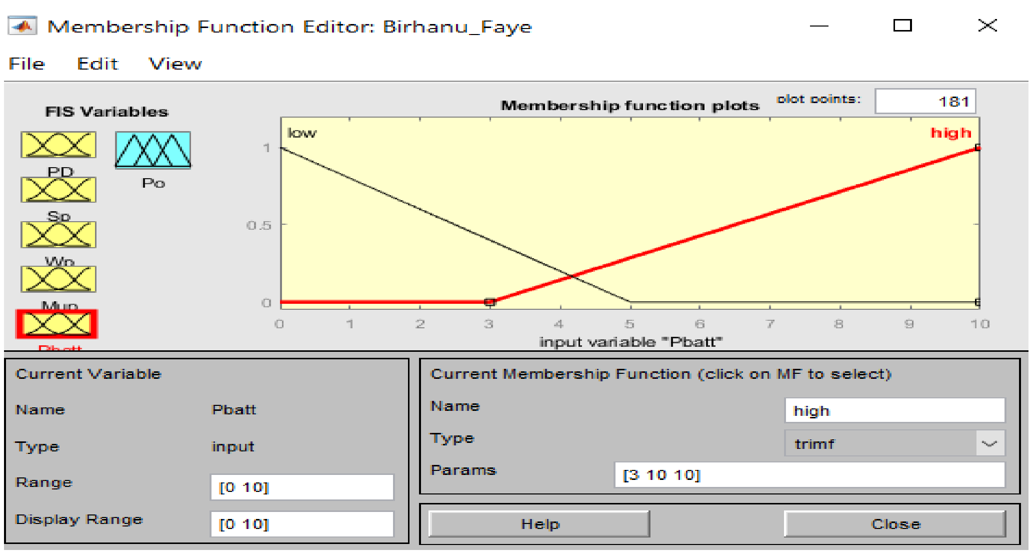

Figure 4. 14 Battery power membership function

6. Output power membership functions (Op)

The output power, which is an output linguistic variable, is characterized by five linguistic values of membership functions. These linguistic values can be defined as; Bp only(0 0 9.44), Wp only (4.722 14.17 23.61), Sp only (18.89 37.78 66.11), Mup only (70.83 85 85), and Sp+Wp (47.22 66.11 83.11).

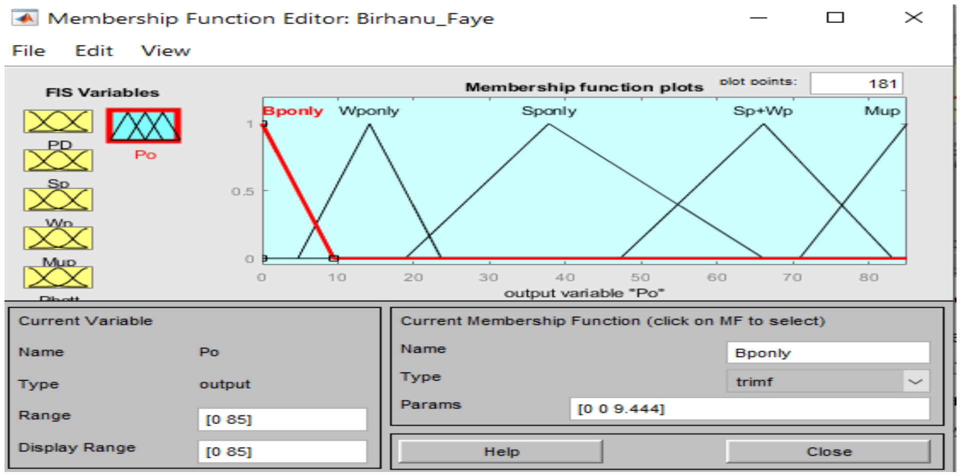

Figure 4. 15 Output power membership function

4.7.2 Fuzzy logic rule modeling

This is a real-time fuzzy logic control system that takes in five input variables and produces a single output variable. The system contains a collection of rules that are written in the control box, the system is designed to abide by these rules during its operation.

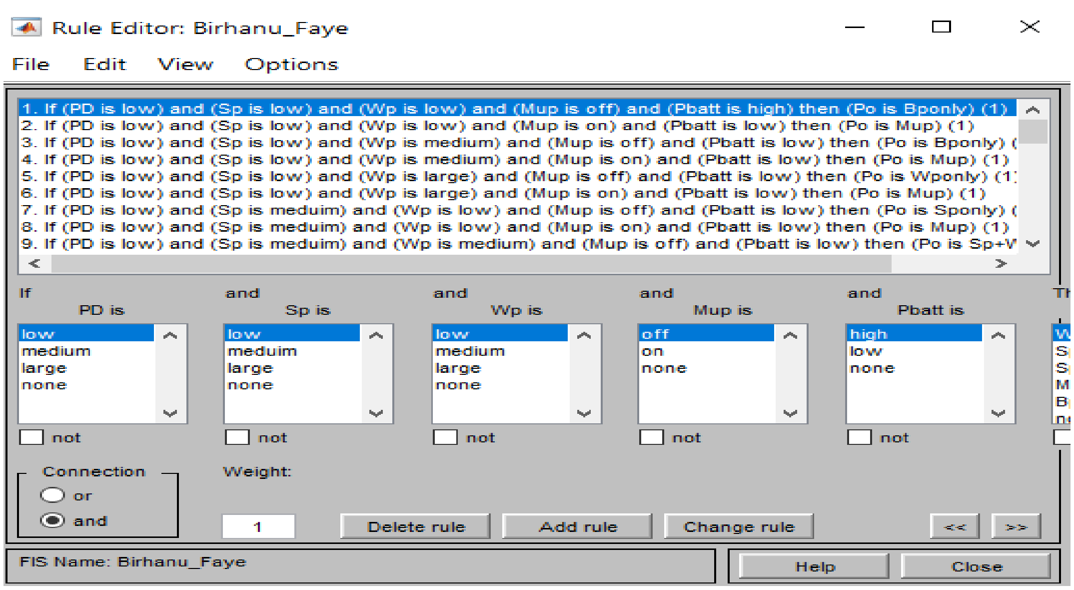

Figure 4. 16 Modelling of fuzzy logic rule editor view

MATLAB provides a feature that allows users to assess whether a system is functioning by predefined rules. In the following example, two renewable energy resources (wind and solar power), the main utility power and battery bank are intentionally configured to align with these rules. It was meet a power demand of 53.3 kW, and the result output power is measured at 53.5 kW when the main utility power is zero (off) and the battery status is low. This outcome indicates that the fuzzy rule is effectively operational in this specific case. The evaluation of these rules is visualized in Figure 4.18. Again, while constructing a fuzzy logic control, it is possible to evaluate the efficiency of the written rules viewer. In this case, let's consider the input power demand of 79.6 kW (Dp) and the corresponding output power (Op) determined by the controller, which is measured at 80.5 kW (Op) when renewable energy is not available but the main utility power is available and battery status low. The graphical representation of these rules can be observed in Figure 4.19. This outcome demonstrates that the controller is successfully utilizing the available sources in an appropriate manner to meet the given power demand.

Figure 4. 17 Fuzzy rule viewer when solar, wind power and main utility power are not available

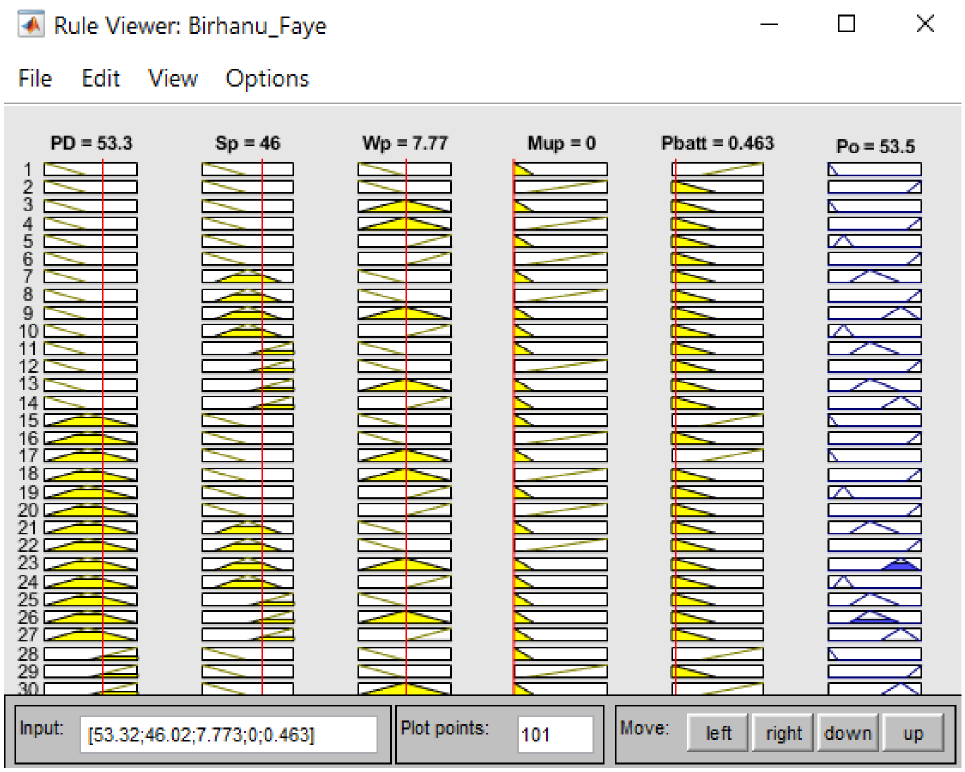

Figure 4. 18 Fuzzy rule viewer when solar and wind power is available

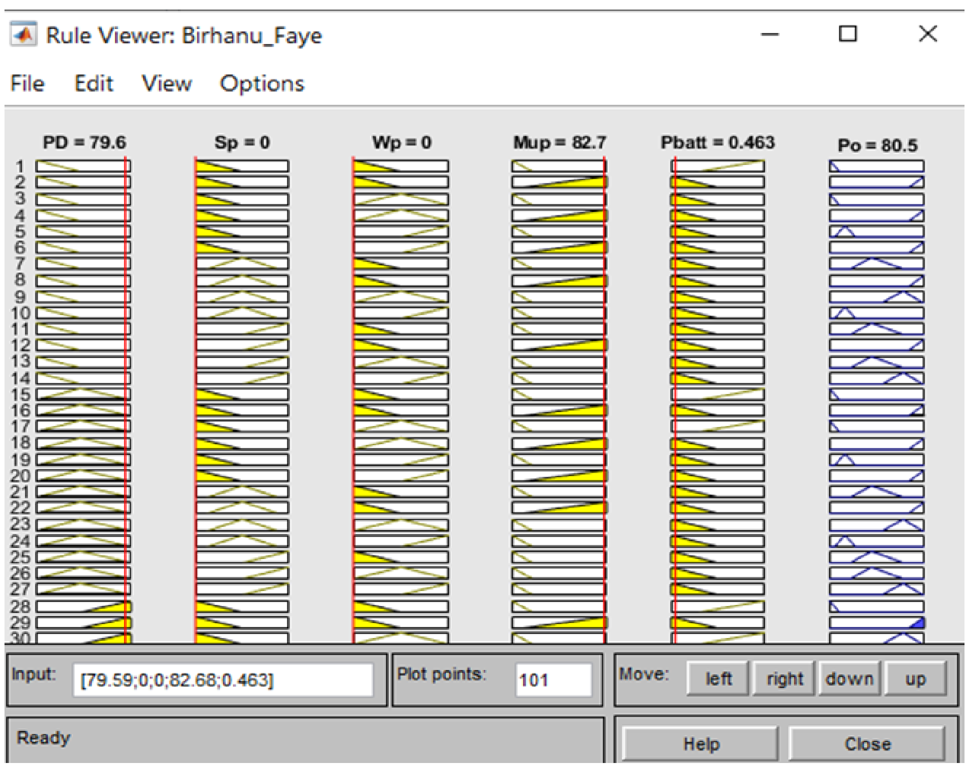

Figure 4. 19 Fuzzy logic rule viewer when main utility power is available

4.8 Overall hybrid microgrid energy management system

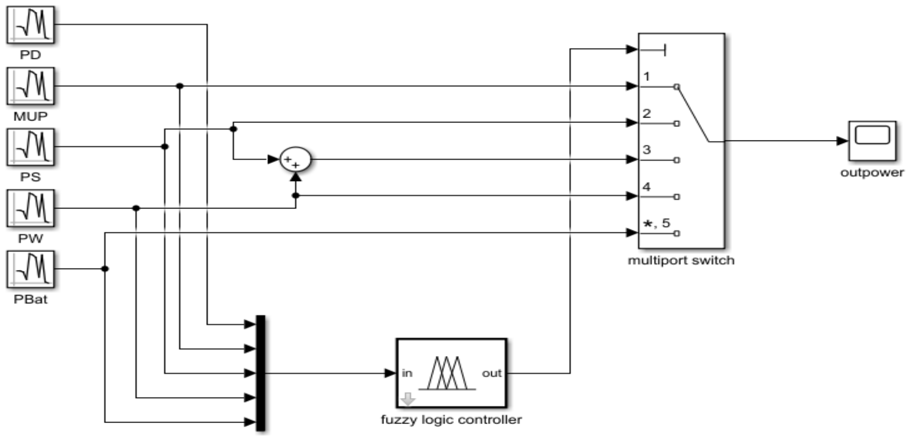

Figure 4. 20 Fuzzy logic-based microgrid energy management system

To account for the fluctuating nature of renewable energy sources, it is important to ensure that the controller can effectively adapt to these variations and make accurate decisions for multiport switches. To test this capability, a Gaussian random number generator was chosen to generate inputs for the five variables, namely power demand, main utility power, battery power, wind power, and solar power. Ac load demand power varied, main utility power(Mup) was off, the status of battery power(Bp) was low, wind power(Wp) and solar power(Sp) available which given power to load demand as shown Figure 4.21.

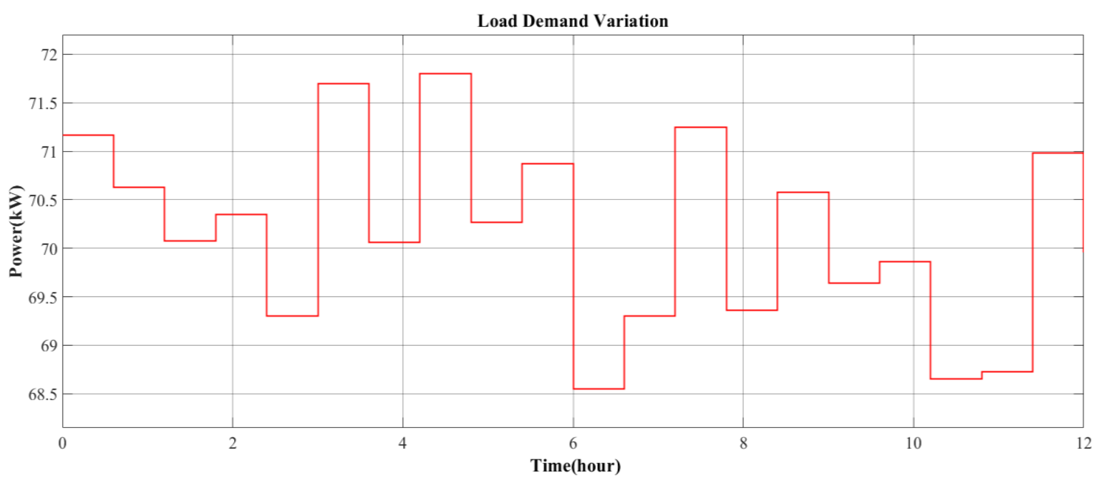

Figure 4. 21 Fuzzy logic control ouput load demand power

CHAPTER 5

5. CONCLUSIONS AND RECOMMENDATIONS

5.1 Conclusion

This thesis was design a hybrid solar/wind and battery storage microgrid system at Oda Bultum University in Chiro City, Ethiopia. The university is located at coordinates 9.0607'N and 40.8665'E at an elevation of 1540.12 meters. Due to technological restrictions in the country, there is a shortage of standardized wind speed data taken at a height of 10 meters. As an alternative, wind speed data was collected every 15 minutes at a height of 2 meters from the recorded at chiro station for 10 years (2014-2023). Mathematical models were then utilized to predict wind speed at the desired height by comparing the recorded data to NASA's wind speed data collected at 10 meters. Wind speeds were determined to be very comparable. The monthly average wind speed at the location was found to be more than 4m/s at 35-meter height, hence a small wind turbine designed to generate power 15kW capacity based on a wind speed of 5.12m/s. In terms of solar radiation, a sunlight hour recorder was used throughout a 10 year period (2014-2023). The observed sunshine hour measurements were used as input to a mathematical modeled based on the Angstrom correlation to calculate the expected monthly mean daily solar radiation levels. These forecasts were then compared against solar radiation data acquired from NASA and PVGIS-SARAH2.

Analyze load demand accurately is a critical step in designing a hybrid solar/wind microgrid system. The performance characteristics of the loads have an impact on load demand. However, analyzing the load demand at Oda Bultum University (particularly at the library, data center, and registeral office) was difficult due to the lack of a defined load calculation method. Different approaches were used to collect load demand. This entailed obtaining information from staff members and collected from Oda Bultum University's electrical technician and maintenance team. The collected daily power usage for the library, data center, and registeral office was calculated by gathering data from the site, and it came out to be 197.1kWh/day, 103.1kWh/day, and 66.74 kWh/day respectively. Consequently, the total annual energy demand for the university 367kWh/day. Solar panels at university are subject to varying levels of solar radiation of 1000W, at other times, the solar radiation levels drop to around 800W and there are also occasions when solar panels receive a relatively lower solar radiation of 600W. Hybrid solar/ wind microgrid energy system to produce efficient power by use of energy resources, a fuzzy logic control system detects available resources and picks the most suitable alternative source. The fuzzy rule editor was used to create the fuzzy rules and Matlab/Simulink was used to simulate the hybrid system components. Based on the energy requirements of the target site, the thesis has selected specific components for the proposed microgrid system. This includes SPR-305E-WHT-D photovoltaic panels, a wind turbine H15 class II, and 12V, 200Ah deep cycle batteries. The simulation results show that the system can maintain a stable DC link voltage of 400V. The hybrid solar and wind generation system produces a DC power output of around 70kW from the solar panels and an additional 15kW from the wind turbine, totaling 85kW of DC power generation.This DC power is supplemented by a 10kW battery storage capacity to meet the demands of high-priority loads. An inverter is then used to convert the 400V DC voltage to a 400V AC voltage, with a current of 125A, resulting in an 85kW AC power output to satisfy the overall load requirements.

Generally, a hybrid solar/wind microgrid system with battery backup allows for the generation of power from renewable resources. To ensure efficient power generation, a fuzzy logic was employed. The analysis of the simulation results showed that the designed fuzzy logic control system was able to successfully meet the power requirements for specific facilities at Oda Bultum University, such as the library, data center, and registrar's office. The system demonstrated its capability to meet the intended power requirements under various cases, with a targeted peak power demand of 85 kW.

5.2 Recommendation

Energy is the essential force that powers everything humans do and helps society move forward. The hybrid solar/wind microgrid energy management system played a crucial role in addressing energy crises at Oda Bultum University, particularly in the library, data center, and registeral office. The research successfully designed a hybrid combination of solar/wind energy sources with a battery backup system and a main utility power grid. This research was specifically conducted for the university, and its findings should be considered for the actual implementation. It is important to note that the study area selected for this research was limited to Oda Bultum University in the Oromia region, and future studies should explore similar hybrid solar/wind microgrid systems in other areas facing similar energy challenges. In the future, different combinations of available energy resources can be explored. The governmental bodies must prioritize and support such initiatives, including providing financial assistance for the procurement and installation of hybrid solar/wind systems. Promoting the use of the design of fuzzy logic-based microgrid energy management systems in various sectors such as clinics, schools, buildings, and others should be encouraged. The use of fuzzy logic membership functions in controlling the hybrid system was demonstrated in this research. However, interested researchers can explore other controllers such as Fuzzy-PID, Neural Network, Neuro-Fuzzy, and ANFIS for different study areas and different types of hybrid systems. The was lack of reliable and accessible data poses a challenge in our country. Therefore, I recommend that the government actively participate in improving data handling practices and supporting research efforts in the field of hybrid systems.

* * *

Special Acknowledgement: This research was founded by Adama Science and Technology University with a grant number **ASTU/SM-R/1005/24.**

REFERENCE

Ahmad, M. J., & Tiwari, G. N. (2016). *Study of Models for Predicting the Mean Hourly Global Radiation from Daily Study of Models for Predicting the Mean Hourly Global Radiation from Daily Summations*. *November 2008*. https://doi.org/10.2174/1876325100802010006

Al-Ezzi, A. S., & Ansari, M. N. M. (2022). Photovoltaic Solar Cells: A Review. *Applied System Innovation*, *5*(4), 1–17. https://doi.org/10.3390/asi5040067

Algburi, S., & Saadoon Al-Juboori, S. (2017). *Stand-Alone Photovoltaic System 5 Stand-Alone Photovoltaic System*. *March*. https://www.researchgate.net/publication/315493603

Alhamrouni, I., Hairullah, M. A., Omar, N. S., Salem, M., Jusoh, A., & Sutikno, T. (2019). Modelling and design of PID controller for voltage control of AC hybrid micro-grid. *International Journal of Power Electronics and Drive Systems*, *10*(1), 151–159. https://doi.org/10.11591/ijpeds.v10.i1.pp151-159

Ali McBride. (2021). Comprehensive Guide to Solar Panel Types - Aurora Solar. *Aurora Solar*, *August*, 1–9. https://doi.org/10.13140/RG.2.2.31128.16644

Asian Development Bank. (2020). *Asian Development Bank: Handbook on Microgrids for Power Quality and Connectivity* (Issue July). http://dx.doi.org/10.22617/TIM200182-2

Aslam Husain, M., & Tariq, A. (2014). Modeling and Study of a Standalone PMSG Wind Generation System Using MATLAB/SIMULINK. *Universal Journal of Electrical and Electronic Engineering*, *2*(7), 270–277. https://doi.org/10.13189/ujeee.2014.020702

Ayele, S., & Shen, W. (2022). *Renewable Energy Procurement by Private Suppliers in Ethiopia*. *187*.

Babaa, S. E., Armstrong, M., & Pickert, V. (2014). Overview of Maximum Power Point Tracking Control Methods for PV Systems. *Journal of Power and Energy Engineering*, *02*(08), 59–72. https://doi.org/10.4236/jpee.2014.28006

Bangga, G. (2022). Progress and Outlook in Wind Energy Research. *Energies*, *15*(18). https://doi.org/10.3390/en15186527

Benti, N. E., Aneseyee, A. B., Asfaw, A. A., Geffe, C. A., Tiruye, G. A., & Mekonnen, Y. S. (2022). Estimation of global solar radiation using sunshine-based models in Ethiopia. *Cogent Engineering*, *9*(1). https://doi.org/10.1080/23311916.2022.2114200

Bilendo, F., Meyer, A., Badihi, H., Lu, N., Cambron, P., & Jiang, B. (2023). Applications and Modeling Techniques of Wind Turbine Power Curve for Wind Farms—A Review.

Energies, *16*(1). https://doi.org/10.3390/en16010180

Borkute, R., Prof, A., & Malwar, N. (n.d.). *ICIREST-19 An Innovative Design Strategies To Control Grid Connected Intentional Islanding Operation Of Distributed Power Genration*. 1–5.

Bunting, A. (2010). *Solar Radiation Geometry*. 1–78.

Chitra, S., & Jackson, S. (2022). *A Review : Some Application on Fuzzy Logic*. *71*(4), 12619–12627.

Das, C. K., Bass, O., Kothapalli, G., Mahmoud, T. S., & Habibi, D. (2018). Overview of energy storage systems in distribution networks: Placement, sizing, operation, and power quality. *Renewable and Sustainable Energy Reviews*, *91*(November 2016), 1205–1230. https://doi.org/10.1016/j.rser.2018.03.068

Dumitrescu, C., Ciotirnae, P., & Vizitiu, C. (2021). Fuzzy logic for intelligent control system using soft computing applications. *Sensors*, *21*(8), 1–33. https://doi.org/10.3390/s21082617

El-Ahmar, M. H., El-Sayed, A. H. M., & Hemeida, A. M. (2017). Evaluation of factors affecting wind turbine output power. *2017 19th International Middle-East Power Systems Conference, MEPCON 2017 - Proceedings*, *2018-Febru*(December), 1471–1476. https://doi.org/10.1109/MEPCON.2017.8301377

Fissaha, S. G. (2017). *Hybrid Solar Pv-Genset- Battery Storage Power System for a Remote Off- Grid Application : Case Study in Ethiopia*. 2016–2017.

Fitwi, S. (2014). *Feasibility Study of Standalone PV/Wind/Biogas Hybrid System for Rural Electrification: (A Case Study of Midrwa Community in Adigrat District)*. *August*.

Green Energy and Technology. (2006). In *Green Energy and Technology*. https://doi.org/10.2174/97816080528511060101

Jain, S., & Sen, K. (2020). *PID Controller Tuning for Microgrid*. *68*(01), 58–63.

Jäkel, J., & Bretthauer, G. (n.d.). *SA NE M SC PL O E – C EO AP LS TE S M SC PL O E – C EO*. *XVII*(Section 1).

Kahlane, A. E. W. H., Hassaine, L., & Kherchi, M. (2014). *LCL filter design for photovoltaic grid connected systems*. 227–232.

Kefelegn, C. G. (2023). *Feasibility Study and Optimal Design of Hybrid Renewable Energy Microgrid System for Rural Electrification in Ethiopia (A Case Study : Jimma-Gera-Kola-*

Kinibibit) Feasibility Study and Optimal Design of Hybrid Renewable Energy Microgrid System for Rural . July.

Kumar, Y. V. P., & Bhimasingu, R. (2021). Design of voltage and current controller parameters using small signal model - based pole - zero cancellation method for improved transient response in microgrids. *SN Applied Sciences*. https://doi.org/10.1007/s42452-021-04815-x

Kuo, M. T., & Lu, S. Der. (2013). Design and implementation of real-time intelligent control and structure based on multi-agent systems in microgrids. *Energies*, *6*(11), 6045–6059. https://doi.org/10.3390/en6116045

Madvar, M. D., Ahmadi, F., Shirmohammadi, R., & Aslani, A. (2019). Forecasting of wind energy technology domains based on the technology life cycle approach. *Energy Reports*, *5*(December 2020), 1236–1248. https://doi.org/10.1016/j.egyr.2019.08.069

Maegaard, P., & Krenz, A. (2016). *Catalogue of Small Wind Turbines Under 50 Kw*.

Makkar, R., & Renu Makkar, C. (2018). Application of Fuzzy Logic. *International Journal of Statistics and Applied Mathematics*, *3*(1), 357–359. www.ijari.org

Mallon, K. R., Assadian, F., & Fu, B. (2017). Analysis of on-board photovoltaics for a battery electric bus and their impact on battery lifespan. *Energies*, *10*(7). https://doi.org/10.3390/en10070943

Manyonge, A. W., Ochieng, R. M., Onyango, F. N., & Shichikha, J. M. (2012). Mathematical modelling of wind turbine in a wind energy conversion system: Power coefficient analysis. *Applied Mathematical Sciences*, *6*(89–92), 4527–4536.

MathWorks. (2014). *Statistics Toolbox TM User ' s Guide R 2018 a*. 5700. www.mathworks.com

Matsiko, O. (2019). *Optimal Method of Generating Power at the Train Rooftop for the Auxiliary Power Supply System Case Study: Solar and Wind Power Generation on Electric Multiple Units (EMU) at Addis Ababa Light Rail Transit System (AALRT).*

Nandakumar, N., & Sekar, T. (2022). Analysis of Thermal Energy Storing and Selfcleaning Coating for Solar Panel By Using Titanium Dioxide, Melamine Formaldehyde. *International Research Journal of Modernization in Engineering Technology and Science*, *06*, 2582–5208. www.irjmets.com

Nebey, A. H. (2020). Energy management system for grid-connected solar photovoltaic with battery using MATLAB simulation tool. *Cogent Engineering*, *7*(1).

https://doi.org/10.1080/23311916.2020.1827702

Nomandela, S., Mnguni, M. E. S., & Raji, A. K. (2023). Modeling and Simulation of a Large-Scale Wind Power Plant Considering Grid Code Requirements. *Energies*, *16*(6). https://doi.org/10.3390/en16062897

Papageorgiou, P. C., & Alexandridis, A. T. (2017). Stabilizing the VSI response in microgrids via novel PI controllers. *19th International Symposium on Power Electronics, Ee 2017*, *2017-December*(October 2017), 1–6. https://doi.org/10.1109/PEE.2017.8171705

Pattanayak, P., Panigrahy, N., & Mishra, S. (2015). Overcome of energy crisis using hybrid renewable energy sources in India: HOMER application. *Proceedings of 2015 IEEE 9th International Conference on Intelligent Systems and Control, ISCO 2015*. https://doi.org/10.1109/ISCO.2015.7282263

POPESCU, V. F., & PİSTOL, M. S. (2021). Fuzzy logic expert system for evaluating the activity of university teachers. *International Journal of Assessment Tools in Education*, *8*(4), 991–1008. https://doi.org/10.21449/ijate.1025690

Rajashekar Reddy Palle, Jens Schuster, Yousuf Pasha Shaik, M. K. (2018). Solar Photovoltaic (PV) System Components. *University of Arizona - Cooperative Extension*, *May*, 1–8.

Reddy, K., N, S. A., Naga, N., Lakshmi, M., Reddy, A. V. K., Rajesh, B., Kumar, K., & Ali, S. (2015). A Brief Research , Study , Design and Analysis on Wind turbine. *Journal Of Modern Engineering Research (IJMER)*, *5*(October 2015), 26.

Roine, L., Therani, K., Sahraei Manjili, Y., & Jamshidi, M. (2014). Microgrid energy management system using fuzzy logic control. *World Automation Congress Proceedings*, 462–467. https://doi.org/10.1109/WAC.2014.6936001

Saha, A., Misra, S., & Progya, P. M. (2019). Design and simulation based stand-alone solar micro grid system for island areas. *2019 5th International Conference on Advances in Electrical Engineering, ICAEE 2019*, 229–234. https://doi.org/10.1109/ICAEE48663.2019.8975488

Shallo, L., Ayele, M., & Sime, G. (2020). Determinants of biogas technology adoption in southern Ethiopia. *Energy, Sustainability and Society*, *10*(1), 1–13. https://doi.org/10.1186/s13705-019-0236-x

Stephie, A. (2023). A Comprehensive Guide to Primary and Secondary Batteries Commentary. *Rrjpap|*, *11*(2), 45. https://doi.org/10.4172/2320-2459.11.2.010.

Sumit S.Chaudhari, O.Chaudhary, A., Gole, P. P., & Kapil.T.Patil. (2017). Design & Construction of Combined Axis Wind Mill Turbine for Maximise Efficiency. *Ijariie*, *3*(3), 1914–1921.

SunPower. (2007). *SunPower 305 Datasheet*. 0–1. http://www.pocosolar.com/wp-content/themes/twentyfifteen/pdfs/Sunpower SolarPanels/sunpower_305wht_spec_sheet.pdf

Teshale, A., & Science, A. (2012). *Irrigation System in case of Wonji-Shoa Villages*.

Thirunavukkarasu, M., & Sawle, Y. (2020). Design, analysis and optimal sizing of standalone PV/diesel/battery hybrid energy system using HOMER. *IOP Conference Series: Materials Science and Engineering*, *937*(1). https://doi.org/10.1088/1757-899X/937/1/012034

Weiß, C. I., Gohm, A., Rotach, M. W., & Minda, T. T. (2022). Dynamics of gap winds in the Great Rift Valley, Ethiopia: emphasis on strong winds at Lake Abaya. *Weather and Climate Dynamics*, *3*(3), 1003–1019. https://doi.org/10.5194/wcd-3-1003-2022

Yaqobi, M. A., Matayoshi, H., Danish, M. S. S., Urasaki, N., Howlader, A. M., & Senjyu, T. (2018). Control and Energy Management Strategy of Standalone DC Microgrid Cluster using PV and Battery Storage for Rural Application. *International Journal of Power and Energy Research*, *2*(4), 53–68. https://doi.org/10.22606/ijper.2018.24001

APPENDIX

Appendix i. Specification of SunPower 305 solar panels and battery

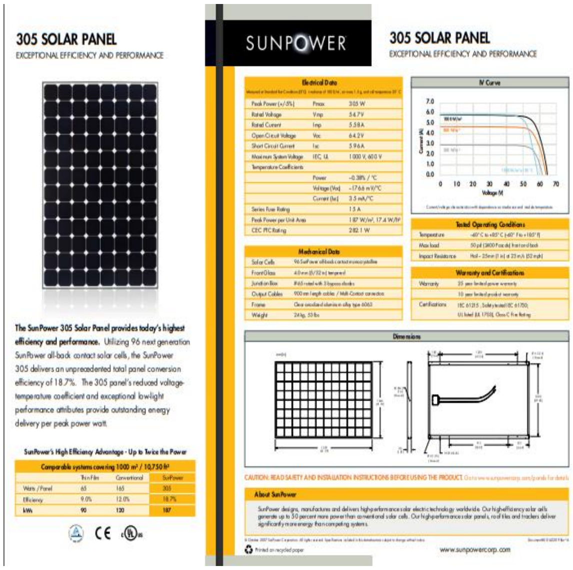

DC12-200 (12V200Ah)

DC (Deep Cycle) series is specially designed for frequent cyclic discharge. By using strong grids and specially designed active material, the DC series battery offers 30% more cyclic life than the standby series. It is suitable for solar energy systems, marine and RV etc.

Specification

Cells Per Unit	6
Voltage Per Unit	12
Capacity	200Ah@10hr-rate to 1.80V per cell @25℃
Weight	Approx. 60.0 Kg (Tolerance±1.5%)
Max. Discharge Current	2000 A (5 sec)
Internal Resistance	Approx. 4 mΩ
Operating Temperature Range	Discharge: -20℃~60℃ Charge: 0℃~50℃ Storage: -20℃~60℃
Normal Operating Temperature Range	25℃±5℃
Float charging Voltage	13.6 to 13.8 VDC/unit Average at 25℃
Recommended Maximum Charging Current	60 A
Equalization and Cycle Service	14.6 to 14.8 VDC/unit Average at 25℃
Self Discharge	RITAR Valve Regulated Lead Acid (VRLA) batteries can be stored for more than 6 months at 25℃. Self-discharge ratio less than 3% per month at 25℃. Please charge batteries before using.
Terminal	Terminal F10
Container Material	A.B.S. UL94-HB, UL94-V0 Optional.

Appendix ii. Voltage source inverter control system

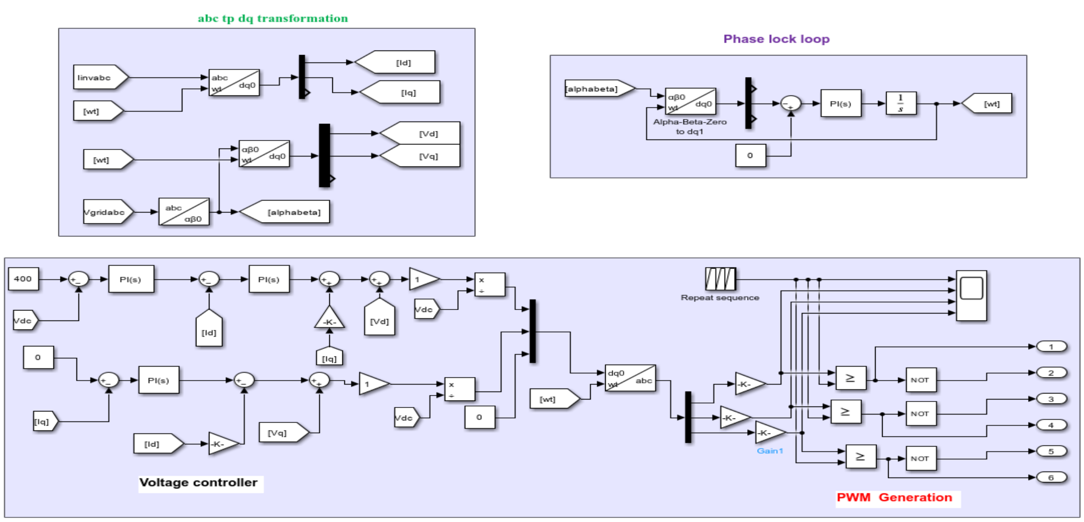

Appendix iii. Battery design and control system